New Strategies to Improve the Sensitivity of Capillary Electrophoresis for Carbohydrate Analysis

by

Artaches Alexandrovich Kazarian

A thesis submitted in fulfilment of the requirements for the degree of

Doctor of Philosophy

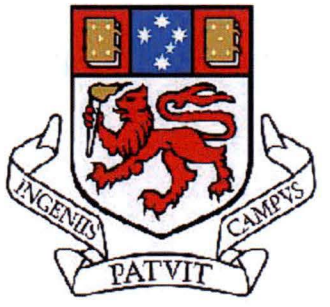

UNIVERSITY OF TASMANIA

Submitted 28 May 2010

Declaration

To the best of my knowledge, this thesis contains no copy or paraphrases of material previously written or published, except where due reference is made.

Artaches Kazarian

28 May 2010

This thesis may be available for loan and limited copying in accordance with the Copyright Act 1968.

Artaches Kazarian

28 May 2010

Acknowledgements

First of all I would like to thank my supervisors Dr. Michael Breadmore and Dr. Emily Hilder for their excellent help and support throughout the years. Also thank you for sending me to the international conferences in Europe and Asia, it was a great learning experience and a chance to have a great vacation too :)

Thanks to the members of ACROSS for providing a great working atmosphere, including the weekly meetings with cakes and other goodies.

Thanks to all the PhD students, their support, interesting conversations and their help throughout the years.

I would also like thank my family, all my relatives and friends for their understanding and support, without you guys I would not have got this far.

Artaches Kazarian

List of Abbreviations

2-AA	2-Aminobenzoic acid
2-D	2-Dimensional
3-AA	3-Aminobenzoic acid
3-ABA	3-Aminobenzamide
3-APP	2-Amino-3-phenylpyrazine
ABEE	4-Aminobenzoic acid ethyl ester
ANTS	8-Aminonaphthalene-1,3,6-trisulfonic acid
APTS	8-Aminopyrene-1,3,6-trisulfonic acid
bd	Broad doublet
BGE	Background electrolyte
bs	Broad singlet
CBQCA	3-(4-Carboxybenzoyl) quinoline-2-carboxaldehyde
CDCCs	*Cis*-diol-containing compounds
$CDCl_3$	Deuterated chloroform
CE	Capillary electrophoresis
CL	Chemiluminescence
CZE	Capillary zone electrophoresis
d	Doublet
D_2 lamp	Deuterium lamp
DAD	Diode array detector
dd	Doublet of doublets
DMF	Dimethyl formamide
DMSO	Dimethylsulfoxide
DMSO-d_6	Deuterated dimethyl sulfoxide
DNA	Deoxyribonucleic acid
dp	Degree of polymerisaton
EOF	Electro-osmotic flow
FASS	Field amplified sample stacking
GC	Gas chromatography
HPLC	High performance liquid chromatography
HVA	Homovanillic acid

ITP	Isotachophoresis
J	Coupling constant
LED	Light-emitting diode
LEDIF	Light-emitting diode induced fluorescence
LIF	Laser-induced fluorescence
LOD	Limit of detection
LPA	Linear polyacrylamide
Luminol	3-Aminophthalhydrazide
LVSS	Large volume sample stacking
M	Moles L^{-1}
m	Multiplet
MALDI	Matrix-assisted laser desorption
MCRB	Moving chemical reaction boundary
MEKC	Micellar electrokinetic chromatography
MNPs	Magnetic nanoparticles
MS	Mass spectrometry
NBD-F	7-Nitro-2,1,3-benzoxadiazole 4-fluoride
NMP	1-(2-Naphthyl)-3-methyl-5-pyrazolone
NMR	Nuclear magnetic resonance
NPBA	3-Nitrophenylboronic acid
PABA	*p*-Aminobenzoic acid
PDADMAC	Poly(diallyldimethylammonium chloride)
PDMS	Polydimethylsiloxane
p*I*	Isoelectric point
PITC	Phenylisothiocyanate
pK_a	Negative logarithm of acid dissociation constant
PMP	1-Phenyl-3-methyl-2-pyrazolin-5-one
PNA	*p*-Nitroaniline
PSS	Poly(styrene sulfonate)
QY	Quantum yield
RSD	Relative standard deviation
SDS	Sodium dodecylsulfate
SEC	Size exclusion chromatography

SFC	Supercritical fluid chromatography
THF	Tetrahydrofuran
TLC	Thin layer chromatography
tris	Tris (hydroxymethyl) aminomethane
TRSE	4-Carboxytetramethylrhodamine succinimidyl ester
UV	Ultra-violet
Vis	Visible
γ-MAPS	γ-Methacryloxypropyltrimethoxysilane
δ	Chemical shift

List of Publications

Publication type	Number	Reference
Journal publications	4	1-2, 4-5
Book chapter	1	3
Poster presentations	3	6-8
Oral presentations	4	9-12

(1) A. A. Kazarian, M. C. Breadmore and E. F. Hilder, Capillary electrophoresis separation of mono- and di-saccharides with dynamic pH junction and implementation in microchips, Analyst, submitted on 18 Jan 2010. (Accepted for publication on 26 Apr 2010). **(Chapter 5)**

(2) A. A. Kazarian, J. A. Smith, E. F. Hilder, M. C. Breadmore, J. P. Quirino and J. Suttil, Development of a novel fluorescent tag O-2-[aminoethyl]fluorescein for the electrophoretic separation of oligosaccharides, Analytica Chimica Acta, 2010, 662, 206-213. **(Chapter 4)**

(3) A. A. Kazarian, M. C. Breadmore, E.F. Hilder, Fluorophores and chromophores for the separation of carbohydrates by CE, in N. Volpi (Editor), Capillary Electrophoresis of Carbohydrates: From monosaccharides to complex polysaccharides, accepted for publication 23 October 2009. **(Chapter 1)**

(4) M. C. Breadmore, J. R. E. Thabano, M. Dawod, A. A. Kazarian, J. P. Quirino and R. M. Guijt, Recent advances in enhancing the sensitivity of electrophoresis and electrochromatography in capillaries and microchips (2006-2008), Electrophoresis, 2009, 30, 230-248. **(Chapter 1)**

(5) A. A. Kazarian, E. F. Hilder and M. C. Breadmore, Utilisation of pH stacking in conjunction with a highly absorbing chromophore, 5-aminofluorescein, to improve the sensitivity of capillary electrophoresis for carbohydrate analysis, Journal of Chromatography A, 2008, 1200, 84-91. **(Chapter 3)**

(6) A. A. Kazarian, E. F. Hilder and M. C. Breadmore, Investigation of New Strategies to Improve the Sensitivity of Capillary Electrophoresis in Carbohydrate Analysis, The 14th Annual Royal Australian Chemical Institute Research & Development Topics, Gold Coast, Australia, 2009, **poster presentation.**

(7) A. A. Kazarian, E. F. Hilder and M. C. Breadmore, Development of a Novel Fluorescent Tag O-2-[Aminoethyl]fluorescein Hydrochloride to Improve the Sensitivity of Capillary Electrophoresis for Carbohydrate Analysis, Australian Centre for Research on Separation Science Symposium on Advances in Separation Science, Hobart, Australia, 2009, **poster presentation.**

(8) A. A. Kazarian, E. F. Hilder and M. C. Breadmore, Investigation of New Strategies to Improve the Sensitivity in Capillary Electrophoresis, The 14th Annual Royal Australian Chemical Institute, Research & Development Topics, Woolongong, Australia, 2006, **poster presentation.**

(9) A. A. Kazarian, E. F. Hilder and M. C. Breadmore, Investigation of New Strategies to Improve the Sensitivity of Capillary Electrophoresis for Carbohydrate Analysis,8th Asia-Pacific International Symposium on Microscale Separation and Analysis, Kaohsiung, Taiwan, 2008, **oral presentation.**

(10) A. A. Kazarian, E. F. Hilder and M. C. Breadmore, Novel Fluorescent Tag O-2-[Aminoethyl]fluorescein Hydrochloride to Improve the Sensitivity of Capillary Electrophoresis for Carbohydrate Analysis, University of Tasmania Conference for Postgraduate Students, Hobart, Australia, 2008, **oral presentation.**

(11) A. A. Kazarian, E. F. Hilder and M. C. Breadmore, Investigation of New Strategies to Improve the Sensitivity of Capillary Electrophoresis in Carbohydrate Analysis, 15th Annual RACI Research & Development Topics, Adelaide, Australia, 2007, **oral presentation.**

(12) A. A. Kazarian, E. F. Hilder and M. C. Breadmore, Investigation of New Strategies to Improve the Sensitivity of Capillary Electrophoresis for Carbohydrate Analysis, 31st International Symposium on High Performance Liquid Phase Separations and Related Techniques, Ghent, Belgium, 2007, **oral presentation.**

Abstract

This study describes various strategies to improve the sensitivity of carbohydrate analysis in capillary electrophoresis (CE).

The use of pH stacking is investigated in conjunction with 5-aminofluorescein as a derivatisation agent for the sensitive analysis of simple sugars such as glucose, lactose and maltotriose by CE. The derivatisation agent was selected on the basis of its extremely high molar absorptivity, its compatibility with a 488 nm light-emitting diode (LED) and the fact that it has two ionisable groups making it compatible with on-line stacking using a dynamic pH junction. The influence of both acetic and formic acids were investigated with regard to both derivatisation efficiency and the ability to stack using a dynamic pH junction. Superior sensitivity and resolution was obtained in formic acid over acetic acid. Simulation studies combined with experimental data showed the separation with the best resolution and greatest sensitivity when the carbohydrates were derivatised with the 95 mM formic acid. Using this method efficiencies of 150,000 plates and detection limits at 8.5×10^{-8} M for mono-, di- and tri-saccharides were achieved. The current system demonstrates a 515 times improvement factoring sensitivity when compared to using a normal deuterium (D_2) lamp, and 16 times improvement over other systems using light-emitting diodes (LEDs).

A novel fluorescent tag, O-2-[aminoethyl]fluorescein, was developed for the separation of sugars by CE with laser-induced fluorescence (LIF) detection using an argon ion laser. The tag was synthesised using three consecutive steps namely: esterification, alkylation and hydrolysis, specifically designed to offer a flexible way in which to make an assortment of fluorescent tags from cheap and readily available starting reagents (typically less than $1 per g of fluorescent tag).

O-2-[Aminoethyl]fluorescein was equipped with a spacer group to lower steric effects between the fluorescein backbone and the reducing end of the carbohydrate which were anticipated to improve the reactivity of the tag. Fluorescence studies of the novel tag revealed a quantum yield (QY) of 0.24, when using fluorescein as a standard. Kinetic studies were also conducted to compare and assess the performance of aromatic and aliphatic amines using the novel tag and two commercial fluorescent fluorescein motifs where the aromatic amine derivative demonstrated better labelling performance. The separation performance of all the tags was also benchmarked using a range of corn syrup oligosaccharides. The application of the novel tag to a set of oligosaccharides produced a baseline separation of seven different sugar units, with 1 nM detection limit for maltoheptaose.

A CE method was designed with on-line concentration which can be translated directly to a microchip format allowing preconcentration *via* dynamic pH junction. Optimisation of the separation selectivity yielded best separations using a 170 mM ammonium borate buffer at pH 8.60 in an acrylamide coated capillary. When using the current system *via* LIF, limits of detection (LODs) as low as 0.13 nM for maltose were obtained, which were 10 times lower than could be achieved without on-line concentration. In order to implement this system in a glass/polydimethylsiloxane (PDMS) microchip, the low pH sample was introduced into the microchannels via a cathodic pH independent electro-osmotic flow (EOF) generated using a polyelectrolyte multilayer coating. Microchip separations of maltose, glucose, galactose and allose with dynamic pH junction, were achieved within 120 s, with the limit of detection (LOD) of maltose using a light-emitting diode induced fluorescence (LEDIF) detection system being 790 nM. This is the first implementation of on-line concentration via a dynamic pH junction in a microchip,

and significantly, the improvement in sensitivity achieved when translated to the microchip was equivalent to that achieved in capillaries.

Table of Contents

Chapter 1

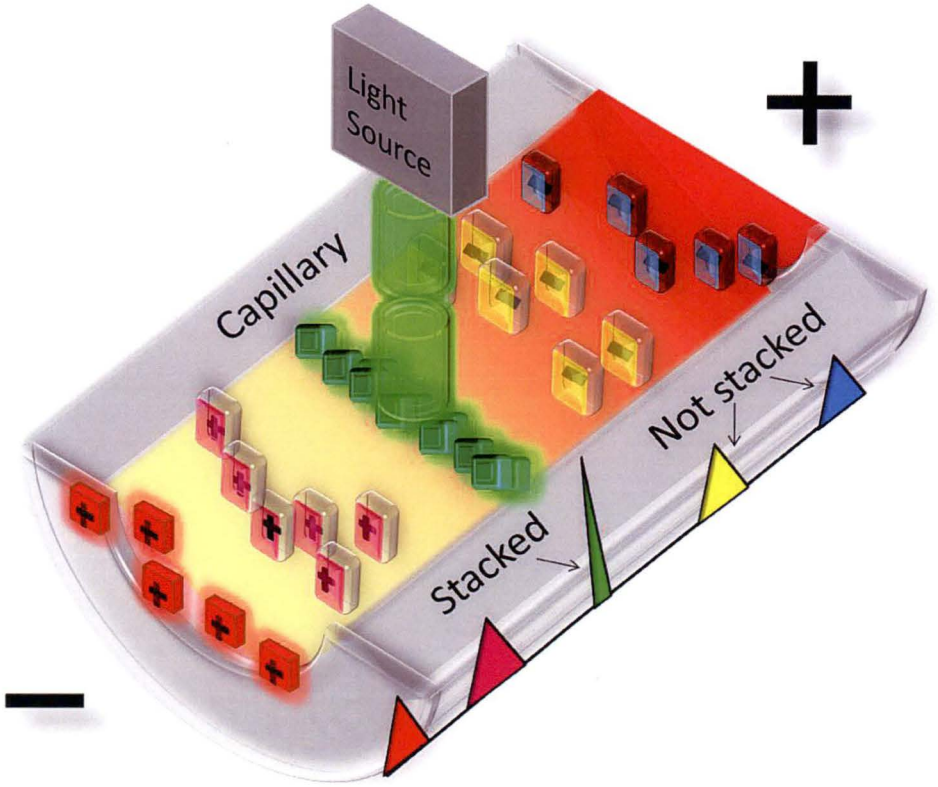

1 Literature review

1.1 Overview

These days there is an increased interest among the scientific community worldwide to analyse carbohydrates and their bioconjugates starting with simple oligosaccharides and progressing to more complex glycoprotein biocomposites. Carbohydrates are known to be the most abundant assembly of biopolymers resulting in an immense diversity as a result of complex glycosylation processes occurring in the body which inevitably complicates the ability to study these structures [1]. It has been documented that carbohydrates are responsible for numerous regulatory processes occurring on the cell surface as well as causing specific receptor communication such as antigen/antibody recognition and cell/cell interaction [2-4]. Further applications are found in production of pharmaceuticals where carbohydrates have demonstrated vital roles in bioactivity [5], stability of glycoproteins [6] and efficacy [7]. Viral infection [8] and tumour metathesis [9] have been pinpointed as a consequence of carbohydrate involvement implying the significance of carbohydrates and ultimately the importance of the field of glycobiology. Carbohydrates also contribute to the global issues of organic carbon deposits [1], directly affecting the carbon cycle and therefore unequivocally highlighting the importance of detection and analysis of these micro composites. A large proportion of the functionally important carbohydrates are numerous in their diversity and are typically present in extremely low amounts which clearly highlights the need to develop highly sophisticated and sensitive methods for their identification.

Over the years the fast pace of advancing technology enabled the development of various analytical tools for the analysis of carbohydrates namely: high performance

liquid chromatography (HPLC) using normal-phase, reversed-phase and anion-exchange chromatography, gas chromatography (GC), nuclear magnetic resonance (NMR), mass spectrometry (MS), size exclusion chromatography (SEC), supercritical fluid chromatography (SFC) and capillary electrophoresis (CE). All of these methods have some limitations: HPLC shows difficulties resolving structural isomers, SFC and GC require labelling of chain carbohydrates to improve solubility and volatility respectively, while MS requires internal standards to obtain necessary quantitation. Quantitation is further compromised due to matrix-induced ion suppression effects. SEC is another useful method to study carbohydrates although the technique is unable to separate smaller sugars and therefore requires additional methods to analyse a complete range of these biopolymers. Anion-exchange liquid chromatography-pulsed amperometric detection allows analysis of carbohydrates at picomole levels via the use of strong anion exchange stationary phases which produce selective separations of weakly acidic carbohydrates [10]. Nevertheless this technique still requires large sample volumes and can be challenging when trying to resolve structural isomers. Other techniques such as NMR have been trialled however this lacks sensitivity and is inappropriate when dealing with small sample quantities [11]. CE is excellent for the separation of carbohydrates as it is complementary to SEC and it offers better separation efficiency, shorter separation times and smaller sample volumes than HPLC techniques [12].

This particular study will focus on the applications of CE as the means to study carbohydrates with the aim of achieving ultra-sensitive detection. Later sections of this literature review will identify and explain strategies utilised to improve the detection and sensitivity of CE for carbohydrate analysis.

1.2 CE

Historical accounts reveal that expression "electrophoresis" was pioneered by Michaelis who initiated protein separation by the means of isoelectric focusing in 1909 [13]. The origin of modern electrophoresis dates back to the year 1937 when the concept of moving boundary electrophoresis was confirmed by observing movement of proteins induced by electric field [14]. Years of research described various electrophoresis modes starting with fused-silica gels and thin layers of Sephadex beads which led to the development of polyacrylamide gel electrophoresis [15]. In the late 1960s sodium dodecyl sulfate (SDS)-PAGE [16], electrophoresis and the term isotachophoresis (ITP) were established and finally the year 1981 brought about the first demonstration of CE [15, 17-18].

The basic model of CE involves the movement of charged analytes in a capillary, dissolved in a conductive electrolyte where an electric field is present. Thus charged species will occupy their positions in accordance with their velocity which is affected by the applied electric field and their individual mobility. The electrophoretic mobility of an ion is governed by its size, charge and the viscosity of the solution. The difference in the mobilities of different ions enables different rates of movement, resulting in their separation [19]. The basic set up of CE instrumentation is shown in Figure 1.1 including the buffer vials where the electrolyte is placed, sample vials where the analytes are introduced, electrodes, high-voltage power supply, capillary where the separation occurs and the detector to interpret the signal output on the computer [19].

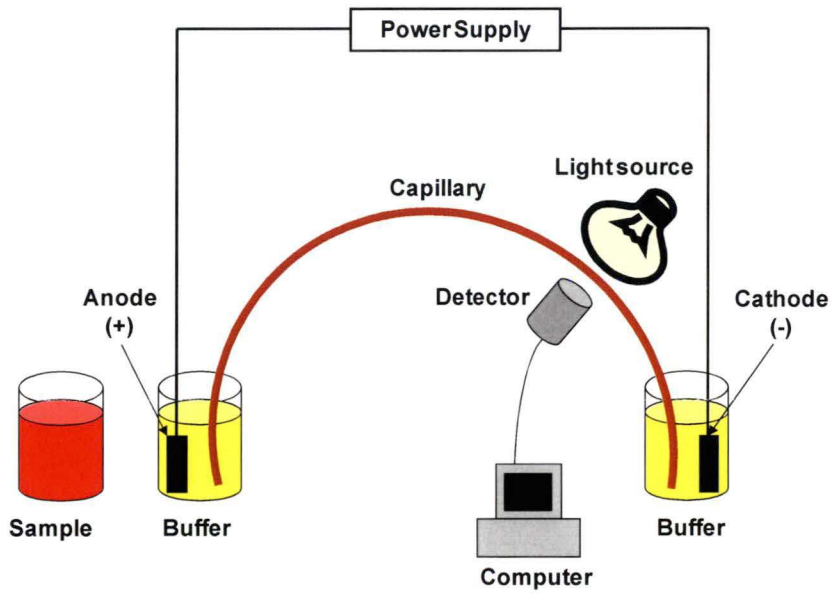

Figure 1.1. Capillary electrophoresis (CE) set up demonstrating buffer vials, sample vials, capillary, light source, detector, computer, power supply, anode and cathode.

1.2.1 Electro-osmotic flow and modes of separation

Electro-osmotic flow (EOF) is the movement of liquid, generated as a result of potential applied throughout a microchannel or a capillary. This phenomenon has been known for 200 years and these days is heavily applied in CE to separate various biomolecules. The early signs of EOF were reported by Reuss in 1809, who demonstrated that water can move through clay by inducing applied potential, reporting the findings in the Proceedings of the Imperial Society of Naturalists of Moscow [20]. The underlying cause of EOF is rationalised by formation of an electric double layer at the wall of the capillary. Typical capillaries in CE are composed of silica which contains silanol functionalities throughout the surface of the capillary column. Introduction of high pH buffer deprotonates the silanol groups resulting in a negatively charged surface, which ultimately attracts the cations in solution allowing electric double layer formation. This double layer is the result of a fixed layer where the cations are immobile and a diffuse layer where the cations are free to move towards the cathode. High solvation of these cations drags the bulk solution in the direction of the cathode which consequently generates EOF as shown in Figure 1.2. [19].

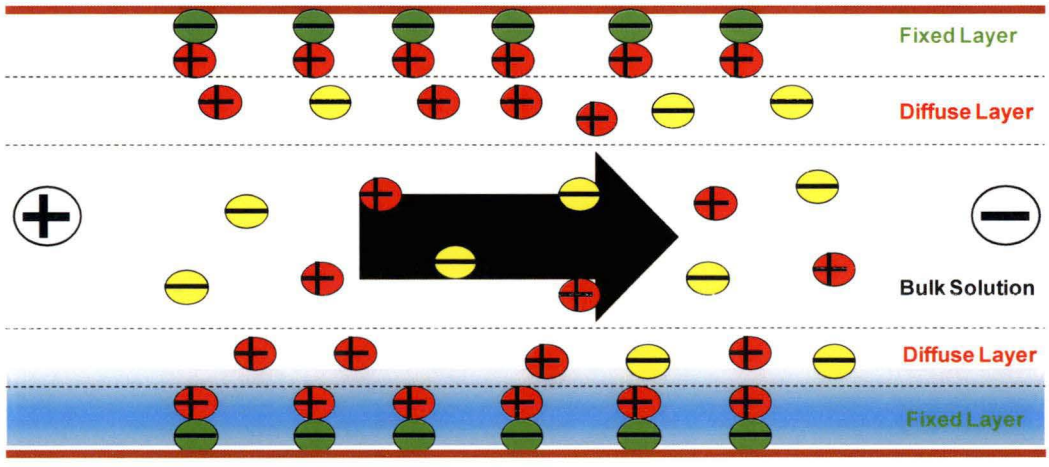

Figure 1.2. Diagram describing the concept of electro-osmotic flow (EOF).

Chapter 1.3 has been removed for copyright or proprietary reasons.

It has been published as: Breadmore, M. C., Hilder, E. F., Kazarian, A. A. Fluorophores and chromophores for the separation of carbohydrates by capillary electrophoresis, in, Volpi, N., (editor), Capillary electrophoresis of carbohydrates: from monosaccharides to complex polysaccharides, 2011, Humana Press, 978-1-60761-874-4

1.4.2 Common trends (buffer, sample composition and pH)

The preconcentration concept of dynamic pH junction has been known for approximately 20 years covering a wide range of analytes, buffer systems, sample matrixes, pH media and various mechanistic designs for stacking. A broad spectrum of the dynamic pH junction systems involving various analytes and their applications has been published, nevertheless it is clear that some common trends can be summarised to produce a universally accepted model with its generic conditions. Table 1.2 covers mostly application based literature related to dynamic pH junction from the 1990 and until Jan 2010, with the emphasis on understanding the basic conditions required for dynamic pH junction. It is also worth mentioning that a large portion of the literature does not exclusively incorporate dynamic pH junction but rather employs a combination of stacking techniques to achieve the best sensitivity improvement. Some of these hyphenated preconcentration techniques are dynamic pH junction-sweeping [94-100], full-capillary sample stacking/sweeping MEKC [101], ITP/dynamic pH junction [102], pH-mediated sample stacking/dynamic pH junction [103], acid barrage [104-105], field amplified migration/pH mediated

stacking/sweeping [106], thermal dynamic junctions [107-108], large volume sample stacking (LVSS) and dynamic pH junction [109-110], LVSS/reversed pH junction [111] and many more. To ensure a descriptive comparison of the literature is made an extensive list of condition variables is included in the table such as: analyte properties, pK_a or isoelectric point (p*I*), and the sample and BGE conditions, such as their respective pH values, components and concentrations, and the LODs and enhancement factors achieved are also provided. Careful examination of Table 1.2 focusing specifically on BGE application in dynamic pH junction systems reveals that nearly half of the summarised references employ borate as their BGE allowing analysis of a very extensive spectrum of analytes including alkaloids, hormones, catecholamines, phenols, flavins, metabolites, amines, nucleotides , deoxyribonucleic acid (DNA) markers, amino acids, proteins, cationic compounds, carbohydrates, isoflavones, peptides and carboxylic acids. Undoubtedly borate demonstrates frequent use and superior performance over other background electrolytes (BGEs) and appears to be the preferred option used by the research groups around the globe. Some of the reasons responsible for that are most likely attributed to the favourable pK_a of borate (9.14) [112] with its useful working range of 8.1-10.1 [113] providing a large degree of ionisation for many carboxyl functions found in many biomolecules, while a low pH sample matrix can offer extensive degree of ionisation for amine functionalities primarily found in amines, amino acids and proteins, providing a change in electrophoretic mobility and securing a perfect foundation for dynamic pH junction. Borate also induces complexation with vicinal diols, introducing additional charge which gives it further flexibility in regard to manipulation of electrophoretic mobility in CE. Further insight into borate buffers reveals its ability to maintain relatively low currents while operating at high ionic

strength, and concentrations ranging from 20 mM to 1,500 mM are reported in Table 1.2, with a typical concentration of 140-160 mM [114]. Other BGEs also include phosphate, nevertheless this buffer is highly conductive and should only be used at relatively low concentrations to eliminate Joule heating effects. A typical range reported for this type of electrolyte according to Table 1.2 is 30-50 mM with a maximum reported concentration of 80 mM. Of some benefit may be the fact that this buffer can be used at both low and high pH, with a working range of 1.1-3.1 and 6.2-8.2 which offers some flexibility depending on the application and the analyte of interest. The literature suggests that this type of buffer is also applied to a wide variety of compounds namely proteins, amino acids, amines, carboxylic acids, arsenic compounds and antifolate drugs. Further overview of the buffer preference in dynamic pH junction can be gained from the work of Cao and colleagues who conducted much research using formate buffers to generate a dynamic pH junction, which they call a moving chemical reaction boundary (MCRB) [115-120]. Various other groups employed ammonium buffers to analyse proteins with a particular emphasis on myoglobin, while acetate buffers were infrequently utilised to analyse cationic analytes, proteins, amino acids and hormones. Unlike borate and phosphate, these buffers offer compatibility with MS detection.

The next point of imperative significance in relation to dynamic pH junction is the relation between the sample matrix and electrolyte composition and their respective pH values which inevitably governs the formation of a pH boundary. Analysis of Table 1.2 unravels a large variety of sample/BGE combinations where phosphate/borate, phosphate/phosphate, acetate/borate, borate/borate, ammonium/formate, acetate/acetate, acetate/ammonia, formate/formate, acetate/phosphate with various other combinations are observed. It is clearly evident

from the table that the phosphate/borate, sample/BGE arrangement is the most prevalent option utilised in dynamic pH junction. A typical phosphate sample matrix is at acidic pH of 4.0-6.5 where as the BGE is at pH 8.2-10.0 which is consistent with the previously discussed working ranges for the both phosphate and borate buffers. Other less popular combinations such as acetate/borate and acetate/ammonia follow similar trends reporting acidic pH for the sample matrix and alkaline for the BGE, meanwhile formate/formate, ammonium/formate, borate/phosphate convey reversed pH conditions for the sample and the BGE. Overall the literature advocates that the sample matrix with acidic pH and the BGE with basic pH is the most frequently used model, although it is vital to recognise that these conditions are heavily dependent on the set of analytes and their pK_a values employed in the study. This brings about the necessity to discuss the pK_a values in relation to buffer and sample matrix pH values. To make the discussion comprehensible it is necessary to consider a general example from the literature such as the protein/amino acid model where the analytes are stacked on the basis of their p*I* values. A study by Monton *et al.* [92] explicitly examined dynamic pH junction of peptides with marginally different p*I* values between 4.7-12.0. The sample and buffer pHs were set at 4.0 and 11.0, respectively, providing a large range over which the analytes charge is altered from positive to negative. The results conclude that the peptides with p*I* values of 6.9 and 6.7 undergo ionisation changes over 4-5 pH units which means the p*I* values are approximately 2-2.5 units away from the pH values of the sample or the BGE. This in turn governs the cation to anion transition which abruptly alters the direction of the analyte's travel. Further observations of the study state that bigger changes in electrophoretic mobility lead to the prospect of better focusing. It is also worth noting that it is not just the directional changes in electrophoretic mobilities such as the case for amino acids and

proteins that induce stacking, but also a change in electrophoretic mobility in the same direction from a neutral to a charged state that would encourage stacking for typical weak acids and bases. From this the general trend suggests that amino acids and proteins would undergo a higher degree of stacking due these abrupt directional mobility changes while weak acids and bases would be stacked to a lesser extent.

Using the basis of this model in conjunction with the current trends observed in Table 1.2, for most of the analytes it is apparent that sufficient changes in electrophoretic mobilities and successful focusing is achieved when the pK_a values of analytes differ by at least 2 pH units from the sample matrix and/or BGE. Nevertheless it is vital to realise that this statement is very generic for most analytes, and should therefore serve as a flexible guideline for designing a system based on dynamic pH junction.

To conclude the current section of the literature review, it is clear that many studies do not solely rely on dynamic pH junction to preconcentrate analytes, but rather incorporate hyphenated preconcentration techniques, depending on the set of analytes and their properties. Combinations of preconcentration methods are ultimately directed at achieving impressive sensitivity enhancements. Currently borate is the preferred option as the BGE for stacking of various analytes in dynamic pH junction while the pK_a values of the analytes must be carefully adapted to the pHs of the sample, and the BGE to induce adequate stacking.

Table 1.2. Summary of dynamic pH junction related research encompassing analyte, pK_a and p*I* values, sample matrix and background electrolyte (BGE) conditions, limit of detection (LOD), enhancement factor (EF) and references (Ref).

Analyte	pK_a	p*I*	Sample matrix	BGE	LOD (nM)	EF	Ref
Serkinkine senecionine retrosine seneciphylline	6.7[a] 5.4[a] 5.4[a] 5.4[a]		pH 4.0, 10 mM phosphate	pH 9.1, 20 mM borate	30	23.8-90	[94]
Oxymatrine matrine	7.7[b] 5.8[b]		pH 10.7, 20 mM formate	pH 2.6, 40 mM formic acid - stacking section pH 4.8, 100 mM formic acid - separation section	0.26 μg mL^{-1} 0.19 μg mL^{-1}	60	[120]
Bradykinin angiotensin I angiotensin II [Sar^1, Ile^8]- angiotensin II myoglobin β-lactoglobulin B[c] β-lactoglobulin A[c] bovine serum albumin		12.0 6.9 6.7 8.8 7.2 5.2[121] 5.2[121] 4.7[122]	pH 4.0, 1,000 mM acetate	pH 11.0, 200 mM borate	NS	113 124 65 67 43	[92]

[a] Acid
[b] Base
[c] Just β-lactoglobulin

Angiotensin I [Sar[1], Ile[8]]-angiotensin II bradykinin β-lactoglobulin A Glu-Val-Phe (EVF) cytochrome C ribonuclease B (1) m/z 585.1 (2) m/z 634.5 (3) m/z 678.4 (4) m/z 779.5 (5) m/z 964.6 (6) m/z 736.2		see[92] see[92] see[92] see[121] 9.3[123] 8.9[124] 9.4 8.6 8.6 8.5 4.4 5.5	pH 8.0, 50 mM ammonium bicarbonate	pH 2.0, 1,000 mM formate	NS	 691 600 546 896 1,029 1,028	[93]
Peptides			pH > 10 ammonia	pH 2.5, 10 mM citrate	5-20 ng μL^{-1}	5	[90]
rRGD-hirudin		4.1	pH 6.0, 25 mM ammonium formate	pH 2.4, 25 mM formic acid	≈11[d]	100	[125]
Trimethoprim sulfamethoxazole	7.2[e,b] 1.4[b,e]; 5.8[b,e]		50 mM HCl	pH 8.5, 30 mM phosphate	0.31 μg mL^{-1} 0.70 μg mL^{-1}	4.5 4.7	[126]
m-anisidine *p*-bromoaniline aniline	4.2[b] 3.9[b] 4.6[b]		pH 2.0, 100 mM phosphate	pH 4.5, 250 mM acetate, 2 mM CTAC[f]	1.9 3.7 3.1	160 140 100	[127]
Tetstosterone corticosterone prednisone	 12.4[a,e]		pH 8.0, 160 mM borate	pH 11.0, 160 mM borate	NS	100	[95]

[d] Limits of detection estimated from limits of quantitation of 35 nM
[e] pKa values calculated using ACD Labs 7.0 / pKa dB
[f] Cetyltrimethylammonium chloride

hydrocortisone β-estradiol estriol	12.5[a,e] 10.4[a] 10.4[a]						
Epinephrine norepinephrine dopamine DOPA[g] tyrosine catechol phenol	9.2[b,e]; 9.6[a,e] 8.4[b,e]; 9.6[a,e] 9.4[a,e]; 10.1[b,e] 9.3[b,e]; 9.9[a,e] 9.4[b,e]; 10.0[a,e] 9.5[a,e] 10.1[a,e]		pH 8.5, 160 mM borate, 3 mM sodium metabisulfite 1 mM EDTA[h], 155 mM NaCl	pH 10.7, 160 mM borate, 150 mM NaCl, 1 mM EDTA	40	250	[128]
Epinephrine	See pK_a section[128]		30 mM para-hydroxy benzoic acid, 220 mM glucose	pH 10.2, 160 mM borate 1 mM EDTA	500	NS	[129]
			pH 3-3.5, 1 mM EDTA 3.0 mM sodium metabisulfite 155 mM sodium chloride	pH 10.1, 160 mM borate, 1 mM EDTA	500	NS	[91]
p-cresol m-nitrophenol 2,4-dinitrophenol 2,4,6-trinitrophenol	10.3[a] 8.3[a] 4.1[a] 0.4[a]		pH 4.5, 450 mM acetate	pH 10.0, 160 mM borate	NS	60-450	[130]
Myoglobin		7.2[123]	pH 4.75, acetate pH 3.75, formate pH 6.0, citrate pH 4.75, acetate	pH 9.25, ammonium pH 9.25, ammonium pH 8.0, tris pH 8.0, tris	NS	2,000	[131]

[g] D/L-3,4-dihydroxyphenylalanine
[h] Ethylenediaminetetraacetic acid

		see[123]	pH 4.75, 20 mM , acetate	pH 9.25, 20 mM acetate	NS	NS	[132]
Myoglobin bovine serum albumin trypsin		see[123] see[122] 10.0	pH 4.25, 10 mM acetate	pH 9.75, 10 mM ammonium	NS	NS	[122]
Myoglobin bovine serum albumin β-lactoglobulin		see[123] see[122] see[121]	pH 4.25, 10 mM acetate	pH 9.75, 10 mM ammonium	NS	100	[133]
Myoglobin insulin		see[123] 5.3[134]	pH 4.20, 5 mM phosphate	pH 9.20, 20 mM phosphate	NS	1,500	[135]
Myoglobin asparagine		see[123] 5.4[136]	pH 7.8, water pH 7.5, water	pH 8.8, 50 mM tris	NS	3,000 7,000	[137]
Myoglobin amyloglucosidase cytochrome C carbonic anhydrase I		see[123] 3.6 see[124] 6.6	pH 4.75, 10 mM AcOH	pH 9.25, 10 mM ammonium	NS	1,700	[123]
Lysozyme myoglobin carbonic anhydrase α-lactalbumin ribonuclease A[i] trypsinogen β-lactoglobulin ovalbumin β-casein		9.3[124] see[123] 6.2 4.3[138] see[124] 4.3 see[121] 4.7[124] 5.1[139]	pH 2.8, 200 mM propanoic acid	pH 3.8, 200 mM propanoate	1.9 3.2 11.3 6.5	76 107 89 47	[140]

[1] Ribonuclease B is being reported

Riboflavin (RF)	10.2		pH 6.0, 75 mM phosphate	pH 8.5, 140 mM tetraborate	3-7	NS	[141]
			pH 5.9, 80 mM phosphate	pH 8.2, 100 mM tetraborate	1	NS	[96]
RF flavin mononucleotide (FMN) flavin adenine dinucleotide (FAD)	see[141] 1.8[a,e]; 4.4[b,e]; 6.3[a,e] 1.1[a,e]; 1.3[b,e]; 1.5[a,e], 3.4[b,e]; 6.7[b]		pH 6.0, 75 mM phosphate	pH 10.0, 140 mM borate, 100 mM SDS[J]	0.004	1,200	[97]
			pH 6.0, 75 mM phosphate	pH 8.5,140 mM borate, 100 mM SDS, 5mM β-cyclodextrin	0.004	60	[98]
RF FMN FAD NAD^{+}[k] acetyl coenzyme A (AcCoA) $NADP^{+}$[l] coenzyme A (CoA) ADP ATP prednisone hydrocortisone estriol cortisol testosterone estradiol	see[141] see pK_a section[97-98] see pK_a section[97-98] 3.9[142] 4.0; 6.3[143] 4.0; 6.5[143] see pK_a section[95] see pK_a section[95] see pKa section[95] see pK_a section[95]		pH 6.0, 75 mM phosphate	pH 10.0, 140 mM borate, pH 8.5, 140 mM borate, 100 mM SDS.	0.004	1,200	[99]

[J] Sodium dodecyl sulfate
[k] Oxidised form of nicotinamide adenine dinucleotide
[l] Oxidised form of nicotinamide adenine dinucleotide phosphate

RF catechol quinol	see[141] 9.9[a,e] 6.7[a]; 9.2[b][144]		pH 4.0, 20 mM phosphate	pH 10.0, 20 mM sodium tetraborate	2.7	42	[145]
Thiamine hydrochloride RF pyridoxal hydrochloride pyridoxine hydrochloride D-biotin ascorbic acid calcium pantothenate nicotinic acid folic acid	4.8[b]; 9.0[b][146] see[141] 3.3[b,e]; 8.1[a,e] 5.1[b,e]; 8.4[a,e] 4.5[a][147] 4.2[a][148] 4.5[a][149] 2.2[a][150] 2.3[a]; 8.3[a][151]		pH 6.0, 75 mM phosphate	pH 8.5, 160 mM borate	95 66 172 44 291 534 249 49 27	NS	[152]
Phenylalanine tryptophan		5.9[153] 5.5[153]	pH 8.34, 80 mM sodium chloride, 33.8/66 mM formate	pH 2.85, 32.8 mM formic acid	NS	NS	[115]
			pH 8.34, 80 mM NaCl 66 mM formate	pH 2.85, 32.8 mM formic acid	NS	200	[116]
Tryptophan		see[153]	pH 8.3-8.4, formate	pH 2.85, 30 mM formate	NS	NS	[117]
			pH 8.1, 8.2-82.5 M sodium formate, NaCl, tryptophan	pH 2.85, 32.8 M formic acid	4.23 ng mL^{-1}	NS	[118]
L-Histidine L-trytophan		7.6[153] see[153]	pH 7.88-8.27, 10-60 mM format	pH 3.0, 30 mM formic acid NaOH, CTAB[m]	NS	NS	[119]

[m] Cetyltrimethylammonium bromide

Isoleucine tryptophan		6.0[153] see[153]	pH 4.6, 0.4 mM sodium dihydrogen phosphate, 0.06 mM phosphoric acid	pH 2.0, 30 mM phosphoric acid	1.4 1.1	400	[101]
Dopamine DOPA 5-hydroxyindole-3-acetic acid 5-hydroxytryptamine 3-indoxyl sulfate L-tryptophan D/L-vanillomandelic acid epinephrine tryptamine	see pK_a section[128] see pK_a section[128] 9.7[a,e]; 10.31[a,e] see[153] 3.4[a,e]; 10.2[a,e] see pK_a section[128] 10.6[b,e]		pH 3.1, 10 mM citric acid 89% ACN[n] in H_2O	pH 10.0, 1,500 mM borate	0.6 17.6 0.31 0.19 0.27 0.27 19.8 0.3 0.017	 800 400 14,000 5,200	[154]
Guanosine uridine	9.4[b] 9.7[b]		pH 9.7, 160 mM borate	pH 7.0, 160 mM borate 150 mM NaCl	40 40	50	[155]
Glycine alanine serine proline valine threonine cysteine leucine isoleucine asparagine glutamine lysine glutamic acid methionine		6.0[153] 6.0[153] 5.7[153] 6.3[153] 6.0[153] 5.6[153] 5.1[153] 6.0[153] see[153] 5.4[153] 5.7[153] 9.7[153] 3.2[153] 5.7[153]	pH 7.0, 200 mM ammonium acetate	pH 1.8, 1,000 mM formic acid	 1 25	50	[156]

[n] Acetonitrile

phenylalanine		see[153]					
arginine		10.8[153]					
tyrosine		5.7[153]					
tryptophan		see[153]					
γ-aminobutyric acid (GABA)	4.2[156]						
tyramine	9.7[b][156]						
adenosine	3.2[b][156]						
guanosine	2.2[b][156]						
Cytosine	4.2[b,e]		pH 6.0, 75 mM sodium phosphate	pH 9.4, 160 mM borate	0.2-30 ng mL^{-1}	NS	[100]
uracil	9.2[b,e]						
cortisone	12.4[a,e]						
adenine	4.2[b]; 9.9[b][157]						
guanine	9.4[b][158]						
hypoxanthine	2.0[b]; 8.9[b][157]						
uric acid	5.5[b]; 10.3[b][159]						
xanthine	7.4[b];12.4[b][157]						
uridine	see[155]						
thymine	9.9[b][158]						
inosine	9.0[b][157]						
adenosine	see[156]						
guanosine	see[156]						
theobromine	10.0[b][160]						
theophylline	8.8[b][160]						
caffeine	14.0[b][160]						
ADP	see[143]						
ATP	see[143]						
guanosine diphosphate (GDP)	2.9[b]; 9.6[b]; < 2[a]; 7.2[a] [161]						
guanosine triphosphate (GTP)	3.3[b]; 9.3[b], <2[a]; 7.7[a] [161]						
inosine triphosphate (ITP)							
uridine diphosphate (UDP)	9.4[b]; < 2[a]; 7.2[a][161]						
uridine triphosphate (UTP)	9.6[b]; < 2[a]; 7.6[a][161]						

NADP[o]							
cytidine (C)	4.1[b][143]						
cytidine monophosphate (CMP)	4.5[b]; < 2[a]; 6.6[a][161]						
uridine monophosphate (UMP)	9.5[b]; < 2[a]; 6.6[a][161]						
inosine monophosphate (5'IMP)	8.9[b]; 1.5[a]; 6.0[a][162]						
adenosine monophosphate (AMP)	3.9[b]; < 2[a]; 6.4[a][161]						
guanosine monophosphate(GMP)	2,4[b]; 9.4[b]; < 2[a]; 6.7[a] [161]						
NAD[p]	see[142]						
nicotinic acid	see[150]						
protocatechuic acid	4.4[a][163]						
3,4-dihydroxyphenylacetic acid	4.4[a,e]; 9.8[a,e]						
phenylpyruvic acid	2.61[a,e]						
4-hydroxybenzoic acid	4.6[a][163]						
4-hydroxyphenylacetic acid	4.4[a]; 9.1[a][164]						
anthranilic acid	2.1[a][165]						
4-hydroxyphenylpyrivic acid	2.5[a,e]; 9.9[a,e]						
benzoic acid	4.2[a][166]						
trans-cinnamic acid	4.57[a][167]						
FAD	see pK_a section[97-98]						
FMN	see pK_a section[97-98]						
RF	see [141]						
5-methyl THF[q]	see[151]						
folic acid	see pK_a section[95]						
estriol	see pK_a section[95]						
hydrocortisone							
4-androstene-3,17-dione							
estrone							
17-β-estradiol							

[o] Nicotinamide adenine dinucleotide phosphate

[p] Nicotinamide adenine dinucleotide

[q] 5-Methyl-5,6,7,8-tetrahydrofolate disodium salt

testosterone 17-α-hydroxyprogesterone progesterone							
4-Nitrophenol 4-aminobenzoic acid sulfanilic acid fluorescein 2,7-dichlorofluorescein AMP CMP ADP GMP UMP	7.2[a][168] 4.9[a][169] 3.1[169] 4.5[a]; 6.8[a][170] 4.0[a]; 5.2[a][170] see[161] see[161] see[143] see[161] see[161]5		200 mM NaCl	pH 9.0, 20 mM triethyamine/ TAPS[r]	NS	521 511 481 282 1,187 512 624 548 484 698	[102]
8-hydroxy-2′-de oxyguanosine (8OHdG)	8.0[b][171]		pH 6.5, 30 mM phosphate	pH 9.1, 30 mM borate	20	NS	[172]
			pH 6.5, 30 mM phosphate	pH 9.1, 30 mM borate	4.3	NS	[173]
8OHdG 2'-deoxyguanosine thymidine hydroxybenzoic acid glutathione disulfide naproxen, corticosterone	see[171] 9.2[174] 9.8[174] see[163] 3.5[103] 4.9[a][174]		Sample followed by pH 10.7 NaOH, methylamine, 0.5 mM TTAB[s],	pH 6.0, 100 mM imidazole, 0.5 mM TTAB	NS	24	[103]
Deoxyadenosine adenine guanine theobromine	3.4[b,e] see[157] see[158] see[160]		pH 6.0, 20 mM phosphate	pH 9.5, 70 mM borate	80	50	[175]

[r] *N*-Tris(hyroxymethyl)methyl-3-aminopropanesulfonic acid

[s] Tetradecyltrimethylammonium bromide

allopurinol hypoxanthine xanthine	2.7[b,e]; 9.2[b,e] see[157] see[157]						
Xanthine caffeine adenine guanine theophylline hypoxanthine uric acid	see[157] see[160] see[157] see[158] see[160] see[157] see[159]		pH 6.0, 75 mM phosphate	pH 9.5, 160 mM borate	<40	50	[176]
FMOC-leucine FMOC-alanine FMOC-glutamic acid FMOC-aspartic acid			pH 9.4, 5.5 mM KCl 2.3 mM $CaCl_2$, 107 mM borate, (acid barrage – pH 2.4, 100 mM tartaric acid)	pH 10.5, 60 mM borate	NS	1,000	[104]
Arginine histidine β-alanine	see[153] see[153] 10.4[177]		pH 4.0, 13 mM acetate	pH 11.0, 13 mM acetate	0.75	100	[178]
ortho-phthalaldehyde (OPA) N-acetyl-L-cysteine (NAC) NAD^+ taurine L-alanine dehydrogenase L-lysine oxidase D/L-serine D/L-alanine D/L-glutamic acid D/L-aspartic acid	 see[142] 9.1[179]	 see[153] see[153] see[153] see[153]	pH 6.0, 40 mM phosphate	pH 9.5, 140 mM tetraborate	 0.4 0.4 0.6 0.6	40	[180]

NDA[t] cyanobenz[*f*]isoindole D/L CBI-tyrosine D/L CBI-threonine D/L CBI-asparagine D/L CBI-phenylalanine D/L CBI-histidine D/L CBI-glutamic acid D/L CBI-methionine D/L CBI-alanine D/L CBI-arginine D/L CBI-aspartic acid D/L CBI-isoleucine D/L CBI-serine D/L CBI-tryptophan D/L CBI-glutamine D/L CBI-valine D/L CBI-leucine D/L CBI-lysine			pH 6.0 in water	pH 2.0, 25 mM phosphate, 2% wt sulfated sodium deoxycholate (S-β-CD)	0.3	100	[106]
Amino acids			Plug of NH_4OH, 12.5% followed by sample plug in formic acid	2,000 mM formic acid, 20% MeOH	50	NS	[181]
NDA serine fluorescamine aspartic acid glutamic acid		 see[153] see[153] see[153] see[153]	0.5-1 mM tris or 0.5-1 mM phosphate	pH 7.0, 50 mM tris or pH 7.0, 30 mM phosphate stacking occurs as a result of cooling and heating producing pH boundary between 8.4 and 6.4	NS	2	[107]
NDA Lysine, serine	8.8 at 25 C°[108]		pH 7.1, in ethanolamine	pH 8.7, 20 mM borate	NS	NS	[108]

[t] Naphthalene-2,3-dicarboxaldehyde

Phosphoserine phosphothreonine phosphotyrosine	1.7[a,e]; 2.0[a,e]; 6.3[a,e] 1.7[a,e]; 6.2[a,e]; 6.8[b,e] 1.8[a,e]; 2.2[a,e]; 7.5[a,e]		pH 6.5, 40 mM phosphate	pH 9.6, 140 mM borate	130 100 60	200	[182]
Serotonin (derivatised with 3,4-dimethoxybenzylamine)	10.2[b]; 12.0[b]		pH 8.0, 40 mM borate	pH 10.0, 15 mM phosphate 30 mM borate	< 10	NS	[183]
Albumin		see[122]	pH 8.2, 150 mM borate	pH 10.2, 150 mM borate	0.06 μg mL^{-1}	31	[184]
Lentil lectin β-casein trypsin		8.6 see[139]	pH 4.3, acetate	pH 9.8, ammonium	NS	NS	[139]
Benzoic acid sorbic acid	see[166] 4.8[a][166]		pH 9.5, 50 mM sodium borate	pH 2.5, 50 mM phosphate 150 mM SDS	11 10	2,120[u] 1,225[u]	[109]
			pH 2.5, 50 mM phosphate	pH 9.5, 50 mM phosphate	5 7.2	4,600	[110]
Sinapic acid ferulic acid coumarinic acid caffeic acid syringic acid vanillic acid 4-hydroxybenzoic acid	4.6[a,e]; 10.2[a,e] 4.5[a]; 9.4[a] 4.1[a,e]; 10.2[a,e] 4.4[a]; 8.7[a] 4.3[a,e]; 9.3[a,e] 4.5[a,e]; 9.3[a,e] see[163]		pH 9.5, 50 mM borate	pH 2.5, 50 mM phosphate	2.23 ng mL^{-1} 4.20 ng mL^{-1} 0.71 ng mL^{-1} 2.04 ng mL^{-1} 1.14 ng mL^{-1} 0.62 ng mL^{-1} 0.38 ng mL^{-1}	723 780 4,048 1,627 2,544 3,762 5,565	[185]
Lovastatin	4.3[a,e]		pH 4.9, 20 mM , Glycine, HCl	pH 11.5, 100 mM Glycine, NaOH	8.8 ng mL^{-1}	105-130	[186]

[u] Estimated improvement factor recorded by comparing CZE and LVSS/dynamic pH junction methods.

R/S propranolol hydrochloride R/S metoprolol tartrate nifedipine nitrendipine nimodipine	4.5[b] 4.3[b] 8.8[b] 8.8[b] 8.8[b]		pH 2.8, 25 mM acetate, 20% acetonitrile	pH 9.0, 50 mM tetraborate, 30 mM SDS 20% acetonitrile	0.08 μg L^{-1} 0.1 μg L^{-1} 0.05 μg L^{-1} 0.05 μg L^{-1} 0.03 μg L^{-1}	14,000-35,000	[187]
Muramic acid diaminopimelic acid	3.4[a,e]; 8.4[b,e] 2.2[a,e]; 2.8[a,e]; 9.4[b,e]; 10.1[b,e]		pH 6.5, 40 mM, phosphate	pH 9.5, 140 mM borate	2,000 μM 200 μM	100	[188]
Glucose lactose maltose 5-aminofluorescein	4.6[a,e]; 9.4[a,e]		pH 2.4, 95 mM formate	pH 9.2, 100 mM borate	85 42 85	515	[v]
Galactose, allose, arabinose, mannose, glucose, xylose, rhamnose, lactose, maltose O-2-[aminoethyl]fluorescein	3.6[a,e]		pH 4.2, sample diluted in water	pH 8.6, 170 mM borate	0.13	10	[w]
Arsenite arsenate monomethylarsonic acid dimethylarsinic acid roxarsone phenylarsonic acid	9.2[a]; 12.1[a] 2.3[a]; 6.7[a]; 11.6[a] 4.6[a]; 7.8[a] 6.2[a] 3.5[a] 3.6[a]; 8.8[a]		pH 3.5, 15 mM acetic acid	pH 10, 15 mM phosphate	1.29 1.33 1.93 1.13 0.44 0.34	100-800	[189]
Barbital phenobarbital secobarbital	7.5[b] 7.6[b] 7.8[b]		pH 5.5, 60 mM glycine HCl	pH 11.0, 10 mM glycine NaOH	0.26μg mL^{-1} 0.27 μg mL^{-1}	20.5 22.6	[190]

[v] Chapter 3 describes the use of 5-aminofluorescein
[w] Chapter 5 describes the use of O-2-[aminoethyl]fluorescein

Weak bases	3.0[a] 4.5[a] 6.0[a] 7.5[a]		pH 8.60, 65.6 mM formate 50 mM NaCl	pH 2.85, 65.6 mM formic acid NaOH	NS	NS	[191]
Methotrexate hyoxymethotrexate 2,4-diaminoN[10]-methylpteroic acid MTX-polyglutamate	3.5[a,e]; 4.8[a,e]; 5.1[b,e] 4.6[a,e] 5.1[a,e] 3.5[a,e]; 4.8[a,e]; 5.5[a,e]		0.01 M NaOH	pH 2.5, 80 mM phosphate, SDS, 1.5 mL THF[x]	100-500	NS	[192]
EPO-β glycoforms (hormone)			pH 8.23, 1 mM phosphate	pH 5.50, 10 mM acetate 7 M urea, 10 mM tricine 2.5 mM putrescine, 0.15 NaCl	50-100	NS	[111]
(-)-Epicatechin gallate (-)-gallocatechin gallate (-)-epigallocatechin	8.4[a][193] > 8.0[194] > 8.0[194]		pH 9.5, 200 mM boric acid, 1 mM sodium dihydrogen phosphate, 6 mM sodium metabisulfate	pH 2.0, 50 mM phosphate, 100 mM sodium chloride	1.4 3.8 17.5	1,850	[195]
Genistein	7.2[a]; 10.1[a][196]		pH 9.2, 20 mM borax, acid barrage: pH 1.7, 200 mM citric acid	pH 10.5, 20 mM borax	0.03 mg L^{-1}	> 50	[105]

[x] Tetrahydrofuran

1.4.3 Optimum sensitivity enhancement and LODs

Another issue of imperative significance in the current chapter is the sensitivity enhancement and the LODs offered by preconcentration methods based on dynamic pH junction. Over the years various groups around the world have been striving to push the sensitivity limits allowing three orders of magnitude enhancement factors using dynamic pH junction. Meanwhile combinations of other stacking techniques in conjunction with dynamic pH junction recently provided impressive improvements in the range of 10,000 and above. This section of the review will describe in more detail the systems employed to attain the best sensitivity enhancements and most impressive LODs obtained up to this day by dynamic pH junction. To set a benchmark for this particular topic one should consider the previously discussed work of Aebersold and Morrison who in 1990 established improvements in sensitivity of up to 5-10 times.

In 2002-2003 Britz-McKibbin *et al.* [97-99] published a number of studies relating to assessment of flavins in biological samples using a combination of pH junction and sweeping. The earliest of these studies published in *Analytical Chemistry* claimed that this was the first encounter of dynamic pH junction-sweeping [97] mode applied in CE, therefore highlighting the significance of the research. All of the studies shared superior LODs at a 4.0 pM mark as well as reporting excellent enhancements in sensitivity of up to 1,200-fold when compared against conventional CE injection modes. One of these reports led by Britz-Mckibbin and Terabe effectively attempted to conduct a comprehensive metabolome analysis where biological samples were analysed to yield stacking and separation of coenzyme metabolites and steroids [99]. The proposed benefits of dynamic pH

junction/sweeping can be understood when considering mixtures of hydrophilic and hydrophobic analytes thus permitting analyses of a large diversity of compounds.

In 2005-2006 a few reports were published by Nesbitt *et al.*, [123] Li *et al.*, [137] and Jurcic *et al.*, [131] where the main focus was directed at focusing myoglobin and other analytes. Nesbitt and colleagues managed to obtain impressive 1,700 enhancement in the sensitivity while the group by Jurcic *et al.* obtained 2,000-fold preconcentration factors. The latter study employed an intricate method design through the use of pH indicators which assisted understanding of the preconcentration performance, making this a very unique system. More specifically absorption profiles of bromothymol blue made it possible to predict and assess the performance of focusing and buffer selection and provide insights regarding the mechanism of protein stacking by observing pH junctions throughout the duration of the run [131]. The previously stated work by Li *et al.* [137] enabled impressive stacking *via* the use of microextraction through sol-gel coatings and dynamic pH junction producing outstanding preconcentration factors of 3,000 and 7,000 for myoglobin and asparagine respectively. The authors recommend that this technique may find applications in trace analysis.

Year 2005 also registered another impressive application where biologically active amines and acids were subjected to stacking, by pH junction, changes in viscosity and field amplification. This in turn produced LODs of 17 pM to 0.3 nM and remarkable sensitivity enhancements of 5,200 to 14,000-fold for tryptamine and epinephrine respectively [154]. The merit of the work is also realised by successful analysis of urine samples as well as future capability to examine blood and cerebrospinal fluids.

The onset of 2007 introduced a study by Imami *et al.* [93] who made a valuable contribution to the field by analysing a number of peptides using a simple formic acid/ammonium formate system. The simplicity of the design enabled evaluation of the effects of the sample matrix on the focusing mechanism. The biggest advance of the system was the ability to analyse and focus numerous peptides simultaneously with a broad range of p*I*s. Experimental data suggested that very slight changes in the analyte mobility allowed high degree of focusing, not something previously considered credible by the same group. Under optimal conditions injection volumes in the order of 30% of the capillary volume were used resulting in a 550-1,000-fold improvement in sensitivity with the optimum method applied to the analysis of a tryptic digest of cytochrome c.

Horakova *et al.* [110] conducted a study exploring preconcentration of acids using electrokinetic accumulation. This system involved formation of a pH boundary *via* LVSS using electrokinetic injection followed by a sweeping step to mobilise the analytes. The authors made some interesting observations revealing that SDS does not induce any focusing of analytes but merely carries them to the detection site. The presence of a moving pH boundary was confirmed using a computer program (Simul), which assisted to obtain 5 nM LODs for benzoic acid. Furthermore a 2 h electrokinetic injection resulted in a 4,600 preconcentration when compared to a typical CZE method. The same team of authors researched another very similar dual strategy by the means of LVSS and dynamic pH junction to preconcentrate previously described acids [109]. This time the preferred injection was hydrodynamic which resulted in LODs at 10 nM and11 nM levels for benzoic and sorbic acids respectively, which is slightly higher than for the electrokinetic injection discussed in the previous study. Nevertheless the sensitivity enhancements were still

rather impressive recording the range of 1,225-2,120 when compared to routine CZE methods. The significance of the current method is further supported by its application to real samples such as food analysis.

At last some of the more recent literature published by Xu *et al.*, [135] Petr *et al.*, [185] and Zhang *et al.* [187] in 2008-2009 offers a variety of preconcentration strategies based on dynamic pH junction with: tentacle-type polymer coatings, accumulation/mobilisation and ITP-CZE/MEKC. Some of these methods show a very minor contribution of dynamic pH junction to the overall preconcentration effect in the study, nevertheless these reports are of principal importance realising the necessity of using combinatorial preconcentration methods.

Xu and colleagues described a new polymer coating with a tentacle-type architecture which assists extraction of proteins based on electrostatic interactions, followed by desorption and focusing on a dynamic pH junction. In particular myoglobin was preconcentrated allowing 1,500 times sensitivity enhancement in relation to a standard CZE approach. Further results indicated that the presence of the novel coating improved protein capture by 30 times producing a clear benefit for the established method.

Petr *et al.* investigated phenolic acids through a concept of electrokinetic accumulation/mobilisation which was ultimately based on a model of dynamic pH junction [185]. The basis of this method was taken from the previously described work of Horakova *et al.*, [110] where the analytes are introduced electrokinetically, accumulated using dynamic pH junction and mobilised by the means of sweeping. The remarkable outcomes reveal very impressive sensitivity enhancement in the order of 720-5,560 times.

Finally the work of Zhang and colleagues in 2009 was based on the separation of cationic compounds using a 2-dimensional (2-D) system where the first dimension employed ITP-CZE while the second utilised MEKC by way of cyclodextrins incorporation [187]. Formation of a pH junction was only a small part of the study which was established between the two dimensions as a result of a low pH CZE buffer and a high pH MEKC buffer. The outcomes of the study produced unbelievable improvement factors of 14,000-35,000 which to our knowledge is the most extraordinary and the best sensitivity enhancement recorded to this day in the literature associated with dynamic pH junction. From this study it is also evident that the 2-D system offers outstanding resolving power, allowing separations of neutral, ionic compounds and structural isomers simultaneously. The credibility of the method was further scrutinised by analysing real wastewater samples, where the end result demonstrated preconcentration and separation of all target analytes. Recent research involving dynamic pH junction and other preconcentration techniques has undoubtedly illustrated impressive sensitivity enhancements suggesting a great potential for the technique in the years to come.

1.4.4 Latest novel developments in dynamic pH junction

The niche of dynamic pH has generated sufficient interest amongst the scientific community where various reviews by Breadmore *et al.* [197] and Britz-McKibbin *et al.* [198] have captured and discussed many novel developments in dynamic pH junction throughout the existence of this preconcentration methodology. This section considers the previously described reviews and makes a brief chronological extension reporting some of the latest advances related to dynamic pH junction.

In 2008 Nesbitt *et al.* [122] and Yeung *et al.* continued their research based on a very recent publication involving preconcentration of myoglobin on a pH junction

and trypsin introduction to generate in-capillary digestion followed by reconcentration of newly formed peptides and ultimately their separation [123]. The current work is carried out using a very similar in-capillary digestion model apart from using proteins with a wide range of p*I* values [122]. The study was a success underscoring the enhanced degree of digestion and a rapid incubation time of 2 h when evaluated against a typical large-scale procedure performed overnight. The importance of dynamic pH junction is also attributed to its ability to differentiate acidic peptides from basic, allowing selective segregation of the initial peptides from the latter ones, which lead to a decrease in ionisation suppression and improved sensitivity by MALDI-MS. According to the authors of the publication the best aspect of this research is attributed to the analysis of miniscule quantities of analytes as well as elimination of large scale pre-digestion steps. This makes this strategy perfect for recombinant proteins found in minute quantities.

Booker *et al.* [133] initiated a study using previously established buffer systems employed to focus myoglobin as a model protein [122-123, 131]. Herein the authors effectively attempted to combine capillary isoelectric trapping with desalting and separation using CZE mode for three proteins namely myoglobin, bovine serum albumin and β-lactoglobulin. Coupling CE with MALDI-MS verified the presence of preconcentration producing better sensitivity.

An innovative research by Dou and colleagues [145] investigated the use of magnetic nanoparticles (MNPs) and their applications as nanoextraction probes followed by coupling with CE where pH junction served as an interface for coupling. The design of the system relied on boronate functionalities located on MNPs which facilitated a capture/release concept at different pHs, where the sample was in acidic media, while the BGE was in basic media. The outcomes of the study show that the

application of pH junction converted large riboflavin sample volumes into narrow bands increasing the sensitivity 42-fold. The drawbacks of the study were possibly attributed to the off-line extraction of the sample and its gravity injection into a capillary, which suggests lack of control, automation and a limited opportunity to carry out high throughput analyses.

A study by Liu *et al.* [195] explored a somewhat similar concept of preconcentration as the one described by Dou *et al.*, [145] where borate complexation affects the state of *cis*-diol-containing compounds (CDCCs) as analytes. Even though the authors state that this methodology is based on borate complexation assisted field-enhanced sample injection, the system configuration incorporates a high pH sample zone where the analytes are negatively charged through borate complexation while a low pH BGE reduces electrophoretic mobilities as a consequence of dissociation between CDCCs and borate. This in turn suggests that the electrophoretic mobilities of the analytes change as a function of pH assisted by borate complexation/dissociation which indicates involvement of a pH discontinuity. The end result was impressive offering 1,850-fold improvement in the sensitivity when compared against a standard sample injection.

Mandaji *et al.* [107-108] introduced a succession of two research articles with a very exciting sample stacking strategy which relies on dynamic thermal junctions. The idea of this approach relies on significant pH changes as a result of altered temperature conditions. The fundamental theory dictates that some molecules may exhibit high thermal sensitivity (high dpH/dT) resulting in dramatic pH changes over a certain temperature range while others may portray the opposite effect. To differentiate the two studies the first one is based on analytes possessing carboxyl functions and pK_a values which are tolerant to temperature changes and therefore

dpK_a/dT (analytes with carboxylic acid functionality) approaching zero, while the BGE has high dpH/dT and is much more susceptible to hot and cold temperatures, inducing pH junctions [107]. The second study is the exact opposite leaving the BGE pH unchanged due to its low pH/dT whereas the sample remains more responsive to rising and falling temperatures [108]. The stacking in these studies was accomplished using amino acids labelled to naphthalene-2,3-dicarboxaldehyde and fluorescamine in some cases. The first report registered stacking between the acidic and the basic section of the capillary where the temperature difference was 70°C and the peak height was doubled due to dynamic thermal gradients which ultimately translates into pH junction methodology. This was a very impressive study and a great contribution to the field of dynamic pH junction encouraging more flexibility and novelty in the future method design.

At last research conducted by Su *et al.* [125] is considered to finalise the discussion of dynamic pH junction techniques. The method herein aims to investigate a sensitive analysis of rRGH-hirudin using dynamic pH junction as its mode of preconcentration. The utility of dynamic pH junction enables a preconcentration factor of 100 and estimated LODS of approximately 11 nM. The method is further approved due to its straightforward sample dilution prior to CE-MS analysis and its relevance and suitability towards urine samples.

1.4.5 Conclusion and future directions

Preconcentration *via* dynamic pH junction has shown considerable developments in the field over the past few years where novel mechanism designs and impressive sensitivity improvements have been achieved. High diversity and combination of preconcentration approaches is already showing clear improvements with ultra-sensitive methods being developed. In addition hyphenation of instruments as well as

incorporation of 2-D systems already shows undisputed performance in relation to resolution of highly versatile analytes as well as outstanding LODs. Future research has the potential to develop the insights into the mechanistic detail and monitoring of preconcentration and incorporation of larger analyte diversity and sample size for routine analysis. Further push towards rapid high throughput analyses and additional miniaturisation requires new formats such as application of microfluidic devices as will become evident in the years to come.

1.5 Project aims

Collectively the literature review suggests that various chromophores and fluorophores have been utilised over the years to improve the sensitivity of carbohydrates analysis in CE, although novel tags are still required to allow even better analytical performance in regards to sensitivity and resolution of analytes. It is also evident that preconcentration *via* dynamic pH junction has had very limited application towards the analysis of carbohydrates throughout its existence, especially in combination with derivatisation reagents which improve detection capability and also can improve resolution and selectivity of the analytes. Therefore the aims of the study were:

- To investigate the sensitivity of an inexpensive CE system involving a cheap detection alternative such as LEDs in conjunction with a highly absorbing UV/Vis chromophore and preconcentration *via* dynamic pH junction.
- To synthesise and evaluate novel and commercially available fluorescent tags which can be used in combination with dynamic pH junction and LIF for ultra-sensitive detection.
- To implement on-line preconcentration *via* dynamic pH junction and separation of carbohydrates on a microchip format.

1.6 References

(1) Stenesh, J. *Biochemistry, Volume 2*; Plenum Press: New York, 1998.

(2) Stefansson, M., Novotny, M., *Anal. Chem.* **1994**, *66*, 1134-1140.

(3) Varki, A., *Glycobiology* **1993**, *3*, 97-130.

(4) Liu, J. P., Shirota, O., Novotny, M., *Anal. Chem.* **1991**, *63*, 413-417.

(5) Takamatsu, S., Inoue, N., Katsumata, T., Nakamura, K., Fujibayashi, Y., Takeuchi, M., *Biochem.* **2005**, *44*, 6343-6349.

(6) Fukuda, M. N., Sasaki, H., Lopez, L., Fukuda, M., *Blood* **1989**, *73*, 84-89.

(7) Paulson, J. C., *Trends Biochem. Sci.* **1989**, *14*, 272-276.

(8) Galvan, M., Murali-Krishna, K., Ming, L. L., Baum, L., Ahmed, R., *J. Immunol.* **1998**, *161*, 641-648.

(9) Fukuda, M., *Cancer Res.* **1996**, *56*, 2237-2244.

(10) Guignard, C., Jouve, L., Bogeat-Triboulot, M. B., Dreyer, E., Hausman, J. F., Hoffmann, L., *J. Chromatogr. A* **2005**, *1085*, 137-142.

(11) Eldridge, S. L., Korir, A. K., Merrywell, C. E., Larive , C. K. *Advances in Chromatography*; CRC Press-Taylor & Francis Group: Boca Raton, 2008.

(12) El Rassi, Z. *High Performance Capillary Electrophoresis of Carbohydrates*; Beckman Coulter Inc.: Stillwater, 1996.

(13) Michaelis, L., *Biochemische Zeitschrift* **1909**, *16*, 81-86.

(14) Tiselius, A., *Trans. Faraday Soc.* **1937**, *33*, 524-531.

(15) Righetti, P. G., *J. Chromatogr. A* **2005**, *1079*, 24-40.

(16) Shapiro, A. L., Vinuela, E., Maizel, J. V., *Biochem. Biophys. Res. Commun.* **1967**, *28*, 815-&.

(17) Virtanen, R., Kivalo, P., *Suomen Kemistilehti* **1969**, *42*, 182-&.

(18) Jorgenson, J. W., Lukacs, K. D., *Anal. Chem.* **1981**, *53*, 1298-1302.

(19) Landers, J. P. *Handbook of Capillary Electrophoresis*; CRC Press: London, 1992.

(20) Reuss, F. F., *Memoires de la Soci´et´e Imperiale des Naturalistes de Moskou* **1809**, *2*, 327.

(21) Swinney, K., Bornhop, D. J., *Electrophoresis* **2000**, *21*, 1239-1250.

(22) Arentoft, A. M., Michaelsen, S., Sorensen, H., *J. Chromatogr. A* **1993**, *652*, 517-524.

(23) Paulus, A., Klockow, A., *J. Chromatogr. A* **1996**, *720*, 353-376.

(24) Housecroft, C. E., Constable, E. C. *Chemistry: an introduction to organic, inorganic, and physical chemistry*, 2nd ed.; Pearson Education Limited: Harlow, 2002.

(25) Harris, D. C. *Quantitative Chemical Analysis*; W.H. Freeman and Company: New York, 2003.

(26) *Fluorescence Microscopy,* http://www.microscopyu.com/references/pdfs/Spring_Fluorescence_Microscopy.pdf, (Access Date, Access 2003).

(27) Khandurina, J., Olson, N. A., Anderson, A. A., Gray, K. A., Guttman, A., *Electrophoresis* **2004**, *25*, 3117-3121.

(28) Khandurina, J., Anderson, A. A., Olson, N. A., Stege, J. T., Guttman, A., *Electrophoresis* **2004**, *25*, 3122-3127.

(29) Olajos, M., Hajos, P., Bonn, G. K., Guttman, A., *Anal. Chem.* **2008**, *80*, 4241-4246.

(30) Joucla, G., Brando, T., Remaud-Simeon, M., Monsan, P., Puzo, G., *Electrophoresis* **2004**, *25*, 861-869.

(31) Fraysse, N., Verollet, C., Couderc, F., Poinsot, V., *Electrophoresis* **2003**, *24*, 3364-3370.

(32) Khandurina, J., Blum, D. L., Stege, J. T., Guttman, A., *Electrophoresis* **2004**, *25*, 2326-2331.

(33) Beaudoin, M. E., Gauthier, J., Boucher, I., Waldron, K. C., *J. Sep. Sci.* **2005**, *28*, 1390-1398.

(34) Lv, Z. H., Sun, Y., Wang, Y. H., Jiang, T. F., Yu, G. L., *Chromatographia* **2005**, *61*, 615-618.

(35) Easley, C. J., Jin, L. J., Elgstoen, K. B. P., Jellum, E., Landers, J. P., Ferrance, J. P., *J. Chromatogr. A* **2003**, *1004*, 29-37.

(36) Khandurina, J., Guttman, A., *Chromatographia* **2005**, *62*, S37-S41.

(37) Kabel, M. A., Heijnis, W. H., Bakx, E. J., Kuijpers, R., Voragen, A. G. J., Schols, H. A., *J. Chromatogr. A* **2006**, *1137*, 119-126.

(38) Kamoda, S., Nomura, C., Kinoshita, M., Nishiura, S., Ishikawa, R., Kakehi, K., Kawasaki, N., Hayakawa, T., *J. Chromatogr. A* **2004**, *1050*, 211-216.

(39) Koller, A., Khandurina, J., Li, J. C., Kreps, J., Schieltz, D., Guttman, A., *Electrophoresis* **2004**, *25*, 2003-2009.

(40) Bui, A., Kocsis, B., Kilar, F., *J. Biochem. Biophys. Meth.* **2008**, *70*, 1313-1316.

(41) Kodama, S., Aizawa, S. I., Taga, A., Yamashita, T., Kemmei, T., Yamamoto, A., Hayakawa, K., *Electrophoresis* **2007**, *28*, 3930-3933.

(42) Buzzega, D., Maccari, F., Volpi, N., *Electrophoresis* **2008**, *29*, 4192-4202.

(43) Santos, S. M., Duarte, A. C., Esteves, V. I., *Talanta* **2007**, *72*, 165-171.

(44) Andersen, K. E., Bjergegaard, C., Sorensen, H., *J. Agric. Food Chem.* **2003**, *51*, 7234-7239.

(45) Momenbeik, F., Johns, C., Breadmore, M. C., Hilder, E. F., Macka, M., Haddad, P. R., *Electrophoresis* **2006**, *27*, 4039-4046.

(46) Wang, X. Y., Wang, Q., Chen, Y., Han, H. W., *J. Chromatogr. A* **2003**, *992*, 181-191.

(47) He, L. P., Sato, K., Abo, M., Okubo, A., Yamazaki, S., *Anal. Biochem.* **2003**, *314*, 128-134.

(48) Kakehi, K., Funakubo, T., Suzuki, S., Oda, Y., Kitada, Y., *J. Chromatogr. A* **1999**, *863*, 205-218.

(49) Cortacero-Ramirez, S., Segura-Carretero, A., Cruces-Blanco, C., de Castro, M. H. B., Fernandez-Gutierrez, A., *Food Chem.* **2004**, *87*, 471-476.

(50) An, H. J., Franz, A. H., Lebrilla, C. B., *J. Chromatogr. A* **2003**, *1004*, 121-129.

(51) Yamamoto, K., Hamase, K., Zaitsu, K., *J. Chromatogr. A* **2003**, *1004*, 99-106.

(52) Zhang, L. Y., Xu, J., Zhang, L. H., Zhang, W. B., Zhang, Y. K., *J. Chromatogr. B* **2003**, *793*, 159-165.

(53) Kodama, S., Aizawa, S., Taga, A., Yamashita, T., Yamamoto, A., *Electrophoresis* **2006**, *27*, 4730-4734.

(54) You, J. M., Sheng, X., Ding, C. X., Sun, Z. W., Suo, Y. R., Wang, H. L., Li, W., *Anal. Chim. Acta* **2008**, *609*, 66-75.

(55) Lamari, F. N., Kuhn, R., Karamanos, N. K., *J. Chromatogr. B* **2003**, *793*, 15-36.

(56) Gao, X. B., Yang, J. H., Huang, F., Wu, X., Li, L., Sun, C. X., *Anal. Lett.* **2003**, *36*, 1281-1310.

(57) Suzuki, S., Honda, S., *Chromatography* **2001**, *22*, 171-179.

(58) Shilova, N. V., Bovin, N. V., *Russ. J. Bioorg. Chem.* **2003**, *29*, 309-324.

(59) Oefner, P. J., Chiesa, C., *Glycobiology* **1994**, *4*, 397-412.

(60) Sundberg, R. J., Carey, F. A. *Advanced Organic Chemistry*; Plenum Press: Charlottesville, 1990.

(61) Hase, S., Hara, S., Matsushima, Y., *J. Biochem.* **1979**, *85*, 217-220.

(62) Suzuki, S., Honda, S., *Electrophoresis* **2003**, *24*, 3577-3582.

(63) Evangelista, R. A., Liu, M. S., Chen, F. T. A., *Anal. Chem.* **1995**, *67*, 2239-2245.

(64) Xiao, D., Zhao, S. L., Yuan, H. Y., Yang, X. P., *Electrophoresis* **2007**, *28*, 233-242.

(65) Haugland, R. P. *Handbook of Fluorescent Probes and Research Products* 9th ed.; Molecular Probes: Eugene 2002.

(66) Wong, D. W. C. *Mechanism and Theory in Food Chemistry*; Van Nostrand Reinhold: New York, 1989.

(67) Li, D. T., Her, G. R., *J. Mass Spectrom.* **1998**, *33*, 644-652.

(68) Li, D. T., Sheen, J. F., Her, G. R., *J. Am. Soc. Mass. Spectrom.* **2000**, *11*, 292-300.

(69) Liu, J. P., Hsieh, Y. Z., Wiesler, D., Novotny, M., *Anal. Chem.* **1991**, *63*, 408-412.

(70) Honda, S., Okeda, J., Iwanaga, H., Kawakami, S., Taga, A., Suzuki, S., Imai, K., *Anal. Biochem.* **2000**, *286*, 99-111.

(71) Liu, J. P., Shirota, O., Novotny, M. V., *Anal. Chem.* **1992**, *64*, 973-975.

(72) Zhao, J. Y., Diedrich, P., Zhang, Y. N., Hindsgaul, O., Dovichi, N. J., *J. Chromatogr. B* **1994**, *657*, 307-313.

(73) Spiro, M. J., Spiro, R. G., *Anal. Biochem.* **1992**, *204*, 152-157.

(74) Suzuki S, Honda S, *Chromatography* **2001**, *22*, 171-179.

(75) Miller, A., Solomon, P. H. *Writing Reaction Mechanisms in Organic Chemistry*, 2nd ed.; Academic Press: San Diego, 2000.

(76) Perez, S. A., Colon, L. A., *Electrophoresis* **1996**, *17*, 352-358.

(77) Miksik, I., Gabriel, J., Deyl, Z., *J. Chromatogr. A* **1997**, *772*, 297-303.

(78) Karamanos, N. K., Tsegenidis, T., Antonopoulos, C. A., *J. Chromatogr.* **1987**, *405*, 221-228.

(79) Honda, S., Suzuki, S., Taga, A., *J. Pharm. Biomed. Anal.* **2003**, *30*, 1689-1714.

(80) Mechref, Y., Ostrander, G. K., El Rassi, Z., *J. Chromatogr. A* **1995**, *695*, 83-95.

(81) Khorana, H. G., *Chem. Rev.* **1953**, *53*, 145-166.

(82) Taga, A., Suzuki, S., Honda, S., *J. Chromatogr. A* **2001**, *911*, 259-267.

(83) Wang, X. Y., Chen, Y., Li, Z., Wang, Z., *J. Liq. Chromatogr. Related Technol.* **2002**, *25*, 589-600.

(84) Jin, Z., Chen, R., Colon, L. A., *Anal. Chem.* **1997**, *69*, 1326-1331.

(85) Kaiser, C., Segui-Lines, G., D'Amaral, J. C., Ptolemy, A. S., Britz-McKibbin, P., *Chem. Commun.* **2008**, 338-340.

(86) Mader, H. S., Wolfbeis, O. S., *Microchim. Acta* **2008**, *162*, 1-34.

(87) Robins, W. H., Wright, B. W., *J. Chromatogr. A* **1994**, *680*, 667-673.

(88) Lorand, J. P., Edwards, J. O., *J. Org. Chem.* **1959**, *24*, 769-774.

(89) Britz-McKibbin, P., Terabe, S., *J. Chromatogr. A* **2003**, *1000*, 917-934.

(90) Aebersold, R., Morrison, H. D., *J. Chromatogr.* **1990**, *516*, 79-88.

(91) Britz-Mckibbin, P., Kranack, A. R., Paprica, A., Chen, D. D. Y., *Analyst* **1998**, *123*, 1461-1463.

(92) Monton, M. R. N., Imami, K., Nakanishi, M., Kim, J. B., Terabe, S., *J. Chromatogr. A* **2005**, *1079*, 266-273.

(93) Imami, K., Monton, M. R. N., Ishihama, Y., Terabe, S., *J. Chromatogr. A* **2007**, *1148*, 250-255.

(94) Yu, L. J., Li, S. F. Y., *Electrophoresis* **2005**, *26*, 4360-4367.

(95) Britz-McKibbin, P., Ichihashi, T., Tsubota, K., Chen, D. D. Y., Terabe, S., *J. Chromatogr. A* **2003**, *1013*, 65-76.

(96) Su, A. K., Chang, Y. S., Lin, C. H., *Talanta* **2004**, *64*, 970-974.

(97) Britz-McKibbin, P., Otsuka, K., Terabe, S., *Anal. Chem.* **2002**, *74*, 3736-3743.

(98) Britz-McKibbin, P., Markuszewski, M. J., Iyanagi, T., Matsuda, K., Nishioka, T., Terabe, S., *Anal. Biochem.* **2003**, *313*, 89-96.

(99) Britz-McKibbin, P., Terabe, S., *Chem. Rec.* **2002**, *2*, 397-404.

(100) Jia, L., Liu, B. F., Terabe, S., Nishioka, T., *Anal. Chem.* **2004**, *76*, 1419-1428.

(101) Shih, C. M., Lin, C. H., *Electrophoresis* **2005**, *26*, 3495-3499.

(102) Shim, S. H., Riaz, A., Choi, K. W., Chung, D. S., *Electrophoresis* **2003**, *24*, 1603-1611.

(103) Arnett, S. D., Lunte, C. E., *Electrophoresis* **2007**, *28*, 3786-3793.

(104) Han, Y. L., Zuo, M., Qi, L., Liu, K., Mao, L. Q., Chen, Y., *Electrophoresis* **2006**, *27*, 4240-4248.

(105) Feng, H. Y., Hou, S. R., Zheng, N., Li, X. J., Hu, Z. B., Yuan, Z. B., *Chromatographia* **2008**, *68*, 431-435.

(106) Kirschner, D. L., Jaramillo, M., Green, T. K., *Anal. Chem.* **2007**, *79*, 736-743.

(107) Mandaji, M., Rubensam, G., Hoff, R. B., Hillebrand, S., Carrilho, E., Kist, T. L., *Electrophoresis* **2009**, *30*, 1501-1509.

(108) Mandaji, M., Rubensam, G., Hoff, R. B., Hillebrand, S., Carrilho, E., Kist, T. L., *Electrophoresis* **2009**, *30*, 1510-1515.

(109) Horakova, J., Petr, J., Maier, V., Znaleziona, J., Stanova, A., Marak, J., Kaniansky, D., Sevcik, J., *J. Chromatogr. A* **2007**, *1155*, 193-198.

(110) Horakova, J., Petr, J., Maier, V., Tesarova, E., Veis, L., Armstrong, D. W., Gas, B., Sevcik, J., *Electrophoresis* **2007**, *28*, 1540-1547.

(111) Liu, J., Liu, Z., Kang, M. C., Liu, S. C., Chen, H. Y., *J. Sep. Sci.* **2009**, *32*, 422-429.

(112) The Chemical Rubber Co. *CRC Handbook of Chemistry and Physics: a ready-reference book of chemical and physical data*, 52nd ed.; The Chemical Rubber Co.: Cleveland, 1971.

(113) ed.; Ed.^Eds.; Beckman Coulter; Vol. 2010, pp 47.

(114) Landers, J. P. *Handbook of capillary and microchip electrophoresis and associated microtechniques*; CRC Press-Taylor & Francis Group: Boca Raton, 2008.

(115) Cao, C. X., He, Y. Z., Li, M., Qian, Y. T., Yang, L., Qu, Q. S., Zhou, S. L., Chen, W. K., *J. Chromatogr. A* **2002**, *952*, 39-46.

(116) Cao, C. X., He, Y. Z., Li, M., Qian, Y. T., Gao, M. F., Ge, L. H., Zhou, S. L., Yang, L., Qu, Q. S., *Anal. Chem.* **2002**, *74*, 4167-4174.

(117) Cao, C. X., Zhang, W., Qin, W. H., Li, S., Zhu, W., Liu, W., *Anal. Chem.* **2005**, *77*, 955-963.

(118) Zhu, W., Zhang, W., Fan, L. Y., Shao, J., Li, S., Chen, J. L., Cao, C. X., *Talanta* **2009**, *78*, 1194-1200.

(119) Oin, W. H., Cao, C. X., Li, S., Zhang, W., Liu, W., *Electrophoresis* **2005**, *26*, 3113-3124.

(120) Wang, X., Zhang, W., Fan, L. Y., Hao, B., Ma, A. N., Cao, C. X., Wang, Y. X., *Anal. Chim. Acta* **2007**, *594*, 290-296.

(121) Cannan, R. K., Palmer, A. H., Kibrick, A. C., *J. Biol. Chem.* **1942**, *142*, 803-822.

(122) Nesbitt, C. A., Jurcic, K., Yeung, K. K. C., *Electrophoresis* **2008**, *29*, 466-474.

(123) Nesbitt, C. A., Lo, J. T. M., Yeung, K. K. C., *J. Chromatogr. A* **2005**, *1073*, 175-180.

(124) Moritz, R. L., Simpson, R. J., *Nat. Methods* **2005**, *2*, 863-873.

(125) Su, S. M., Yu, Y. Q., *J. Chromatogr. A* **2009**, *1216*, 1490-1495.

(126) Fan, L. Y., Liu, L. H., Chen, H. L., Chen, X. G., Hu, Z. D., *J. Chromatogr. A* **2005**, *1062*, 133-137.

(127) Kim, J. B., Okamoto, Y., Terabe, S., *J. Chromatogr. A* **2003**, *1018*, 251-256.

(128) Britz-McKibbin, P., Chen, D. D. Y., *Anal. Chem.* **2000**, *72*, 1242-1252.

(129) Britz-Mckibbin, P., Wong, J., Chen, D. D. Y., *J. Chromatogr. A* **1999**, *853*, 535-540.

(130) Kim, J. B., Britz-McKibbin, P., Hirokawa, T., Terabe, S., *Anal. Chem.* **2003**, *75*, 3986-3993.

(131) Jurcic, K., Nesbitt, C. A., Yeung, K. K. C., *J. Chromatogr. A* **2006**, *1134*, 317-325.

(132) Quintas, G., Nunez, E., Vellekoop, M., Lendl, B., *Anal. Bioanal. Chem.* **2007**, *387*, 287-292.

(133) Booker, C. J., Yeung, K. K. C., *Anal. Chem.* **2008**, *80*, 8598-8604.

(134) Wintersteiner, O., Abramson, H. A., *J. Biol. Chem.* **1933**, *99*, 741-753.

(135) Xu, L., Dong, X. Y., Sun, Y., *Electrophoresis* **2009**, *30*, 689-695.

(136) Mathews, C. K., Holde, K. E., Ahern, K. G. *Biochemistry* 3rd ed.; Benjamin Cummings: San Francisco 2000.

(137) Li, W., Fries, D., Malik, A., *J. Sep. Sci.* **2005**, *28*, 2153-2164.

(138) Kronman, M. J., Vitols, R., Andreotti, R., *Biochem.* **1964**, *3*, 1152-&.

(139) Nesbitt, C. A., Yeung, K. K. C., *Analyst* **2009**, *134*, 65-71.

(140) Wang, S. J., Tseng, W. L., Lin, Y. W., Chang, H. T., *J. Chromatogr. A* **2002**, *979*, 261-270.

(141) Chang, Y. S., Shih, C. M., Lin, C. H., *Anal. Sci.* **2006**, *22*, 235-240.

(142) Moore, C. E., Underwood, A. L., *Anal. Biochem.* **1969**, *29*, 149-&.

(143) *pKa Data compiled by Williams, R.,* http://research.chem.psu.edu/brpgroup/pKa_compilation.pdf, (Access Date, Access

(144) Crofts, A. R., Berry, E. A., Kuras, R., Guergova-Kuras, M., Hong, S., Ugulava, N. In *Photosynthesis: Mechanisms and effects* Editon ed.; Garab, G., Ed.^Eds.; Kluwer Academic Publ.: Dordrecht/Boston/London, 1998; Vol. III, pp 1481-1486.

(145) Dou, P., Liang, L., He, J. G., Liu, Z., Chen, H. Y., *J. Chromatogr. A* **2009**, *1216*, 7558-7563.

(146) Wilson, C. H., H., B. J., Gisvold, O., Beale, J. M. *Wilson and Gisvold's textbook of organic medicinal and pharmaceutical chemistry*, 11th ed.; Lippincott Williams & Wilkins: Baltimore, 2004.

(147) Said, H. M., *J. Nutr.* **2009**, *139*, 158-162.

(148) Ivanovic, D., Medenica, M., Nivaudguernet, E., Guernet, M., *Chromatographia* **1995**, *40*, 652-656.

(149) Ball, G. F. M. *Vitamins in foods: analysis, bioavailability, and stability*; CRC Press-Taylor & Francis: Boca Raton, 2006.

(150) Appleby, C. A., Wittenbe, B. A., Wittenbe, J. B., *Proc. Natl. Acad. Sci. U. S. A.* **1973**, *70*, 564-568.

(151) Akhtar, M. J., Khan, M. A., Ahmad, I., *J. Pharm. Biomed. Anal.* **1999**, *19*, 269-275.

(152) Du, Y. Y., Jia, L., Liu, H. Q., Xing, D., *Anal. Lett.* **2007**, *40*, 2005-2015.

(153) McMurry, J. *Fundamentals of Organic Chemistry*, fifth ed.; Thomson-Brooks/Cole: Pacific Grove, 2003.

(154) Hsieh, M. M., Chang, H. T., *Electrophoresis* **2005**, *26*, 187-195.

(155) Britz-McKibbin, P., Bebault, G. M., Chen, D. D. Y., *Anal. Chem.* **2000**, *72*, 1729-1735.

(156) Lee, R., Ptolemy, A. S., Niewczas, L., Britz-McKibbin, P., *Anal. Chem.* **2007**, *79*, 403-415.

(157) Christensen, J. J., Rytting, J. H., Izatt, R. M., *Biochem.* **1970**, *9*, 4907-&.

(158) Wood, D. O., Dinsmore, M. J., Bare, G. A., Lee, J. S., *Nucleic Acids Res.* **2002**, *30*, 2244-2250.

(159) Grove, R. A., Bildfell, R., Henny, C. J., Buhler, D. R., *J. Wildl. Dis.* **2003**, *39*, 914-917.

(160) Pu, Q. S., Fang, Z. L., *Anal. Chim. Acta* **1999**, *398*, 65-74.

(161) *Handbook of Biochemistry and Molecular Biology*, 3rd ed.; CRC Press: Boca Raton.

(162) Dawson, R. M. C., Elliott, D. C., Elliott, W. H., Jones, K. M. *Data for Biochemical Research*; Clarendon Press, Oxford University Press: London, 1959.

(163) Zhang, S. M., Baker, J., Pulay, P., *J. Phys. Chem. A*, *114*, 425-431.

(164) Ishihama, Y., Oda, Y., Asakawa, N., *J. Pharm. Sci.* **1994**, *83*, 1500-1507.

(165) Lynch, D. E., Sandhu, P., Parsons, S., *Aust. J. Chem.* **2000**, *53*, 383-387.

(166) Lide, D. R. *CRC Handbook of Chemistry and Physics*, 85th ed.; CRC Press: Boca Raton, 2004.

(167) Grimes, S. M., Mehta, L. K., Ngwang, H. C., *J. Environ. Sci. Health Part A-Toxic/Hazard. Subst. Environ. Eng.* **2001**, *36*, 599-612.

(168) Harris, D. C. *Exploring Chemical Analysis*; W. H. Freeman: New York, 1997.

(169) Pospichal, J., Gebauer, P., Bocek, P., *Chem. Rev.* **1989**, *89*, 419-430.

(170) McHedlov-Petrossyan, N. O., Kleshchevnikova, V. N., *J. Chem. Soc.-Faraday Trans.* **1994**, *90*, 629-640.

(171) Culp, S. J., Cho, B. P., Kadlubar, F. F., Evans, F. E., *Chem. Res. Toxicol.* **1989**, *2*, 416-422.

(172) Mei, S. R., Yao, C. H., Cai, L. S., Xing, J., Xu, G. W., Wu, C. Y., *Electrophoresis* **2003**, *24*, 1411-1415.

(173) Yao, Q. H., Mei, S. R., Weng, Q. F., Zhang, P. D., Yang, Q., Wu, C. Y., Xu, G. W., *Talanta* **2004**, *63*, 617-623.

(174) Sigel, H., Song, B., Oswald, G., Lippert, B., *Chem.-Eur. J.* **1998**, *4*, 1053-1060.

(175) Britz-McKibbin, P., Nishioka, T., Terabe, S., *Anal. Sci.* **2003**, *19*, 99-104.

(176) Britz-McKibbin, P., Chen, D. D. Y., *Chromatographia* **2003**, *57*, 87-93.

(177) Jensen, A., Faurholt, C., *Acta Chem. Scand.* **1952**, *6*, 385-394.

(178) Prochazkova, B., Glovinova, E., Pospichal, J., *Electrophoresis* **2007**, *28*, 2168-2173.

(179) Kumar, P. S., Hogendoorn, J. A., Versteeg, G. F., Feron, P. H. M., *Aiche J.* **2003**, *49*, 203-213.

(180) Ptolemy, A. S., Tran, L., Britz-McKibbin, P., *Anal. Biochem.* **2006**, *354*, 192-204.

(181) Mayboroda, O. A., Neususs, C., Pelzing, M., Zurek, G., Derks, R., Meulenbelt, I., Kloppenburg, M., Slagboom, E. P., Deelder, A. M., *J. Chromatogr. A* **2007**, *1159*, 149-153.

(182) Ptolemy, A. S., Britz-McKibbin, P., *Analyst* **2005**, *130*, 1263-1270.

(183) Smadja, C., Le Potier, I., Chaminade, P., Jacquot, C., Trouvin, J. H., Taverna, M., *Chromatographia* **2003**, *58*, 79-85.

(184) Bessonova, E. A., Kartsova, L. A., Shmukov, A. U., *J. Chromatogr. A* **2007**, *1150*, 332-338.

(185) Petr, J., Vitkova, K., Ranc, V., Znaleziona, J., Maier, V., Knob, R., Sevcik, J., *J. Agric. Food Chem.* **2008**, *56*, 3940-3944.

(186) Li, M., Fan, L. Y., Zhang, W., Cao, C. X., *Anal. Bioanal. Chem.* **2007**, *387*, 2719-2725.

(187) Zhang, Z. X., Zhang, M. Z., Zhang, S. S., *Electrophoresis* **2009**, *30*, 1958-1966.

(188) Ptolemy, A. S., Le Bihan, M., Britz-McKibbin, P., *Electrophoresis* **2005**, *26*, 4206-4214.

(189) Jaafar, J., Irwan, Z., Ahamad, R., Terabe, S., Ikegami, T., Tanaka, N., *J. Sep. Sci.* **2007**, *30*, 391-398.

(190) Wang, Q. L., Fan, L. Y., Zhang, W., Cao, C. X., *Anal. Chim. Acta* **2006**, *580*, 200-205.

(191) Breadmore, M. C., Mosher, R. A., Thormann, W., *Anal. Chem.* **2006**, *78*, 538-546.

(192) Cheng, H. L., Liao, Y. M., Chiou, S. S., Wu, S. M., *Electrophoresis* **2008**, *29*, 3665-3673.

(193) Vaidyanathan, J. B., Walle, T., *J. Pharmacol. Exp. Ther.* **2003**, *307*, 745-752.

(194) Jovanovic, S. V., Hara, Y., Steenken, S., Simic, M. G., *J. Am. Chem. Soc.* **1997**, *119*, 5337-5343.

(195) Liu, J., Zhu, F. F., Liu, Z., *Talanta* **2009**, *80*, 544-550.

(196) Zielonka, J., Gebicki, J., Grynkiewicz, G., *Free Radic. Biol. Med.* **2003**, *35*, 958-965.

(197) Breadmore, M. C., *Electrophoresis* **2007**, *28*, 254-281.

(198) Ptolemy, A. S., Britz-McKibbin, P., *Analyst* **2008**, *133*, 1643-1648.

Chapter 2

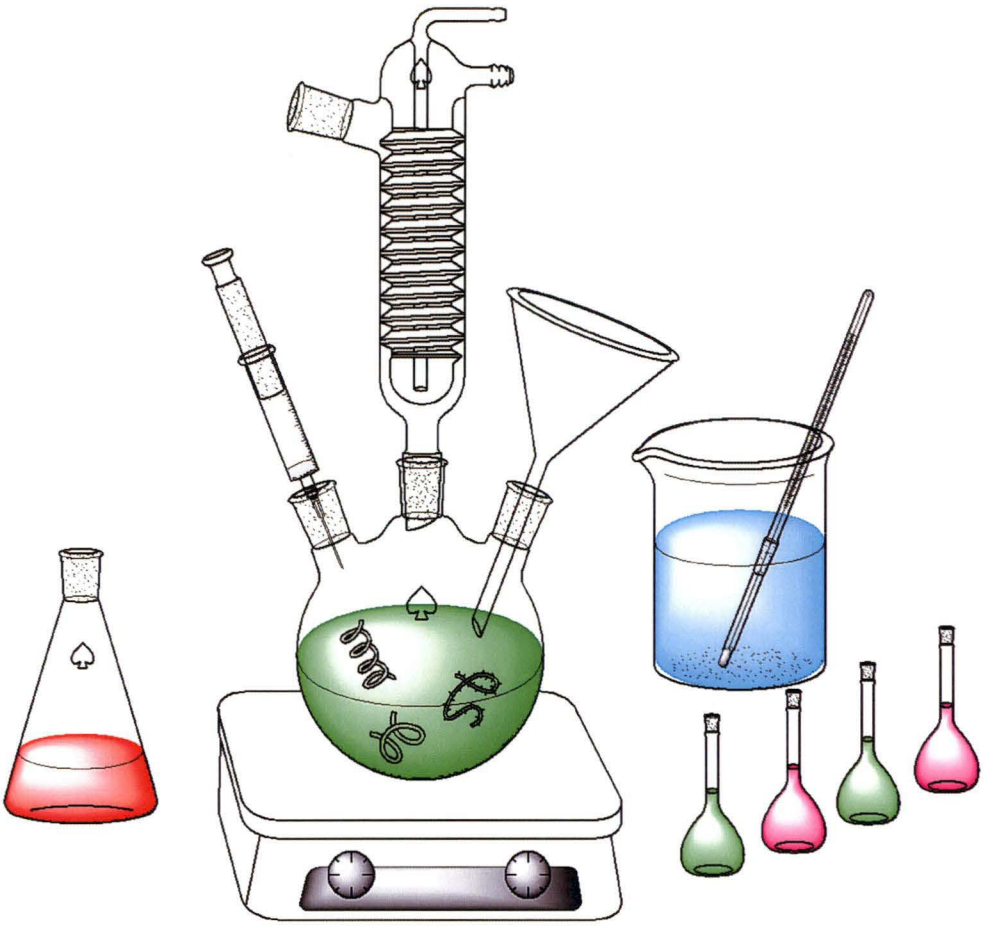

2 Experimental

2.1 Instrumentation

2.1.1 Agilent ^{3D} CE

An Agilent ^{3D}CE (Waldbronn, Germany), equipped with a DAD with a D_2 lamp and a laboratory-built LED detector [1] (Figure 2.1, Figure 2.2) interfaced to the Chemstation software using an Agilent 35900E A/D converter was utilised for photometric detection in CE experiments. Polyimide coated fused silica capillary (Polymicro, Phoenix, AZ, USA), with a 50μm internal diameter (I.D.), 375 μm outer diameter (O.D.), were used for all separations and were permanently coated with acrylamide or purchased from Polymicro with already coated acrylamide surface. Detection windows were burned with a butane torch at 8.5 and 13.5 cm from the capillary end to fit the DAD and LED detection systems respectively. Injection of the sample solutions was performed hydrostatically by applying a pressure of 50 mbar for 10 to 500 s. Electrophoretic separations were performed at 20 kV and 30 kV, with the capillary thermostated at 25 °C. The spectral properties of the LEDs were measured using an Ocean Optics S 1000 diode array fibre-optics visible spectrophotometer (LasTek, Thebarton, Australia).

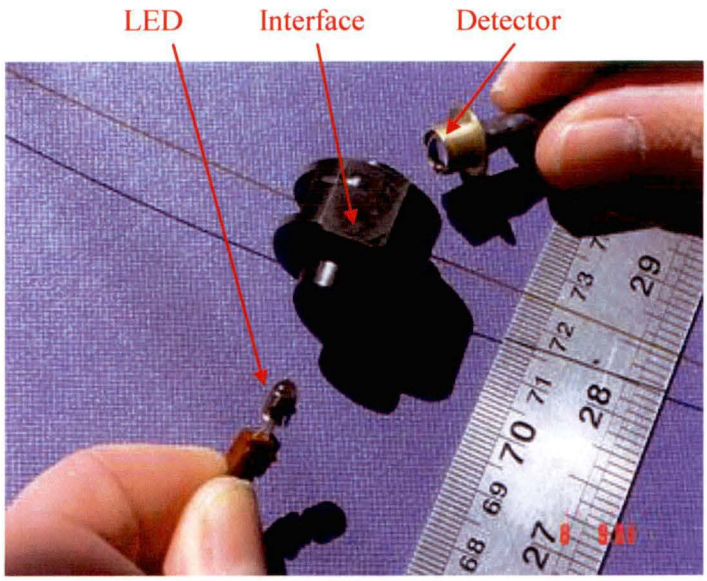

Figure 2.1. LED detection system.

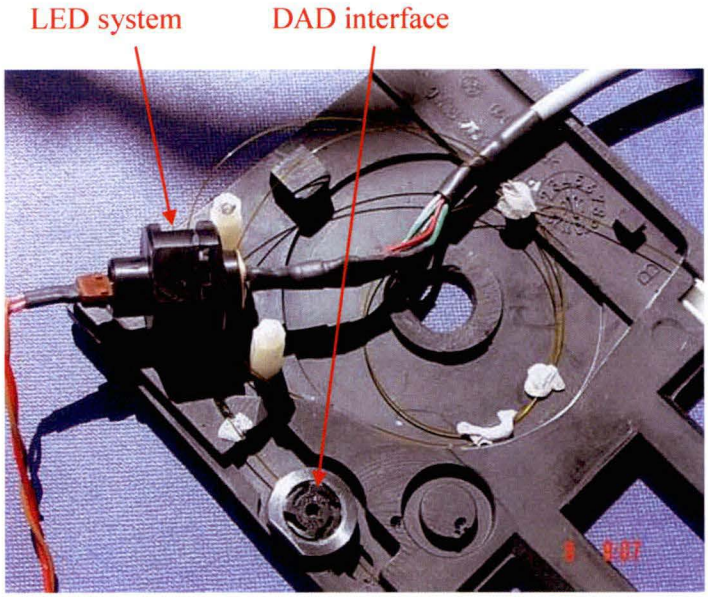

Figure 2.2. LED detection system and DAD interface.

2.1.2 Beckman Coulter P/ACE MDQ

A Beckman Coulter P/ACE MDQ, equipped with a LIF detector interfaced to the Karat software was utilised for fluorescence detection in CE experiments. Polyimide coated linear polyacrylamide (LPA)-coated fused silica capillary (Polymicro, Phoenix, AZ, USA) and bare fused silica capillary coated with PSS or PDADMAC with a 50μm I.D. were used for all separations. Detection windows were created with hot sulfuric acid for acrylamide coated capillaries and using a butane torch for bare fused silica capillaries at 10 cm from the capillary end to fit the LIF detection system. Injection of the sample solutions was performed hydrostatically by applying a pressure of 44 mbar for 4 to 100 s. Electrophoretic separations were performed at 30 kV with the capillary thermostated at 25 °C. LPA-coated capillaries were used to suppress the EOF and to improve the resolution of carbohydrates.

2.2 Reagents

Table 2.1. List of general chemicals used in this work.

Reagent	Supplier	Grade
2-Bromoethylphthalimide	Aldrich	99%
Acetone	Aldrich	AR
Acrylamide	Merck	> 99%
Ammonium carbonate	Fluka	98%
$CDCl_3$	CIL	99.9%
Ceric sulfate	BDH	
D_2O	CIL	99.9%
Dimethyl formamide	Merck	99.5%
DMSO-d_6	CIL	99.9%

Ethanol	BDH	AR
Ethyl acetate	EM Science	AR
Formic acid	Mallinckrodt	99%
Glacial acetic acid	Biolab	99%
Hydrochloric acid	FINECHEM	99%
Methanol	BDH	AR
N, N, N', N'–Tetramethylethylenediamine	Sigma	99%
Phosphomolybdic acid	Hopkin and Williams	99%
Polydimethylsiloxane	Sylgard	
Potassium carbonate	BDH	AR
Potassium persulfate	BDH	AR
Poly(sterene sulfonate)	Sigma	
Poly(dimethyldiallylammonium chloride)	Sigma	
Silica	Merch	Mech
Sodium bicarbonate	Fluka	95%
Sodium cyanoborohydride	Fluka	95%
Sodium hydroxide	AJAX	97%
Sodium phosphate	AJAX	99%
Sodium sulfate	AJAX	98%
Sulfuric acid	Unichrom	99.9%
Tetrahydrofuran	Aldrich	99.9%
3-(Trimethoxysilyl) propyl methacrylate	Sigma	

Table 2.2. Chemicals used as buffers.

Reagent	Supplier	Grade
Tris(hydroxymethyl)aminomethane	Aldrich	99.9%
Boric acid	Standard Labs	AR
Ammonia	Sigma	

Table 2.3. Chemicals used as analytes.

Reagent	Supplier	Grade
Allose	Sigma	
Arabinose	Sigma	
G4-G10 corn syrup	Sigma	
Galactose	Sigma	
Glucose	Sigma	97%
Lactose	Sigma	
Maltoheptaose	Sigma	95%
Maltotriose	Sigma	95%
Maltose	Sigma	
Mannose	Sigma	
Rhamnose	Sigma	
Starch[a]	UQ[a]	Not known
Xylose	Sigma	

[a] Starch debranched and packaged at the University of Queensland (UQ), Brisbane, Australia.

Table 2.4. Chemicals used UV/visible and fluorescent tags.

Reagent	Supplier	Grade
5-Aminofluorescein	Acros Organics	
5-Aminomethylfluorescein	Invitrogen	
8-Aminopyrene-1,3,6 trisulfonic acid	Invitrogen	
Fluorescein	Sigma	
O-2-[Aminoethyl]fluorescein		

2.3 Procedures

2.3.1 Background electrolyte and standard preparation

Preparation of all BGEs and standards was conducted using a Milli-Q (Millipore, Bedford, MA, USA) water system. All buffers were sonicated, degassed using vacuum sonication followed by filtration through a 0.45μm disc filters (Activon, Thornleigh, Australia).

2.3.2 Solvent and reagents

All solvents and reagents were purified by standard laboratory procedure as required. Anhydrous sodium sulfate was used to dry organic extracts. Solvents were removed on a rotary evaporator and a vacuum line under reduced pressure.

2.3.3 Calculations

The EOF was measured from the migration time of acetone in water, injected as neutral marker. The following equation was used to calculate electrophoretic mobilities:

$$\mu_{eff} = \frac{L_T L_D}{V t_m}$$

where L_T signifies the total length of the capillary in metres, L_D defines the length to the detector in metres, V is the separation voltage measured volts and t_m is the migration time of the analyte measured in seconds.

Calculation of LODs was carried out based on a signal-to-noise ratio of 3:1.

2.4 References

(1) Johns, C.; Macka, M.; Haddad, P. R. *Electrophoresis* **2004**, *25*, 3145-3152.

Chapter 3

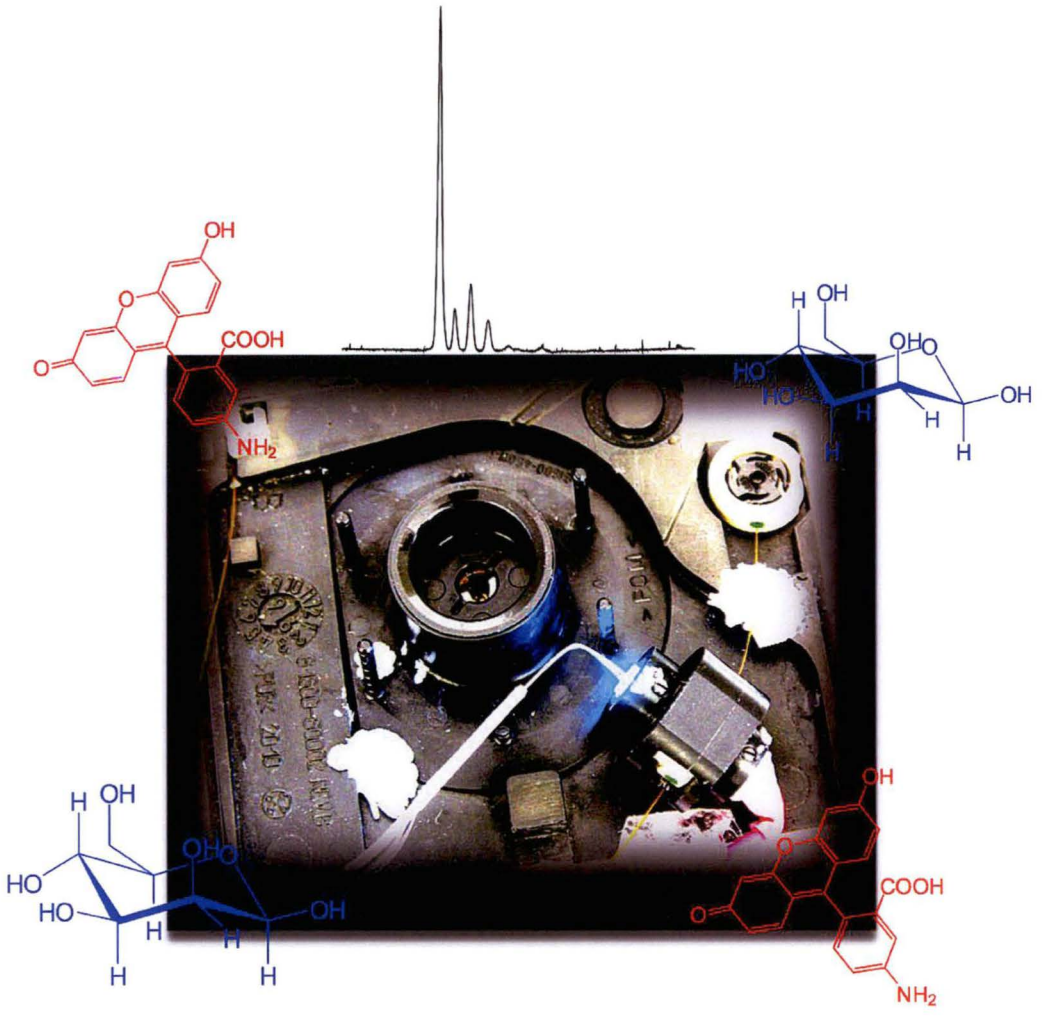

3 Utilisation of pH stacking in conjunction with a highly absorbing chromophore, 5-aminofluorescein, to improve the sensitivity of CE for carbohydrate analysis

3.1 Introduction

One of the typical and popular ways of analysing carbohydrates is by labelling with a fluorescent label such as APTS to a sugar followed by sensitive LIF detection as was discussed in the literature review in Chapter 1. The LODs are superior however the fluorescent label is still very expensive in the order of $ 400 AUD per 10 mg, has a relatively low QY of 0.37 and contains an aromatic nitrogen which could possibly hamper reactivity with carbohydrates. Another way to analyse carbohydrates with fluorescence is using LED-induced fluorescence detection, which has been done by several groups looking at oligosaccharides and proteins [1, 2], nevertheless the system still requires expensive fluorescent tags, costly optics and is hard to miniaturise when fitted in the cassette of a commercial instrument [3].

It is also evident from Chapter 1 that the most common way in which to attach the chromophore or fluorophore to the carbohydrates is based on reductive amination. However one of the limitations is the highly acidic conditions necessary for the derivatisation reaction which can be incompatible with typical basic conditions used in CE analysis of carbohydrates due to the high ionic strength of the sample matrix from the very high concentration of acid required for reductive amination. The best systems therefore require either large dilution of the sample mixture or the injection

of very small volumes to overcome this incompatibility issue [4-7]. This reduces the sensitivity of the system, decreasing the applicability of the method.

An obvious strategy to address this issue is to employ various stacking techniques, however only a few of these are appropriate given the acidic nature of the derivatisation mixture [8]. As derivatisation occurs in acidic conditions and the best separations are obtained in alkaline systems, the most obvious approach is to exploit this pH difference through the use of stacking *via* a dynamic pH junction [9-11]. This approach is also very attractive for the analysis of real samples as it is relatively insensitive to salts and in some cases to the large concentration of acid added for derivatisation. However, in order to ensure that the analytes can be focused on this boundary the label attached to the carbohydrates must be ionisable. This places significant restrictions on the choice of chromophore or fluorophore that can be employed. Of the various labels have been used in the past such as aminopyrine trisulfonate derivatives [7, 12], 9-aminofluorene [13], 2-aminopyridine [14], 6-aminoquinoline [15], aminonapthaline sulfonic acid [16], aminoacridone derivatives [17], 7-amino-4-methylcoumarin [18], PNA [19] and 4-amino-,1,1-azobenzene-3,4-disulphonic acid [20], none of these are ionisable in the acidic separation conditions and are therefore incompatible with dynamic pH junction stacking conditions proposed in this work. We therefore propose the use of a new label, 5-aminofluorescein, which contains two ionisable groups, namely a carboxylic acid (pK_a 4.56)[a] and a phenol group (pK_a 9.36)[a]. These functional groups introduce sufficient charge for electrophoretic separation and show suitable ionisable groups for stacking *via* a dynamic pH junction. The label is also beneficial due to its low cost and its extremely high molar absorptivity (77,000 L mol^{-1} cm^{-1}, λ_{max} = 492 nm),

[a] pKa values calculated using ACDLabs 7.0 pKa dB

which is higher than most other labels, and is also compatible with blue LEDs. It has been used in the past for labelling of fatty acids but to date has not been used for the analysis of carbohydrates [21].

The aim of this study was to understand the fundamentals of dynamic pH junction using 5-aminofluorescein and from that develop a highly sensitive method using a chosen set of commonly known carbohydrates. The sample composition was strategically varied to enhance the performance of the system specifically to exploit the acidic nature of the derivatisation mixture to facilitate on-line stacking. Sample components such as acetic acid, formic acid, sodium cyanoborohydride concentrations and dilution factor of the sample mixture were considered to design a highly sensitive system. This was used in conjunction with a simple miniaturised LED-absorbance detector that shows superior sensitivity in the visible region.

3.2 Experimental

3.2.1 Instrumental

An Agilent ^{3D}CE, equipped with a DAD with a D_2 lamp and a laboratory-built LED detector [22] interfaced to the Chemstation software using an Agilent 35900E A/D converter was utilised for photometric detection in CE experiments. Polyimide coated fused silica capillary (Polymicro, Phoenix, AZ, USA), with a 50μm I.D. were used for all separations and were permanently coated with acrylamide (see below). Detection windows were burned with a butane torch at 8.5 and 13.5 cm from the capillary end to fit the DAD and LED detection systems respectively. Injection of the sample solutions was performed hydrostatically by applying a pressure of 50 mbar for 10 to 500 s. Electrophoretic separations were performed at 20 kV and 30 kV, with the capillary thermostated at 25°C. The spectral properties of the LEDs were

measured using an Ocean Optics S 1,000 diode array fibre-optics visible spectrophotometer (LasTek, Thebarton, Australia) [23].

3.2.2 Capillary coating

Acrylamide-coated capillaries have been found to be important to maintain resolution in the separation of long-chain oligosaccharides [1] and were selected for use in this work on this basis. They were prepared from either vinylised capillaries obtained as a gift from Polymicro or were vinylised by first modifying the fused silica capillary with γ-methacryloxypropyltrimethoxysilane (γ-MAPS) according to the procedure of Rohr *et al.,* [24] followed by attachment of the acrylamide coating using a modification of the procedure of Hjertén *et al.* [25]. Briefly, the 50 μm polyimide coated and vinylised fused silica capillary was flushed with de-aerated 4% (w/v) acrylamide solution containing 1 mg N, N, N', N'–tetramethylethylenediamine and 1 mg potassium persulfate per 10 mL solution. The capillary was attached to a syringe (Hamilton 250 μL gastight, I.D. 2.30 mm) using a microtight capillary fitting (Upchurch, Oak Harbour, WA, USA) and flushed on an electric driven syringe pump (Harvard Model 22) at 0.25 μL min^{-1} as per Hjertén *et al.* [25]. The capillary was then blow dried with pressurised air and left overnight to complete the condensation reaction. Acrylamide capillaries were used to suppress the EOF [12].

Caution: Acrylamide is a suspected carcinogen mutagen and a reproductive hazard. Sodium cyanoborohydride is toxic and γ-MAPS is an irritant. Proper precautions should be taken to avoid contact during the physical handling of these materials.

3.2.3 Labelling reaction

The choice of solvent used for the labelling of the carbohydrates in the current study was an important parameter with poor solubility of 5-aminofluorescein in acidic conditions. The 5-aminofluorescein was soluble at alkaline pH, yet the

labelling reaction was conducted in acidic media to promote formation of an imine. This solubility problem was overcome using 50% methanol, 50% water solution and low concentrations of 5-aminofluorescein.

A solution of 50 μL of 1×10^{-4} M 5-aminofluorescein in methanol was added to a sugar mixture, comprising of 50 μL of 1×10^{-5} M glucose, lactose, and maltotriose in water and 1 μL of a freshly prepared solution of aqueous formic or acetic acid (0.19 or 1.9 or 19 M) and 1 μL of sodium cyanoborohydride (0.01 or 0.1 or 1 M) accordingly. The labelling reaction was studied at various temperatures such as 60, 70, 80°C, where the optimum reductive amination conditions was found at 70°C for 1 hour. The labelling reaction showed that approximately 78% of the glucose reacted with 5-aminofluorescein. The reaction yield was assessed by monitoring the disappearance of the peak area of the labelling reagent and by appearance of the carbohydrate peak area.

The mixture was stirred and heated at 70°C for 1 hour. After completion of the reaction the solution was cooled and homogenised in a Griffin and George, UK (type: UJI 100) centrifuge. The reaction mixture was then injected into the CE with or without dilution as described in the text.

3.2.4 Preparation of background electrolyte

BGE was prepared by taking 100 mM solution of boric acid in water and titrating to pH 9.2 with tris(hydroxymethyl)aminomethane (tris). All BGEs were degassed with a Soniclean ultra-sonic bath under vacuum and filtered through 0.45 μm disc filters (Activon, Thornleigh, Australia).

3.2.5 Simulation studies

Computer simulation studies were performed using the Personal Computer based software developed by Bier *et al.*, [26] and modified by Mosher and Thormann [27-

29] with the latest version described in Breadmore *et al.* [30]. This was recompiled for Unix and executed on Itanium 2 1.6 GHz processors housed in the Tasmanian Partnership for Advanced Computing and Australian Partnership for Advanced Computing facilities and required 3-5 days of computation time. The total capillary length was 50 mm (5 cm) and was divided into 20,000 equal segments. Simulations were performed at a constant voltage of 2,000 V (400 V cm^{-1}), approximating the application of 10 kV over a 25 cm capillary, and without having EOF to simulate the conditions of an acrylamide coated capillary. The sample was placed 5 mm from the anodic end of the capillary and occupied a total length of 20 mm, or 40% of the capillary length. The sample-electrolyte boundary widths were initially set at 0.1% of the capillary length, or 0.05 mm (50 μm). All simulations were for a separation time of 10.0 min with data collection of 101 data points, or every 0.1 min. The electrolyte consisted of 100 mM boric acid ($\mu_{ep,\,bor}$ = -36.2 × 10^{-9} m^2 V^{-1} s^{-1}, pK_a = 9.23) and 700 mM tris ($\mu_{ep,\,tris}$ = 29.5 × 10^{-9} m^2 V^{-1} s^{-1}, pK_a = 8.07). The sample matrix consisted of various concentrations of formic acid ($\mu_{ep,\,for}$ = -56.6 × 10^{-9} m^2 V^{-1} s^{-1}, pK_a = 3.75), 10 mM sodium cyanoborohydride ($\mu_{ep,\,Na}$ = 55 × 10^{-9} m^2 V^{-1} s^{-1}, $\mu_{ep,\,cyano}$ = -20 × 10^{-9} m^2 V^{-1} s^{-1}), 2 μM 5-aminofluorescein ($\mu_{ep,\,amfl}$ = 6.67 × 10^{-9} m^2 V^{-1} s^{-1}, pK_{a1} = 4.56, pK_{a2} = 9.36) and 0.3 μM of glucose, lactose, and maltotriose ($\mu_{ep,\,glu}$ = 6.23 × 10^{-9} m^2 V^{-1} s^{-1}, $\mu_{ep,\,lac}$ = 5.78 × 10^{-9} m^2 V^{-1} s^{-1}, $\mu_{ep,\,mal}$ = 5.34 × 10^{-9} m^2 V^{-1} s^{-1}, pK_{a1} = 4.56, pK_{a2} = 9.36 for all derivatised sugars). Electrophoretic mobilities were based on those estimated from experimental data or obtained from the literature [31, 32].

3.3 Results and discussion

The approach taken in the work was to improve the sensitivity of carbohydrate analysis by incorporating a highly absorbing, ionisable chromophore, 5-

aminofluorescein, as well as through clever optimisation of the chemistry to avoid dilution of the sample after derivatisation through application of pH stacking. The following sections describe the strategy taken to improve each of these components of the separation system.

3.3.1 Detection choice (LED versus DAD)

LEDs offer several advantages over conventional mercury and D_2 light sources used for absorbance detection in CE and it is possible to achieve improvements in sensitivity by 1 to 2 orders of magnitude simply by using an LED as a light source. The derivatisation reagent selected in this work is 5-aminofluorescein, which has a maximum absorptivity at 492 nm. There are a number of commercially available LEDs with an output in this region with the specifications provided by the manufacturers shown in Table 3.1 as well as the experimentally measured output wavelength.

Table 3.1. LED product description.

LED part number	Manufacturer wavelength (nm)	Measured wavelength (nm)	Current (mA)	Luminous intensity max (mcd[a])
ZQ 0182	474	472	40	-
332-4515	475	481	40	4,860
366-4600	488	506	40	3,490
857-6807	505	516	40	21,000

[a] Millicandles

The experimentally measured wavelength agrees closely with the manufacturers for some LEDs, but is significantly different for others. The relevance of this can be seen from Figure 3.1which shows the spectral overlap of 5-aminofluorescein with these LEDs.

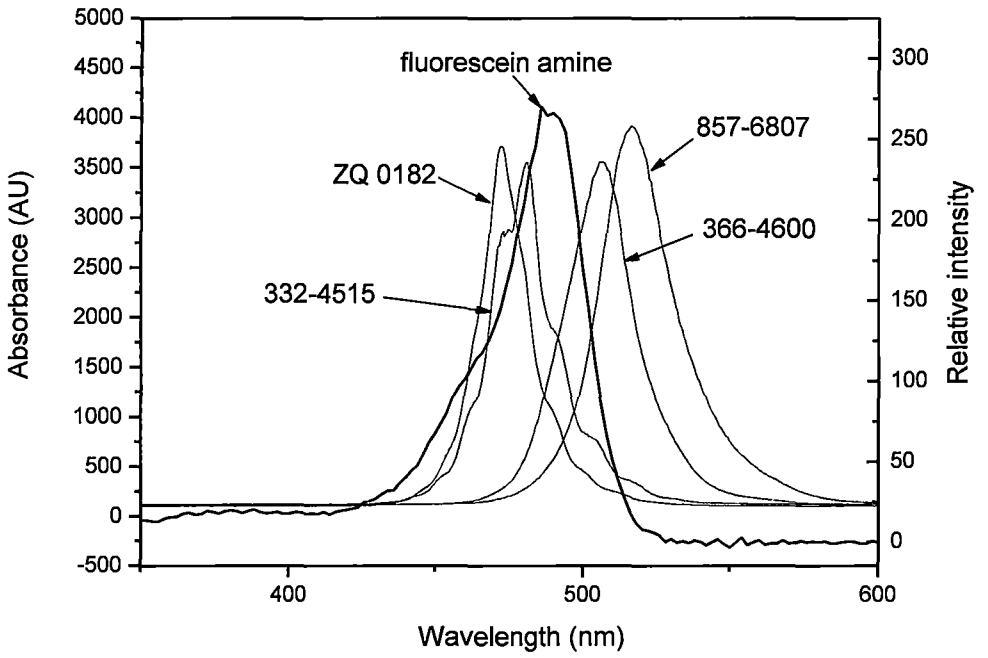

Figure 3.1. Overlay of the absorption spectra of 5-aminofluorescein with the emission spectra of the four LEDs used in this work. Buffer conditions as per "Preparation of background electrolyte section".

The spectra for the 5-aminofluorescein derivatised carbohydrates are not shown due to their identical absorption as 5-aminofluorescein. It can be seen from Figure 3.1. that LED 332-4515 shows the best spectral match, however it is not just the spectral match that is important – it is also the intensity and the noise of the LED that affects sensitivity, which can only truly be determined with appropriate experiments. Separations performed to examine this are shown in Figure 3.2.

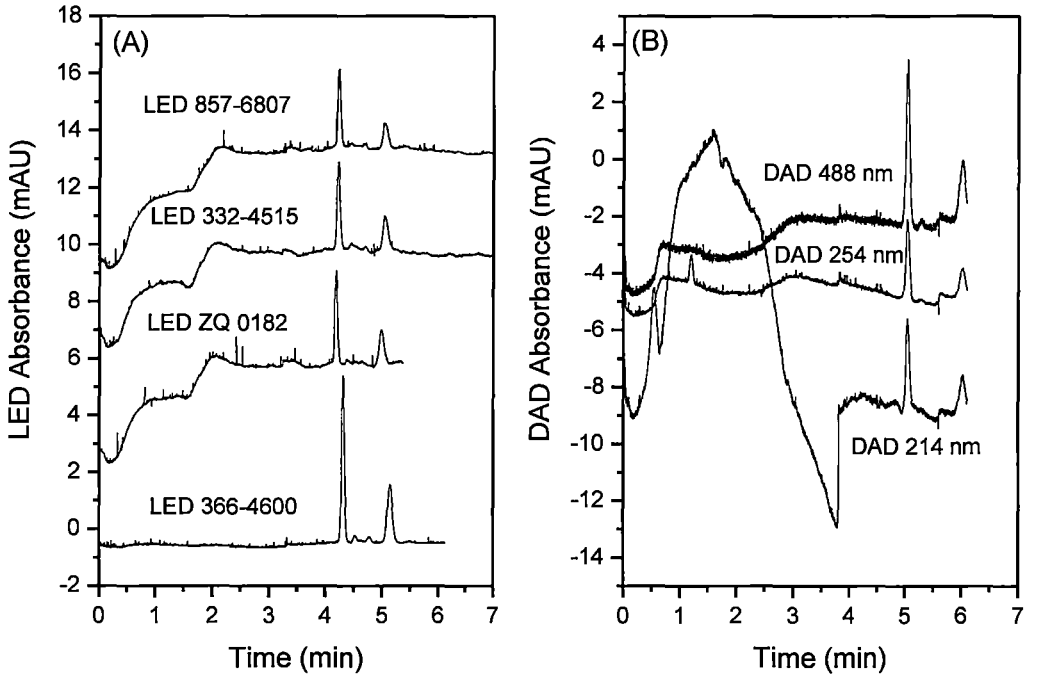

Figure 3.2. Comparison of different (A) LEDs and (B) DAD signal output using a sample of 5-aminofluorescein labelled to glucose (5-aminofluorescein at ≈ 4.4 min, glucose adduct at ≈ 5.5 min) . Conditions: capillary, fused silica (50 μm I.D.), 60 cm (46.5 cm effective length to the LED and 52.1 cm effective length to the DAD); electrolyte 100 mM boric acid, pH 9.2; current -43 μA, voltage -30 kV; injection 100 s at 50 mbar, temperature, 30°C; detection, LED 857-6807, 332-4515, ZQ 0182, 366-4600; DAD at 488 nm, 254 nm, 214 nm.

Comparison of the signal-to-noise ratio highlights that LED 366-4600 proves to be superior showing at least three times improvement when comparing with the second best LED 857-6807, 25 times better sensitivity than DAD and 515 times improvement factoring sensitivity when compared to a normal D_2 lamp . This LED shows better sensitivity when compared to the DAD mainly due to marginally lower noise. This highlights the need to examine a number of LEDs for each specific application as technical details provided from the manufacturer cannot necessarily be used to obtain the best system. In fact Table 3.1shows that the LED with the lowest luminous intensity shows the highest signal to noise ratio which highlights the importance of the LED testing. This LED, 366-4600 was used throughout the remainder of the study.

3.3.2 Dynamic pH junction preconcentration technique

Having determined the appropriate LED to use, experiments were undertaken to improve the sensitivity of the system *via* the use of on-line stacking. Due to the acidic nature of the sample matrix required for reductive amination, stacking employing a dynamic pH junction is the most obvious on-line approach to improving the sensitivity. The mechanism of dynamic pH junction is shown in Figure 3.3 in which the sample has a distinctly different pH to that of the separation electrolyte. As the sample is positioned in the capillary between the borate/tris electrolyte, application of electric field causes borate and acetate ions to move to the anode while tris and hydrogen travel to the cathode, creating a pH junction interface (1). Such arrangement and mobility of ions results in formation of the rear and the front boundaries which are responsible for the pH stacking mechanism. The rear boundary located closer to the inlet (cathode) is a product of the neutralisation reaction between borate and hydrogen, while the front boundary is established due to reaction

between acetate and tris (2). In order for the sample to stack, the rear boundary must move quicker than the front boundary towards the anode to consume the sample matrix and concentrate the sample analytes around the moving pH boundary (3). While the rear boundary is moving through the sample plug the analytes originally in the low pH zone become exposed to the high pH electrolyte. The derivatised analytes bear a double negative charge, as well as additional effect of borate complexation, allowing significant electrophoretic mobility which enables the analytes to move back into the low pH zone. As this boundary moves through the low pH sample zone, analytes concentrate around this moving pH boundary. Of critical importance to this mechanism are the electrophoretic mobilities of the analytes in both the low and high pH electrolytes, as well as the actual velocity at which the pH boundary moves. Once the entire sample has been stacked, the boundary must be allowed to dissipate so that the analytes can separate on the basis of their electrophoretic mobilities (4).

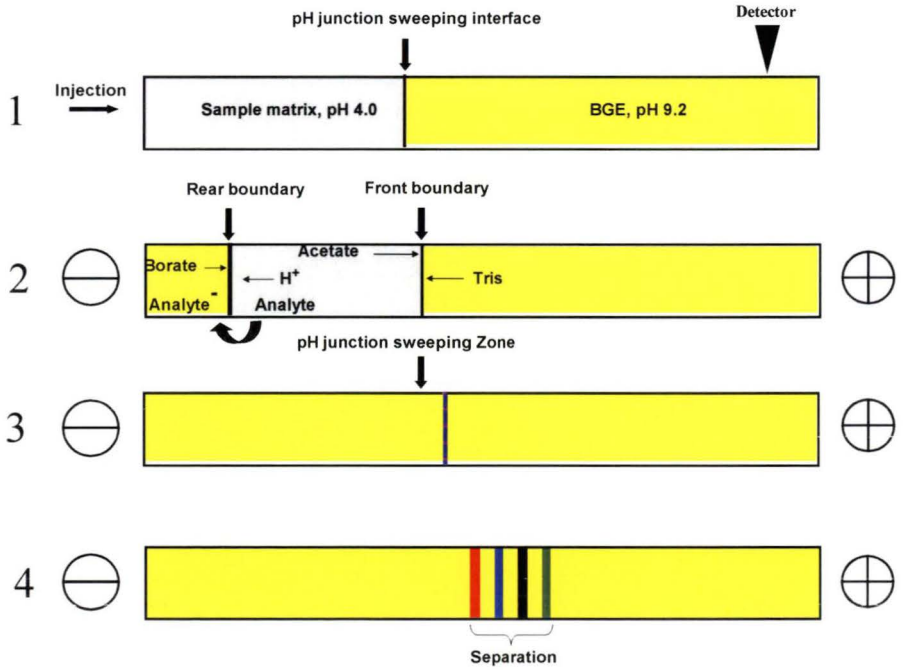

Figure 3.3. Mechanism of stacking *via* dynamic pH junction mode where 1: sample is injected into capillary, 2: formation of rear and front boundary resulting in stacking of the analytes, 3: formation of pH junction sweeping zone after the sample has stacked, 4: separation and detection of the analyte.

3.3.3 Sample composition and stacking *via* dynamic pH junction mode

When employing stacking with a dynamic pH junction, it is essential to be able to control the velocity and duration of the pH boundary to ensure that all of the analytes across the entire sample zone are stacked. This is controlled by the concentration of the separation electrolyte and the sample matrix composition. In this case, the sample matrix cannot simply be varied to enhance stacking without considering the derivatisation reaction between 5-aminofluorescein and carbohydrates. The conditions for both stacking and reductive amination have to be met to ensure sensitive, well resolved separation of the analytes. To understand the best conditions for the labelling and separation of carbohydrates, a mixture of glucose, lactose and maltotriose hydrate was derivatised using 5-aminofluorescein in conditions similar to those reported previously [4-7]. This sample was then injected neat, diluted by 10 and 100 times and the derivatised carbohydrates separated by CE. It must be recognised that dilution of the sample was undertaken to optimise the amount of acid in the sample to control the movement of the boundaries and hence the ability of these systems to stack the derivatised carbohydrates. Without dilution, the concentration of acetic acid in the sample is 190 mM (pH 3.05) and is 1.9 mM (pH 3.70) after dilution by 100. The results of various dilutions can be seen in Figure 3.4, which shows the injection of 7% of the capillary volume (to the window) of undiluted sample, 37% of the 10 times diluted sample and 97% of the 100 times dilution.

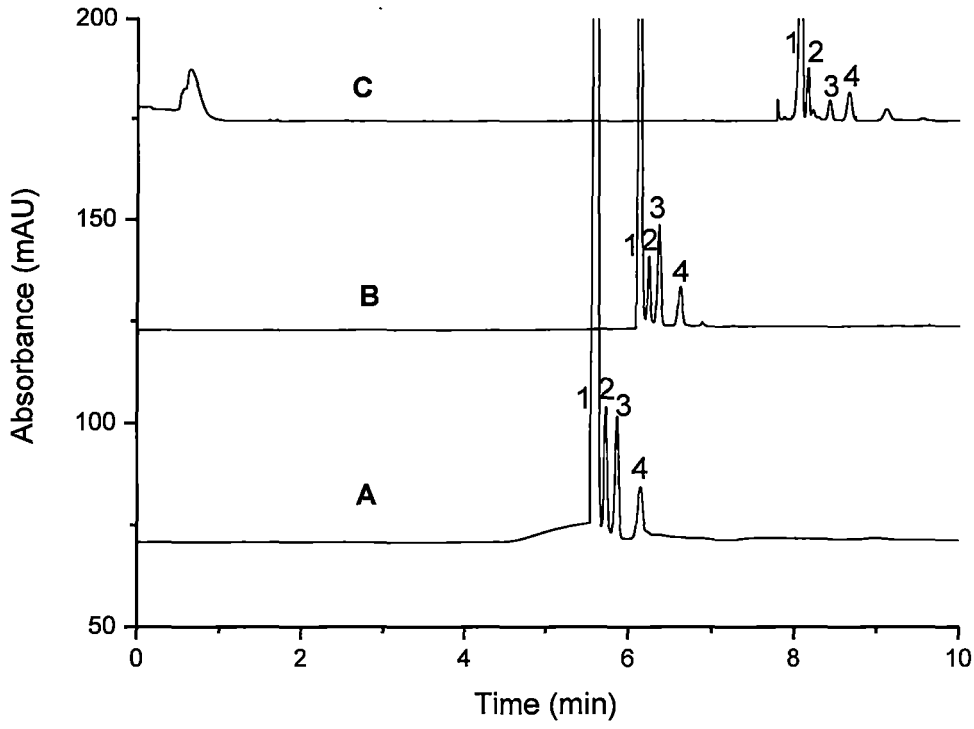

Figure 3.4. An electropherogram showing separations of 5-aminofluorescein and the labelled carbohydrates: 1: 5-aminofluorescein, 2: glucose, 3: lactose, 4: maltotriose hydrate. A) a maximum injection of 15 s for the undiluted sample (5×10^{-3} M 5-aminofluorescein, 5×10^{-4} M of each sugar, in reaction mix), pH 3.10; current -18 μA. B) a maximum injection of 80 s for the 10 times dilution (5×10^{-4} M 5-aminofluorescein and 5×10^{-5} M of each sugar, in reaction mix), pH 3.05; current -20 μA. C) a maximum injectionof 210 s for the 100 times dilution (5×10^{-5} M 5-aminofluorescein and 5×10^{-6} M of each sugar, in reaction mix), pH 3.7; current -22 μA. Conditions: capillary, fused silica (50 μm I.D.); 40 cm (26.5 cm effective length); electrolyte 100 mM boric acid, pH 9.2; voltage -20 kV; injection at 50 mbar; temperature, 30°C; detection, LED 366-4600.

The outcomes of the three injections suggest that that the dilution of the sample and therefore the use of a sample comprising of 1.9 mM acetic acid concentration enables larger injection volumes without substantial deterioration in resolution. The use of similar conditions which contain 1.9 mM acid in the labelling reaction highlights the possibility of directly injecting extremely large injection volumes of thederivatisation mixture without dilution, which should lead to superior sensitivity. These 100 times dilution conditions will be adopted and explored in the next section to obtain better stacking and separation.

The separation obtained from such incredibly large injection of 97% to the capillary window requires some discussion, especially given that there was no significant loss in resolution between the 3 separations and that the end of the sample zone was positioned almost to the detection window leaving very little of the capillary available for electrophoretic separation. We believe that upon application of the voltage, a small residual cathodic EOF is present which causes the entire sample zone to move back towards the inlet, essentially removing the sample matrix from the capillary in an analogous manner to LVSS. This is supported by monitoring the current. Initially a low current of around -5 μA was observed for the first 2 min followed by a rapid increase to -35 μA after 4 min, after which the current was stable and constant for the remainder of the separation. This change in current is indicative of the low conductivity sample zone being removed under EOF. This has the added advantage of concentrating the sample where the rear sample boundary responsible for stacking the analytes is moving towards the detector while the front boundary is being pushed back by the EOF. Ultimately the sample length is shortened producing extra length for electrophoretic separations to maintain the high resolution.

Table 3.2. Efficiency parameters for the 0, 10, 100, dilution samples obtained from Figure 3.4.

Analyte	Efficiency (no dilution) plate number	Efficiency (10 dilution) plate number	Efficiency (100 dilution) plate number
5-Aminofluorescein	39,100	141,800	163,000
Glucose	120,000	201,000	361,000
Lactose	77,600	117,300	162,800
Maltotriose	52,100	80,200	101,100

Table 3.2 shows the efficiencies calculated for the peaks obtained in Figure 3.4 with results suggesting that working at low ionic strength conditions such as the 10 and 100 times dilution sample enables separations to be achieved from large injection volumes with no significant loss in efficiencies. While in this case, dilution of the sample resulted in a reduction in sensitivity as the derivatised sugars were also diluted, it is important to note that these experiments were designed to determine the amount of acid in the sample necessary for large sample volumes to be injected without a loss of separation efficiency. The outcomes of the results also suggest that the concentrations of the carbohydrates and the label in the 100 times dilution will be used in the later separations due to excellent separation efficiencies.

3.3.4 Effect of acetic and formic acids on separation performance and sensitivity

While the amount of acid present in the sample is important for stacking with a dynamic pH junction, it is also important for reductive amination. To examine this effect, we derivatised three mixtures of carbohydrates with 190 mM, 19 mM and 1.9 mM acetic acid containing 100 mM, 10 mM and 1 mM of sodium cyanoborohydride

added accordingly, which had pH values of 3.05, 3.70 and 4.35, respectively. These concentrations match the concentration of acetic acid examined in Figure 3.4 while the injection time was kept constant at 100 s for all three injections. The concentration of sugars and the label were kept in accordance with the 100 times dilution as shown in Figure 3.4 C. With 190 mM acetic acid in the sample only one peak was observed (Figure 3.5 A), while samples containing 19 mM and 1.9 mM acetic acid had poorly resolved separations with a number of peaks as demonstrated in Figure 3.5.

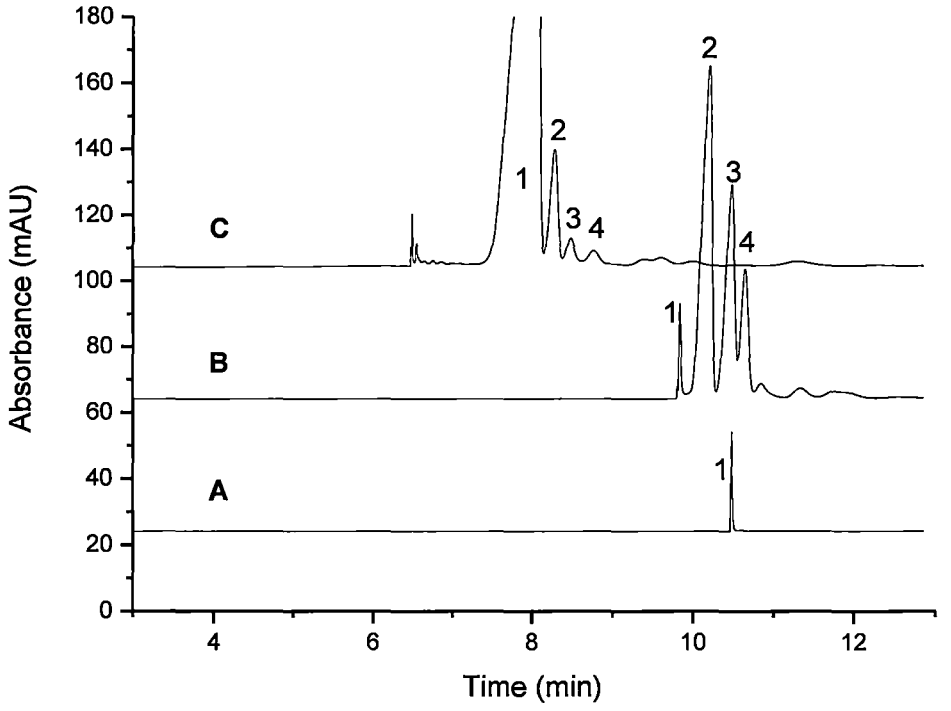

Figure 3.5. An electropherogram showing separations at different acetic acid concentrations (sample mixture of 5×10^{-4} M 5-aminofluorescein and 5×10^{-5} M of each sugar, in reaction mix) where 1: 5-aminofluorescein, 2: glucose, 3: lactose, 4: maltotriose. A) 190 mM acetic acid, pH 3.05; current -21 μA; B) 19 mM acetic acid, pH 3.70; current -22 μA; C) 1.9 mM acetic acid, pH 4.35; current -22 μA. Other conditions as per Figure 3.4.

The presence of one peak in the 190 mM acetic acid is unlikely to be due to insufficient derivatisation of the carbohydrates as peaks were obtained at lower concentrations suggesting that the problem was the movement of the pH boundary which governs the stacking in the system. It is important to note that this system is not completely identical to that conducted in Figure 3.4 as the samples were injected with no dilution into the instrument, while in Figure 3.4 the same sample was injected straight, diluted 10 and 100 times to achieve the shown separations.

While these results suggested that the carbohydrates were suitably derivatised and that the movement of the pH boundary was adequately controlled for stacking with a dynamic pH junction, having a weak acid such as acetic acid (pK_a 4.76) [33] presents the possibility that the derivatised carbohydrates may still be moving in the sample zone. As a result some of the carbohydrates will be focused at the boundary while the remainder would migrate through the sample zone into the separation electrolyte and never be stacked. This potential problem may be overcome by the use of a similar but stronger acid such as formic acid (pK_a 3.75) [33] to create a pH boundary between the buffer and the sample plug. Experiments using 190 (pH 2.40), 19 (pH 2.60) and 1.9 (pH 3.20) mM formic acid in the sample were undertaken and the results are shown in Figure 3.6.

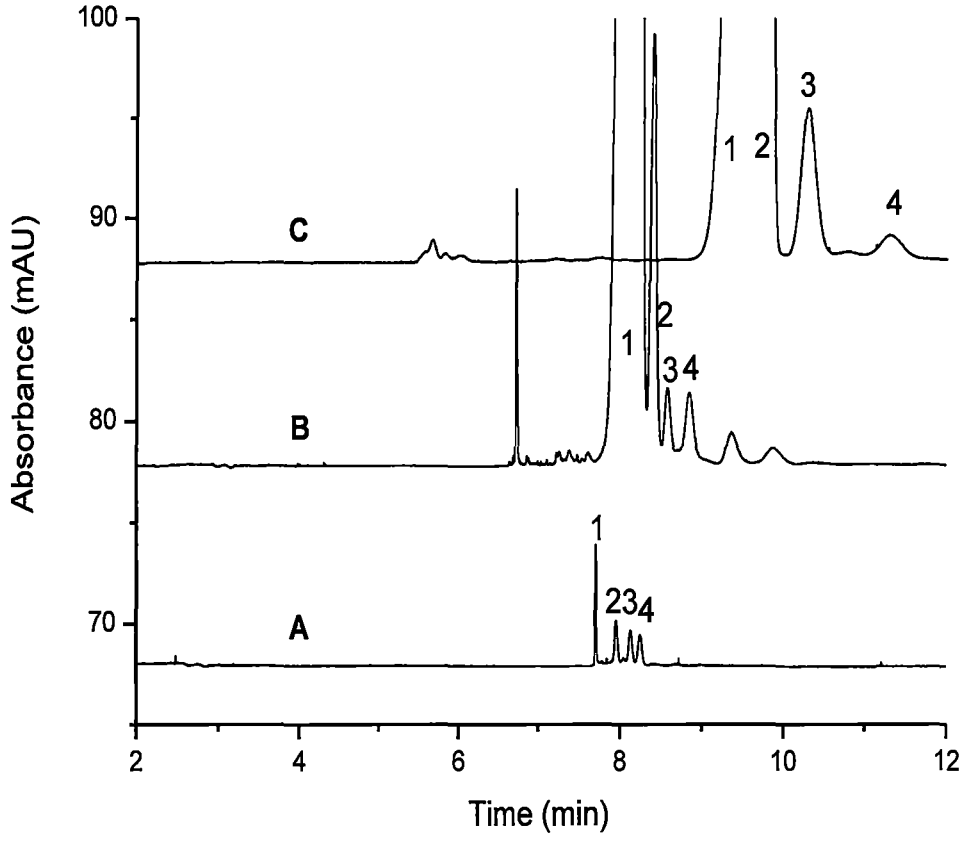

Figure 3.6. An electropherogram showing separations at different formic acid concentrations (sample mixture of 5×10^{-4} M 5-aminofluorescein and 5×10^{-5} M of each sugar, in reaction mix) where 1: 5-aminofluorescein, 2: glucose, 3: lactose, 4: maltotriose. A) 190 mM formic acid, pH 2.40; current -21 μA; B) 19 mM formic acid, pH 2.60; current -22 μA; C) 1.9 mM formic acid, pH 3.21; current -22 μA. Other conditions as per Figure 3.4.

Using formic acid at a concentration of 190 mM we obtained separation of the three analytes which was previously not possible with acetic acid at the same concentration (Figure 3.5) strongly suggesting the involvement of the pH boundary in the system, however these peaks were much smaller than those obtained with lower concentrations of acid. Similar to the results obtained using acetic acid, we noticed a significant change in sensitivity when the concentration of acid was decreased to 19 and 1.9 mM. While the separations with 19 and 1.9 mM formic acid were similar with regard to sensitivity, the resolution with 19 mM was visibly better. In addition, considering lactose, chosen as the most pronounced carbohydrate in all three electropherograms, efficiencies of 28,800 plates in the 19 mM formic acid and 5,600 plates in the 1.9 mM formic acid were recorded. Furthermore, the diminished sensitivity of the 190 mM did result in the highest efficiency with 72,400 plates. We speculate that the decrease in sensitivity at higher formic acid concentration is observed as a result of altered boundary movement and decreased absorption or 5-aminofluorescein at low pH. To confirm and better explain the above experimental observations computational studies were conducted.

3.3.5 Simulation studies

In order to understand the origin of the change in sensitivity with different amounts of formic acid in the sample, computer simulations were performed. Physicochemical parameters for the system were taken from the literature and experimental data to approximate as closely as possible the model to the experimental system used in this work. Figure 3.7 shows simulation results of 5-aminofluorescein derivatised glucose with 190, 19 and 1.9 mM formic acid in the sample. Each panel shows the position along the capillary of one derivatised carbohydrate every 0.1 min for 1.0 min after the application of voltage. It can be seen

from the panels with 19 mM (B) and 1.9 mM (C) formic acid, as the pH boundary moves through the sample zone, the glucose peak stacks into a very sharp peak, however when 190 mM formic acid (A) is used, there is no sharp peak and only small peaks are observed outside the sample zone.

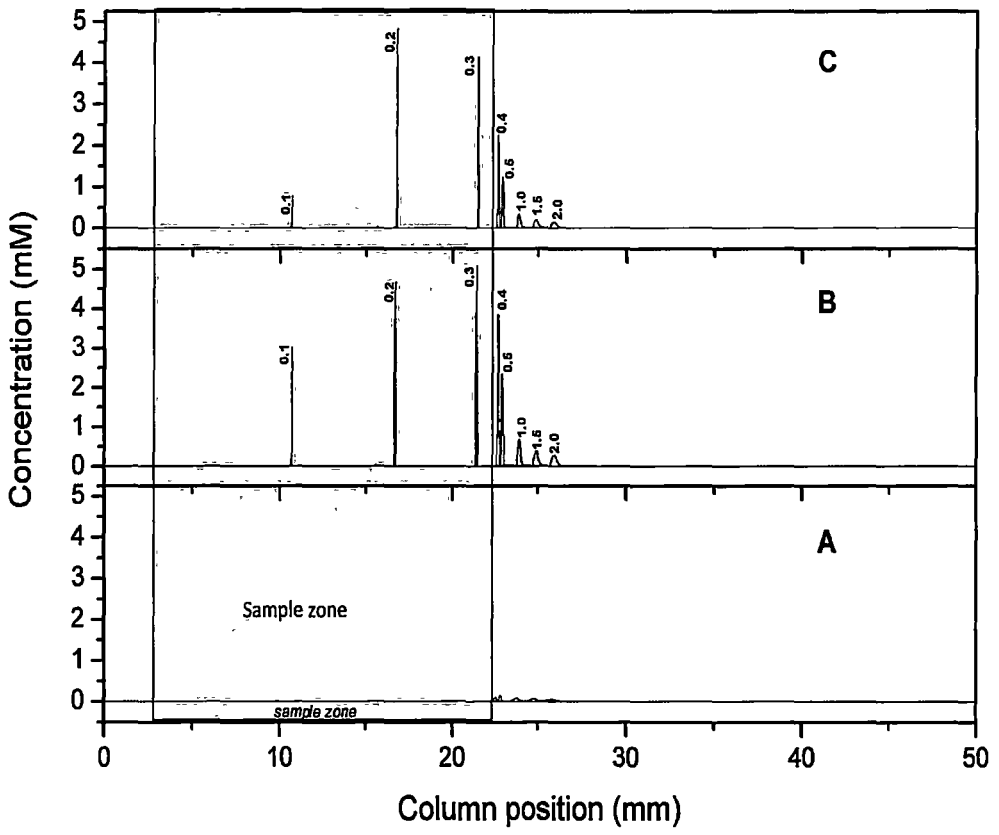

Figure 3.7. Simulation results for A) 190 mM formic acid, B) 19 mM formic and C) 1.9 mM formic acid concentration of the sample mix. Each panel shows the position of glucose derivatised with 5-aminofluorescein every 0.1 min for 1.0 min after the application of voltage. The shaded section indicates the original position of the sample zone. Full details can be found in section 3.2.5.

This is entirely consistent with the experimental results and analysis of the sample and electrolyte data reveal that the pH boundary does not have the correct velocity to stack the derivatised carbohydrates. With 19 mM formic acid the peak height is increasing until 0.3 min after which it has reached the end of the low pH sample zone after which it de-stacks and the peaks broaden between 0.4 and 2 min. This broadening occurs as the stacked analytes stop being focused around the pH boundary and start to migrate according to conventional zone electrophoresis principles. With 1.9 mM formic acid in the sample, the peak is slightly lower at 0.3 min when compared to 0.2 min suggesting that the zone has started to de-stack. This result must however be interpreted with caution as it may be an artefact due to the restricted number of segments into which the capillary is divided imposed by computational resources. It is also necessary to note that the simulation cannot account for complexation with borate, which is known to occur with carbohydrates and will have an additional impact upon the stacking [12, 34]. Nevertheless, the simulation results are in excellent agreement with the experimental results suggesting that the change in sensitivity is most likely due to alteration of the movement of the pH boundary.

Given both the experimental and simulation studies show a sharp discontinuity in terms of stacking between 190 mM (A) and 19 mM (B) formic acid, this region should provide the most optimal conditions with fine sensitivity and superior resolution. Experiments were undertaken in this region at 95 mM formic acid producing superior separations and this concentration of acid was used for further studies.

3.3.6 Conditions and analytical performance of the optimum system

It is important to note that the current study does not provide a completely optimised method for the separation of simple sugars. It is intended as a fundamental study that effectively introduces a new strategy to improve the detection sensitivity of derivatised carbohydrates using simple absorbance detection based on the combination of an LED detector and the use of on-line stacking *via* a dynamic pH junction. Nevertheless, the most suitable conditions applied to the system were as follows: LED 366-4600; fused silica capillary 40 cm × 50 μm I.D.; BGE consisting of 100 mM boric acid and tris at pH 9.2; temperature 30°C; voltage -20 kV as shown in Figure 3.8.

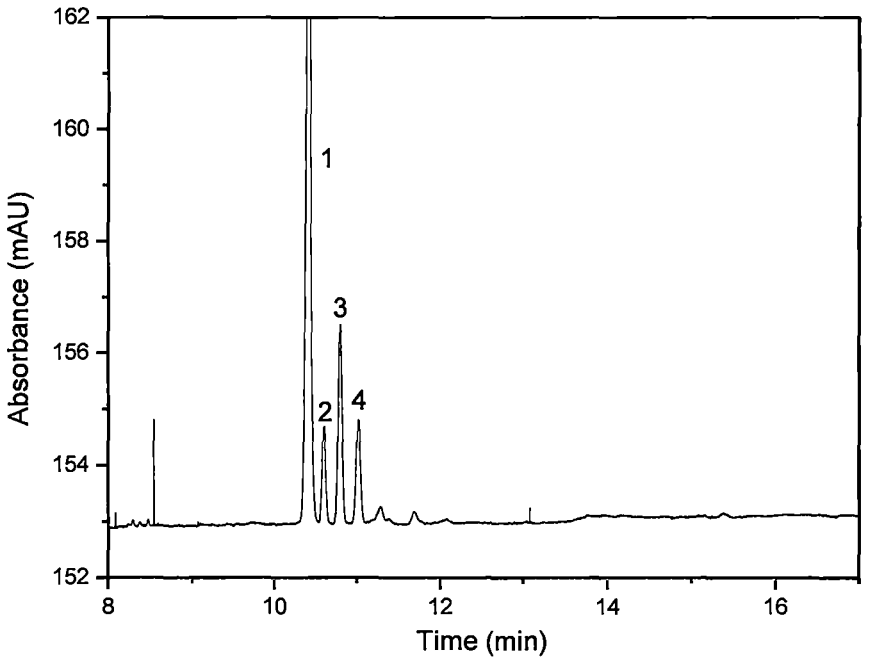

Figure 3.8. An electropherogram showing a separation at 95 mM formic acid (1 × 10^{-5} M 5-aminofluorescein and 1 × 10^{-6} M of each sugar, in reaction mix), pH 2.40, where: 1: 5- amino fluorescein, 2: glucose, 3: lactose, 4: maltotriose. Conditions: capillary, fused silica (50 μm I.D.), 40 cm (26.5 cm effective length); electrolyte 100 mM boric acid, pH 9.2; current -16 μA; voltage -20 kV; injection at 50 mbar 100 s, temperature, 30°C; detection; LED 366-4600.

In this system the separation efficiencies were calculated for each of the analytes to give: glucose = 197,600 plates, lactose = 163,600 plates, maltotriose = 140,000 plates and baseline resolution was achieved for all the analytes. The LODs of the carbohydrates for the above separation were in the order of 8.5×10^{-8} M for glucose and maltotriose, and 4.2×10^{-8} M for lactose, while the literature values reported for APTS labelled glycans by Guttman [16] demonstrated LODs in the order of 5×10^{-10} M. Comparison of the current results with the conventional small injections using a D_2 lamp and an LED as reported by Momenbeik *et al.*, shows a 515 times and 16 times improvement in sensitivity, respectively [34]. This improvement is predominantly due to the ability to directly inject large volumes of the derivatisation mixture without dilution and to stack the analytes using a dynamic pH junction. The lactose peak recorded in Figure 3.8 is larger than the glucose and maltotriose peaks due to either better labelling under reductive amination or improved stacking, however future studies are required to prove the speculations. Using this method the relative standard deviation (RSD) of the migration time and peak area was 0.49-0.94% and 1.1-6.0% respectively. Full optimisation of the current system and its application in LIF detection has a great potential to further enhance the LODs to even lower levels.

3.4 Conclusion

The current study successfully emphasises the utility of pH stacking mode highlighting superior efficiencies in the order of 150,000 plates and detection limits in the order of 8.5×10^{-8} M using simple absorbance detection. The work also emphasised the ability to inject large volumes of undiluted samples, whereby outstanding sensitivity was achieved. Incorporation of LEDs provided highly sensitive detection comparable with other LED and fluorescence-based detection

systems and routinely proved to be at least 25 times better then the commercially available DAD system. Using 5-aminofluorescein as the chromophore, which is a proxy for similar fluorophores based on the fluorescein moiety, also demonstrates the potential to directly translate this methodology to LIF detection for ultra-sensitive detection, as will be discussed in the following chapters, in addition to the applicability to more complex carbohydrate units.

3.5 References

(1) Dang, F.; Zhang, L.; Hagiwara, H.; Mishina, Y.; Baba, Y. *Electrophoresis* **2003**, *24*, 714-721.

(2) Sluszny, C.; He, Y.; Yeung, E. S. *Electrophoresis* **2005**, *26*, 4197-4203.

(3) Xiao, D.; Zhao, S. L.; Yuan, H. Y.; Yang, X. P. *Electrophoresis* **2007**, *28*, 233-242.

(4) Guttman, A.; Chen, F. T. A.; Evangelista, R. A.; Cooke, N. *Anal. Biochem.* **1996**, *233*, 234-242.

(5) O'Shea, M. G.; Samuel, M. S.; Konik, C. M.; Morell, M. K. *Carbohyd. Res.* **1998**, *307*, 1-12.

(6) Suzuki, H.; Muller, O.; Guttman, A.; Karger, B. L. *Anal. Chem.* **1997**, *69*, 4554-4559.

(7) Evangelista, R. A.; Liu, M. S.; Chen, F. T. A. *Anal. Chem.* **1995**, *67*, 2239-2245.

(8) Breadmore, M. C. *Electrophoresis* **2007**, *28*, 254-281.

(9) Mala, Z.; Krivankova, L.; Gebauer, P.; Bocek, P. *Electrophoresis* **2007**, *28*, 243-253.

(10) Yu, L. J.; Li, S. F. Y. *Electrophoresis* **2005**, *26*, 4360-4367.

(11) Britz-McKibbin, P.; Terabe, S. *J. Chromatogr. A* **2003**, *1000*, 917-934.

(12) Stefansson, M., Novotny, M. *Anal. Chem.* **1994**, *66*, 1134-1140.

(13) Franz, A. H.; Molinski, T. F.; Lebrilla, C. B. *J. Am. Soc. Mass Spectr.* **2001**, *12*, 1254-1261.

(14) Hase, S.; Ikenaka, T.; Matsushima, Y. *J. Biochem.* **1981**, *90*, 407-414.

(15) Zhang, M. Q.; Melouk, H. A.; Chenault, K.; El Rassi, Z. *J. Agr. Food Chem.* **2001**, *49*, 5265-5269.

(16) Rethfeld, I.; Blaschke, G. *J. Chromatogr. B* **1997**, *700*, 249-253.

(17) Guttman, A. *J. Chromatogr. A* **1997**, *763*, 271-277.

(18) Vinogradov, E.; Bock, K. *Carbohyd. Res.* **1998**, *309*, 57-64.

(19) Momenbeik, F., Johns, C., Breadmore, M. C., Hilder, E. F., Macka, M., Haddad, P. R. *Electrophoresis* **2006**, *27*, 4039-4046.

(20) Westfall, D. A.; Flores, R. R.; Negrete, G. R.; Martinez, A. O.; Haro, L. S. *Anal. Biochem.* **1998**, *265*, 232-237.

(21) Brando, T.; Pardin, C.; Prandi, J.; Puzo, G. *J. Chromatogr. A* **2002**, *973*, 203-210.

(22) Johns, C.; Macka, M.; Haddad, P. R. *Electrophoresis* **2004**, *25*, 3145-3152.

(23) King, M.; Paull, B.; Haddad, P. R.; Macka, M. *Analyst* **2002**, *127*, 1564-1567.

(24) Rohr, T.; Hilder, E. F.; Donovan, J. J.; Svec, F.; Frechet, J. M. J. *Macromolecules* **2003**, *36*, 1677-1684.

(25) Hjerten, S. *J. Chromatogr.* **1985**, *347*, 191-198.

(26) Bier, M.; Palusinski, O. A.; Mosher, R. A.; Saville, D. A. *Science* **1983**, *219*, 1281-1287.

(27) Mosher, R. A.; Gebauer, P.; Thormann, W. *J. Chromatogr.* **1993**, *638*, 155-164.

(28) Mosher, R. A.; Gebauer, P.; Caslavska, J.; Thormann, W. *Anal. Chem.* **1992**, *64*, 2991-2997.

(29) Mosher, R. A.; Dewey, D.; Thormann, W.; Saville, D. A.; Bier, M. *Anal. Chem.* **1989**, *61*, 362-366.

(30) Breadmore, M. C.; Mosher, R. A.; Thormann, W. *Anal. Chem.* **2006**, *78*, 538-546.

(31) Pospichal, J.; Gebauer, P.; Bocek, P. *Chem. Rev.* **1989**, *89*, 419-430.

(32) Krivankova, L.; Brezkova, M.; Gebauer, P.; Bocek, P. *Electrophoresis* **2004**, *25*, 3406-3415.

(33) Dean, J. A. *Lange's Handbook of Chemistry / John A. Dean*, 14 ed.; McGraw-Hill: New York, 1992.

(34) Hoffstetterkuhn, S.; Paulus, A.; Gassmann, E.; Widmer, H. M. *Anal. Chem.* **1991**, *63*, 1541-1547.

Chapter 4

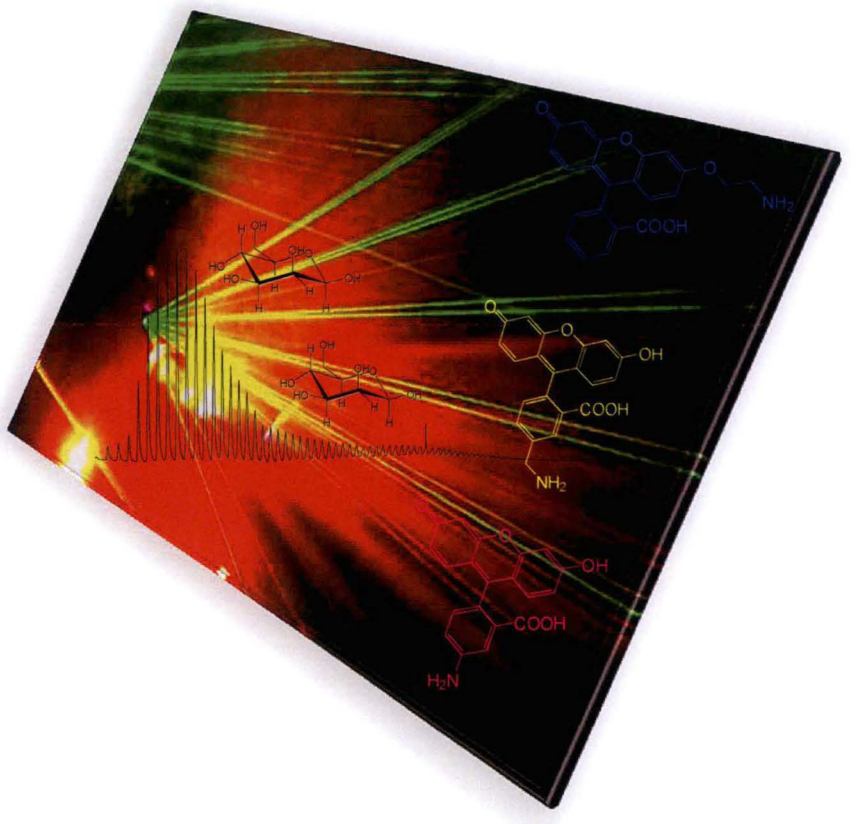

4 Development of a novel fluorescent tag O-2-[aminoethyl]fluorescein for the electrophoretic separation of oligosaccharides

4.1 Introduction

The use of LIF is quite attractive as it provides extremely low LODs allowing better insight into carbohydrate analysis. Some applications requiring sensitive detection are related to characterisation of rice starch and elucidation of its structure. Currently some complex sugars can not be seen in the rice starch profile due to either their absence or inability to be detected. Highly sensitive systems are therefore required to answer these questions.

Derivatisation reagents must not only have good fluorescence properties, but they must also contain a charged group to allow the carbohydrates to be separated by electrophoresis. Taking these factors into consideration fluorescein with its QY of 0.95 is seen as a useful fluorescent molecule and a fluorescein-based carbohydrate reagent would have some appeal. Its QY is significantly higher than for APTS (QY of 0.37) , implying enhanced fluorescence, followed by better suitability for the argon laser and a high molar absorptivity in the range of 80,000 L $mol^{-1}cm^{-1}$ [1]. The fluorescent tag also has charge bearing carboxylic acid and phenol functions, introducing mobility for electrophoretic studies. However some modifications are required to introduce the amino function necessary for labelling. Recent studies by Du *et al.* showed that a fluorescein backbone is gaining growing popularity for HPLC applications where they synthesised a 6-oxy-(acetyl ethylenediamine)fluorescein derivative and successfully labelled 12 fatty acids. Deng *et al.* also prepared a fluorescein derivative, namely *N*-hydroxy-succinimidyl

fluorescein-*O*-acetate and applied it to quantitate biogenic amines with impressive 0.2-0.4 nM LODs [2, 3].

This current study proposes a method for synthesising fluorescent tags based on the commercially available, yet expensive, aminomethylfluorescein as a model. The fundamental design of the molecule considers three main elements: a fluorescent moiety, a spacer and a reactive group where the latter group is an amine that can undergo reductive amination to label carbohydrates. Typically fluorescein derivatives have the functional groups attached at the benzene moiety, which allows dianion formation **II**, however an alternative approach is investigated to incorporate the spacer and the reactive group assembly onto the phenolic site of the fluorescein as shown in **I** Figure 4.1. Such attachment modified the charge bearing phenolic function, resulting in formation of a monoanion, therefore reducing the mobility of the tag, but still making it suitable for CE analysis.

Ideally the synthetic approach adopted would be flexible where a specific intermediate substrate could be modified to construct an assortment of fluorescent analogues, with varied spacer groups. The advantage of the spacer assembly is evident since steric effects are minimised, resulting in a more nucleophilic aliphatic amine, which should provide better labelling efficiency and reactivity. Also by separating the amine from the fluorophore there is no fluorescence quenching due to the reduced donor effects from the amine group [4].

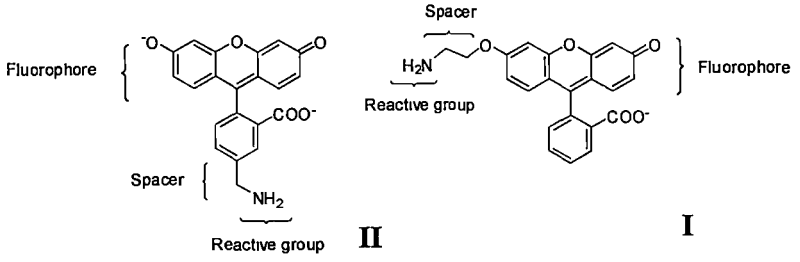

Figure 4.1. Fundamental design of the molecule consisting of three main elements: a fluorescent moiety, a spacer and a reactive group.

This study also evaluates the ability of the newly synthesised tag to label and separate a range of oligosaccharides obtained from corn syrup. To ensure that a meaningful assessment of the tag is made other fluorescein-based motifs are incorporated and compared throughout the study.

4.2 Experimental

4.2.1 General procedures and materials

Commercially available sources were used to purchase reagents and materials. There was no further purification of the reagents unless stated otherwise in the study.

Proton (^{1}H) and carbon (^{13}C) NMR spectroscopy were recorded on a Varian Mercury 2000 Spectrometer operating at a frequency of 300 MHz and 75 MHz respectively. Chemical shifts were recorded as δ values in parts per million (ppm) with a reference to the solvent applied. The solvents used were deuterated chloroform ($CDCl_3$), and dimethyl sulfoxide (DMSO-d_6). The following abbreviations are used to assign ^{1}H NMR spectra: singlet (s[a]); doublet (d); doublet of doublets (dd); triplet (t); broad doublet (bd); broad singlet (bs); multiplet (m); coupling constant (*J*) (Hertz).

A Perkin Elmer FT-IR spectrophotometer Paragon 1000, was used to record infrared spectra. Solids and liquids were recorded as thin films on sodium chloride plates unless stated otherwise.

A Finnigan LCQ ion trap mass spectrometer with electrospray ionisation source was used to determine molecular weights of compounds. The samples were diluted in water and nebulised at 20 μL min^{-1} with a needle voltage of 4.9 kV, and a capillary

[a] When assigning ^{1}H NMR spectra "s" refers to "singlet", while any other use of "s" refers to "seconds".

temperature of 21°C. The experiments were conducted under an inert atmosphere of N_2 gas.

Fluorescence spectra were recorded using a Perkin-Elmer 650-10S Fluorescence Spectrophotometer where the scanning rate of emission wavelength was set to 300 nm min^{-1}.

A Shimadzu UV-Visible Recording Spectrophotometer UV-160 was utilised for recording absorption spectra. The samples were diluted in water and set to scan the spectrum range between 400 nm and 800 nm.

Column and flash chromatography was conducted using Flash grade Silica Gel (32-63 μm), following the general method described by Still [5].

Merck silica gel 60 F_{254} aluminium backed sheets were used for thin layer chromatography (TLC) studies. TLC plates were visualised under a 254 nm UV lamp and by treatment in a ceric (IV) dip containing phosphomolybdic acid (37.5 g), ceric sulfate (7.5 g), sulfuric acid (37.5 mL) and water (720 mL), followed by heating.

4.2.2 Synthesis of O-2-[aminoethyl fluorescein]hydrochloride

4.2.2.1 Synthesis of fluorescein methyl ester

Fluorescein methyl ester was prepared by the method of Adamczyk *et al.* [6]. Concentrated sulfuric acid (1.5 mL) was added drop wise to a mixture of fluorescein, (Figure 4.2) **1**, (2.02 g, 6.02 mmol) in methanol (10 mL) and the reaction mixture was refluxed overnight.

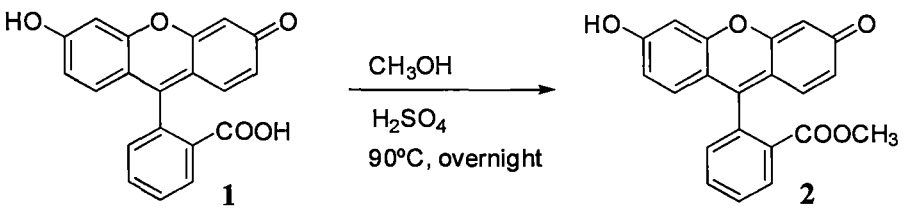

Figure 4.2. Synthesis of fluorescein methyl ester.

The mixture was cooled and cold water (1 mL) and sodium bicarbonate (6 g) added. The mixture was filtered and resuspended in 10 mL of sodium bicarbonate (2% w/v). The solid collected by filtration was washed with cold water, (4 × 10 mL) and dried in an oven for 1 hour at 80°C. The resulting solid was identified as **2** in 84% yield (Figure 4.2).

^{1}H NMR (300 MHz, DMSO-d_6): δ 3.56 (s, 3H), 6.55 (m, 4H), 6.77 (d, J = 9.0 Hz, 2H), 7.46 (d, J = 7.2 Hz, 1H), 7.75 (m, 1H), 7.84 (m, 1H), 8.18 (d, J = 7.2 Hz, 1H). ^{13}C NMR (75 MHz, DMSO-d6) δ: 52.4, 103.2, 114.8, 121.6, 129.5, 130.0, 130.1, 130.6, 130.7, 133.2, 134.0, 151.9, 156.3, 165.2, 173.2. HRMS: (found M^+ 346.08; $C_{21}H_4O_5$ requires M^+ 346.08380). Mass Spectrum m/z: 346 (M^+, 90%), 318 (40), 288 (40), 259 (100), 243 (40), 202 (40). Melting point = 205-210°C.

4.2.2.2 Synthesis of O-[2-phthalimidoethyl]fluorescein methyl ester

Fluorescein methyl ester, (Figure 4.3) **2** (0.214 g, 0.578 mmol) was added to a mixture of potassium carbonate (0.137 g) and 2-bromoethylphthalimide (0.152 g) in dimethyl formamide (DMF) (3 mL) and the reaction mixture stirred overnight at 80°C.

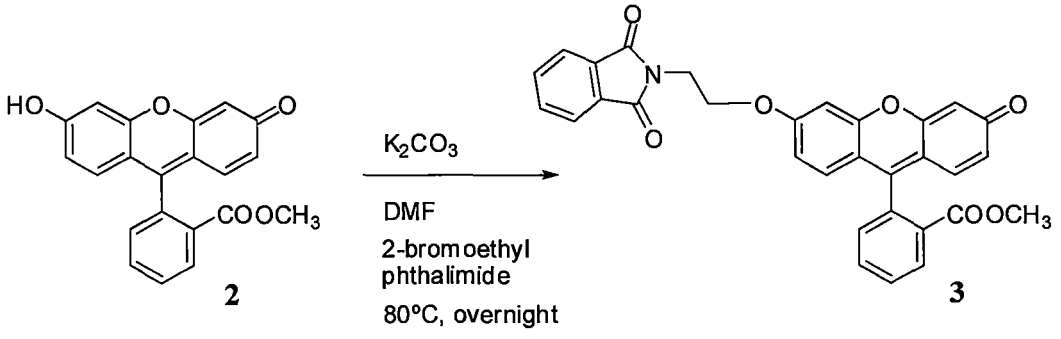

Figure 4.3. O-[2-phthalimidoethyl] fluorescein methyl ester synthesis.

The reaction was cooled, quenched with water (5 mL) and extracted with ethyl acetate (3 × 10 mL). The organic extracts were dried with sodium sulfate, filtered and the solvent removed under reduced pressure. The resulting solid was purified by flash chromatography eluting with 5% methanol in ethyl acetate, appropriate fractions were combined and the solvent removed under reduced pressure. The resulting brown solid was identified as **3** in 34% yield (Figure 4.3).

^{1}H NMR (300 MHz, DMSO-d_6): δ 3.53 (s, 3H), 3.98 (t, J = 5.4 Hz, 2H), 4.37 (t, J = 5.4 Hz, 2H), 6.19 (d, J = 1.8 Hz, 1H), 6.35 (dd, J = 9.6 and 1.5 Hz, 1H), 6.77 (m, 2H), 7.18 (s, 1H) 7.44 (d, J = 7.5 Hz, 1H), 7.81 (m, 3H), 8.17 (d, J = 7.5 Hz, 1H). ^{13}C NMR (75 MHz, DMSO- d_6) δ: 36.7, 52.3, 65.7, 101.1, 104.6, 114.0, 114.5, 116.8, 123.2, 128.9, 129.5, 130.1, 130.4, 130.7, 130.8, 131.5, 133.9, 134.6, 150.0, 153.5, 158.3, 162.5, 165.2, 167.7, 183.9.

4.2.2.3 Synthesis of O-2-[aminoethylfluorescein]hydrochloride

Fluorescein ester phthalimide (Figure 4.4) **3** (0.0529 g, 0.10 mmol) was added to a stirred solution of 5 M hydrochloric acid (2 mL) and refluxed overnight.

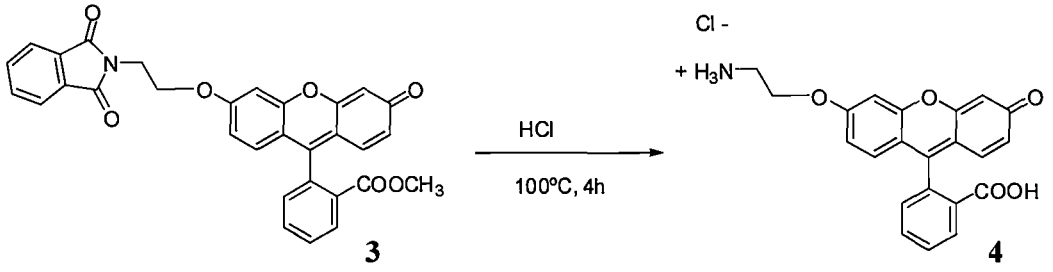

Figure 4.4. O-2-[aminoethylfluorescein] hydrochloride.

The reaction mixture was cooled, water (3 mL) added, the precipitated phthalic acid removed by filtration and the solvent removed under reduced pressure to give the crude product **4** (Figure 4.4) as a yellow oil in quantitative yield of 34%.

^{1}H NMR (300 MHz, D_2O, trifluoroacetic acid): δ 3.41 (m, 2H), 4.41 (m, 2H), 6.54 (db, J = 8.7 Hz, 1H), 6.70 (bs, 1H), 6.85 (bd, J =8.7 Hz, 1H), 6.95 (m, 2H), 7.53 (m, 2H), 7.67 (m, 3H). ^{13}C NMR (75 MHz, D_2O) δ: 37.9, 64.7, 99.8, 113.3, 116.8, 118.7, 120.1, 128.0, 130.3, 130.4, 130.9, 131.1, 131.7, 132.1, 132.5, 158.1, 159.2, 159.5, 167.1, 167.7, 169.3, 170.5, 170.9. EI Fragmentation: 376 (M^+, 376 M^+), 377 (M+H). The product was then purified by HPLC.

4.2.3 Purification of O-2-[aminoethyl fluorescein]hydrochloride (HPLC)

A HPLC instrument equipped with a DAD detector operating at 488 nm was used to purify the synthesised reagent. A reversed phase HPLC method was adopted using an Alltech, Alltima C18, 5 μm, semi-preparative column, 150 mm × 10 mm I.D. as the stationary phase and methanol 90% water 10% as the mobile phase. The flow rate of the mobile phase was set to 0.5 mL min^{-1} and the column heater was set at 25°C. The reagent, 2 mg, was dissolved in 2 mL 50% methanol 50% water and injected onto the column by a series of 100 μL injections. O-2-[Aminoethyl]fluorescein was baseline separated from fluorescein and the fractions were manually collected over a period of 20 min. The fractions were collected by monitoring the colour change of the mobile phase and by observing the elution order of the peaks on the chromatogram. Based on this information the following fractions were collected: 0-9.4 min, 9.4-10.4 min, 10.4-12.5 min, 12.5-14.3 min, 14.3-15.4 min, 15.4-18 min, 18-20 min where fractions 10.4-12.5 and 12.5-14.3 were pure. The purity of the tag was confirmed by CE-ion trap-MS with the M^+ at 376 using a 20 mM ammonium acetate buffer at pH

4.8 and the sample was dissolved in ammonium carbonate 15 mM buffer at pH 9.2. The fractions were combined and subjected to spectral studies.

4.2.4 Quantum yield studies

The fluorescence spectrum of O-2-[aminoethyl]fluorescein was measured using a UV/Vis SP8001 Metertech spectrophotometer and a Perkin Elmer LS 55 fluorimeter. The measurements were obtained by dissolving the tag in 0.1 M NaOH solution. Fluorescein was used as a standard also dissolved in 0.1 M NaOH with $\Phi = 0.95$. Absorbance values of the fluorescein and O-2-[aminoethyl]fluorescein were measured using a spectrophotometer and used in conjunction with the fluorescence intensity with excitation at 484 nm and emission collected at 512 nm to construct a plot of fluorescence emission intensity versus absorbance. The slope of the line is the QY. The fluorescence QY was calculated using the generic formulae:

$\Phi_x = \Phi_s \times (F_x \times A_s)/(F_s \times A_x)$ where Φ_x and Φ_s are the QYs of the novel tag and the standard respectively, F_x and F_s represent the absorbances of the novel tag and the standard while, A_s, A_x signify the area under emission spectra of the novel tag and the standard respectively.

4.2.5 Spectral studies

The excitation and emission spectra of the free and maltoheptaose-conjugated O-2-[aminoethyl]fluorescein were recorded using a Perkin Elmer LS 55 fluorimeter. For the conjugated form, fractions were collected using the CE and pooled to provide sufficient volume for the fluorimeter. The instrument was set to separate for 13 min at 30 kV reversed polarity where the maltoheptaose-conjugated O-2-[aminoethyl]fluorescein was collected. This was followed by a flushing step at 1,380 mbar for 1 min to ensure the removal of impurities. The method was compiled to collect 150 fractions with a 50 s injection each at 50 mbar injection pressure. The

amount of the collected maltoheptaose-conjugated O-2-[aminoethyl]fluorescein was calculated using Beckman CE expert software which accounts for the type of instrument used for the separation, the length of the separation capillary, inside diameter, temperature, sample injection pressure, time of injection and voltage applied across the capillary. Such parameters were utilised to calculate the amount of the maltoheptaose-conjugated O-2-[aminoethyl]fluorescein collected in each run, which was further multiplied by the number of runs to obtain the total amount of the conjugated maltoheptaose O-2-[aminoethyl]fluorescein complex.

4.2.6 Labelling reaction

A bulk solution containing 120 μL methanol, 33.6 μL water and 6.4 μL glacial acetic acid was prepared and stored in an eppendorf tube and refrigerated at 4°C. A 14 μL aliquot was taken and added to 4 μL sodium cyanoborohydride (1 M in THF) and of 1×10^{-6} mol of dry derivatisation reagent. The mixture was sonicated for 5 min to ensure dissolution of the tag. This mixture was then divided into two 9 μL aliquots and 1 μL 99.7% glacial acetic acid was added to each. One portion was added to an empty eppendorf tube to serve as a control while the second was added to an eppendorf tube containing 10-50 nmol of dry carbohydrate. The mixture was placed on a dry bath incubator (Edwards Instrument Co, Model: MD-01N-220) and heated at 60, 70 or 80°C for 1 hour. After completion of the reaction the solution was cooled and homogenised in a Griffin and George, UK (type: UJI 100) centrifuge. The reaction mixture was then injected into the CE with or without dilution as described in the text.

4.2.7 CE

A Beckman Coulter P/ACE MDQ, equipped with a LIF detector interfaced to the Karat software was utilised for fluorescence detection in CE experiments. Polyimide

coated LPA-coated fused silica capillary (Polymicro, Phoenix, AZ, USA), with a 50 μm I.D., 375 μm O.D. was used for all separations. Detection windows were created with hot sulfuric acid at 10 cm from the capillary end to fit the LIF detection system. Injection of the sample solutions was performed hydrostatically by applying a pressure of 50 mbar for 10 s. Electrophoretic separations were performed at 30 kV with the capillary thermostated at 25°C. LPA-coated capillaries were used to suppress the EOF and to improve the resolution of carbohydrates [7].

Separations were performed using an electrolyte prepared from 100 mM solution of boric acid in water titrated to pH 8.65 with tris. All BGEs were degassed with a Soniclean ultra-sonic bath under vacuum and filtered through 0.45 μm disc filters (Activon, Thornleigh, Australia).

4.3 Results and discussion

The approach taken in this work was to develop a simple and flexible synthetic scheme to allow variation of the reagent *via* the incorporation of tailored functionalities to potentially construct an assortment of fluorescent reagents. The reagent was then used for the derivatisation and separation of a range of oligosaccharides by CE using LIF at 488 nm as a means of sensitive detection.

4.3.1 O-2-[aminoethylfluorescein]hydrochloride

4.3.1.1 Fluorescein methyl ester

Before the spacer could be introduced onto the xanthinyl ring of the phenolic function, the carboxylic acid on the fluorescein had to be protected to eliminate possible side reactions, such as dialkylation. This was achieved by Fisher esterification, catalysed under acidic conditions in methanol to yield the methyl ester (Figure 4.2) [8]. The reaction occurred under standard esterification conditions,

starting with a commercially available fluorescein acid to yield the ester **1** as a brown solid in a good yield of 84%. The ^{1}H NMR spectrum of the product showed good agreement with the spectral data published previously, where both spectra recorded methyl protons on the ester at 3.56 ppm [9]. There was a little variation observed in the aromatic region, nevertheless a total of 10 aromatic protons were clearly observed in each of the spectra, supporting the identity of **2**.

4.3.1.2 O-[2-phthalimidoethyl]fluorescein methyl ester synthesis

Having protected the carboxylic acid group as an ester and locking the molecule in the quinoid form an alkylation onto the remaining phenol to introduce the spacer-reactive group assembly could be performed. The alkylation of fluorescein esters has been reported previously by Lohse *et al.* who investigated the coupling of *tert*- butyl bromoacetate and fluorescein, and Shubert *et al.* looking at reacting protected hydroxyalkyl chlorides with fluorescein methyl esters [10, 11]. The former method was more successful obtaining 78% yield, with the latter one showing 33% yield. The synthesis was achieved by reacting 2-bromoethylphthalimide and fluorescein methyl ester with potassium carbonate as a base to generate the phenolic anion to give the desired compound O-[2-phthalimidoethyl] fluorescein methyl ester in 34% yield (Figure 4.3). The yield was lower than might be expected probably due to the mild basic conditions and inability to generate the strong nucleophilic anion on the fluorescein core which could then couple to the electrophilic phthalimide derivative but sufficient compound was obtained. Analysis of the ^{1}H NMR spectrum shows the presence of the methyl group as a singlet at 3.54 ppm with the appearance of two sets of triplets resonating at 3.98 ppm and 4.37 ppm indicating the presence of the ethylene protons of the spacer, which supports the proposed structure of the compound. The aromatic region is quite complex, nevertheless the presence of 14

aromatic hydrogens in the fluorescein core and the phthalimide portion are observed. This alkylation step of the synthesis is essential for introducing the tailored ethylphthalimide functionality on the fluorescent tag backbone. This exact reaction scheme can be applied in future studies to allow incorporation of other desirable functional groups thus assisting the design of new fluorescent tags with new spectral, kinetic and separation properties.

4.3.1.3 O-2-[aminoethylfluorescein]hydrochloride

Having placed the spacer on the desired phenolic site of the fluorescein, the phthalimide and ester groups could be hydrolysed to the desired amine and acid functions under standard acid hydrolysis conditions to yield the target fluorescent reagent. The reaction was performed by refluxing **3** in 5 M HCl and then cooling to precipitate the phthalic acid. The phthalic acid was removed by filtration and the filtrate was then evaporated to dryness to give the fluorescent tag **4** (Figure 4.4). O-2-[Aminoethyl]fluorescein was isolated as a yellow oil in 34% yield while the overall yield of the three-step reaction was 0.5%. Analysis of the ^{1}H NMR spectrum confirmed the identity of the compound. The presence of the ethylene protons on the spacer group were recorded as triplets at 3.42 ppm and 4.43 ppm. Careful examination of the aromatic region supported the presence of only10 distinct protons, consistent with the removal of the phthalimide group. The compound was also characterised by MS to give a molecular weight of 376 a.m.u. consistent with the formation of the fluorescent tag **4**.

4.3.2 Spectral studies

The excitation and emission spectra of the free and maltoheptaose-conjugated O-2-[aminoethyl]fluorescein were recorded. For the conjugated form, fractions were

collected using the CE and pooled to provide sufficient volume for the fluorimeter. The spectra are shown in Figure 4.5. As can be seen, conjugation of the O-2-[aminoethyl]fluorescein to maltoheptaose does not change its spectral properties where both the free and the conjugated form have identical maximum absorption and emission wavelengths of 504 nm and 526 nm accordingly, but the fluorescence intensity has been decreased. In order to quantitatively examine this, the QY of the free and maltoheptaose-conjugated form of the reagent were measured. Fluorescein in 0.1 M sodium hydroxide was used as a standard as it has a known QY of 0.95 [12].

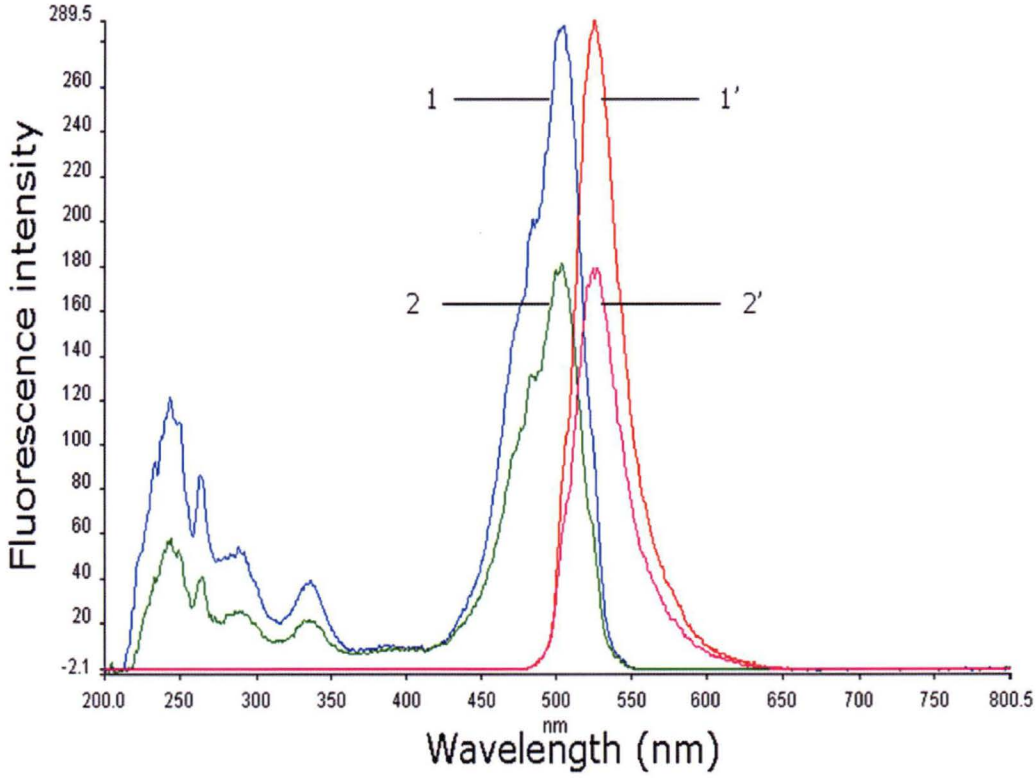

Figure 4.5. Fluorescence excitation and emission spectra of O-2-[aminoethyl]fluorescein in its free form and labelled to maltoheptaose. The free form of O-2-[aminoethyl]fluorescein shown as 1,1', while the labelled maltoheptaose is described as 2,2'. The concentrations of both the free form and the conjugated form of the O-2-[aminoethyl]fluorescein were 2.7×10^{-4} M.

Absorbance values of the fluorescein and O-2-[aminoethyl]fluorescein were measured using a spectrophotometer and used in conjunction with the fluorescence intensity with excitation at 484 nm and emission collected at 512 nm to construct a plot of fluorescence emission intensity versus absorbance. The slope of the line is the QY. The QY of the free O-2-[aminoethyl]fluorescein was 0.24 while for the maltoheptaose conjugate it was 0.19. A related study was conducted by Du and colleagues where a new 6-oxy-(acetyl piperazine) fluorescein was synthesised introducing a reactive group in a similar fashion using the phenolic site of the fluorescein followed by labelling with fatty acids. The outcomes of the research showed that the fluorescence of the labelled fatty acids was higher then of the derivatisation agent itself which is in contrast with the current study [13]. Even though the labelled maltoheptaose was found to be less fluorescent it was still suitable for LIF detection at 488 nm.

4.3.3 Excess tag studies

Numerous studies in the literature suggest that the degree of the derivatisation efficiency of the carbohydrates is governed by the excess of the tag present in the reaction mixture [14-16]. Large excess of the tag is frequently required to obtain high derivatisation efficiency which consequently provides better sensitivity. Figure 4.6 shows a plot of peak area of maltoheptaose as the carbohydrate of choice versus excess of O-2-[aminoethyl]fluorescein. The plot demonstrates a clear upward trend where increasing the amount of the derivatisation reagent enhances the peak area. The initial 5 to 20 times excess of the tag demonstrates a gradual increase where the peak area is raised 4 times. At the 40 and 50 times excess mark the peak areas show significant increase in the order of 20 and 45 times, respectively. Further excess of 100 times registers further rise in the peak area providing 90 times improvement in

the peak area when compared to the initial 5 times excess of the derivatisation reagent. Even though higher excess of the tag can generate further improvement in the sensitivity, the reagent exhibited poor solubility at higher concentrations and this also led to the presence of unknown peaks in the separation. The presence of unknown peaks is possibly due to the elevated number of side reactions which is supported by Klockow *et al.* [15]. Due to these reasons and a limited availability of O-2-[aminoethyl]fluorescein, the 100 times excess was chosen as the maximum excess.

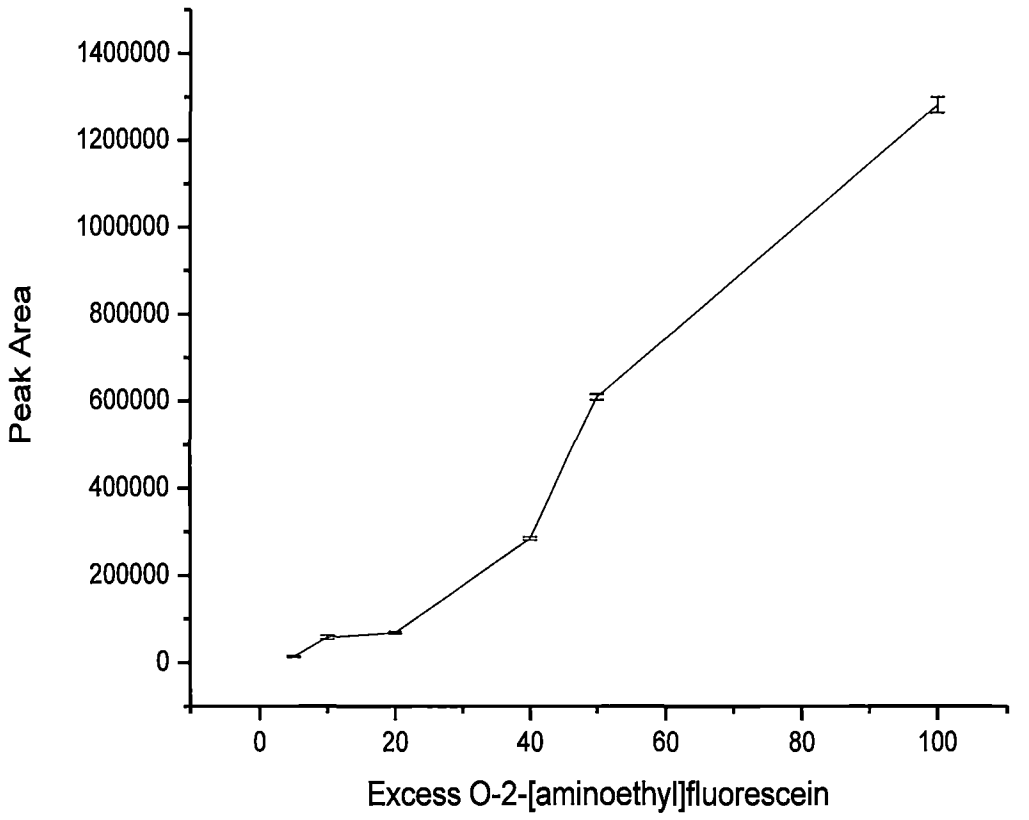

Figure 4.6. Derivatisation of maltoheptaose expressed as peak area of the carbohydrate versus varied excess of O-2-[aminoethyl]fluorescein. Concentration of the tag ranged from 1×10^{-5} M to 5×10^{-4} M, while the maltoheptaose concentration was kept at 5×10^{-6} M.

4.3.4 Kinetic studies

Having established the fluorescent potential of the novel fluorescent tag O-2-[aminoethyl]fluorescein in CE it is important to ensure the tag is capable of derivatising carbohydrates at a suitable reaction rate to make it appropriate for routine high throughput analysis. We therefore introduce an approach whereby kinetic studies are conducted to evaluate the novel O-2-[aminoethyl]fluorescein and compare it against commercial fluorescein based derivatives (analogues of **II** in Figure 4.1) such as 5-aminofluorescein and 5-aminomethylfluorescein, which are absorbance and fluorescence reagents, respectively. The rationale for comparing the reagents is aimed at studying the difference between the 5-aminofluorescein with its aromatic amino function and O-2-[aminoethyl]fluorescein which possesses an aliphatic amino group with potentially higher reactivity. In theory, the presence of the spacer group on the phenolic function of the O-2-[aminoethyl]fluorescein should reduce steric hindrance between the tag and the bulky carbohydrate, therefore providing better labelling reaction and improving the tagging of larger carbohydrates when compared to an aromatic amino function . Furthermore the commercial 5-aminomethylfluorescein is included in the kinetic studies to compare it against the newly synthesised tag, and compare the performance of the two fluorescent motifs. For these comparisons, three parallel reactions were conducted in which 5-aminofluorescein, 5-aminomethylfluorescein and O-2-[aminoethyl]fluorescein were labelled to maltoheptaose under identical conditions. Each reaction mixture was sampled every 10 min for 1 hour and analysed by CE. Figure 4.7 shows a comparison of the labelling performance of the three tags where the reaction kinetics are measured as a function of peak area versus the time of reaction. The two fluorescent tags namely 5-aminomethylfluorescein and O-2-[aminoethyl]fluorescein

were studied using fluorescence with excitation at 488 nm and emission at 512 nm. 5-Aminofluorescein does not fluoresce and the reaction was monitored by detecting the products *via* absorbance detection at 214 nm. Maltoheptaose with dp of 7, expressed as G7, was selected as the carbohydrate of choice for the kinetic studies as it is commercially available in relatively high purity and has enough bulk to induce previously discussed steric hindrance.

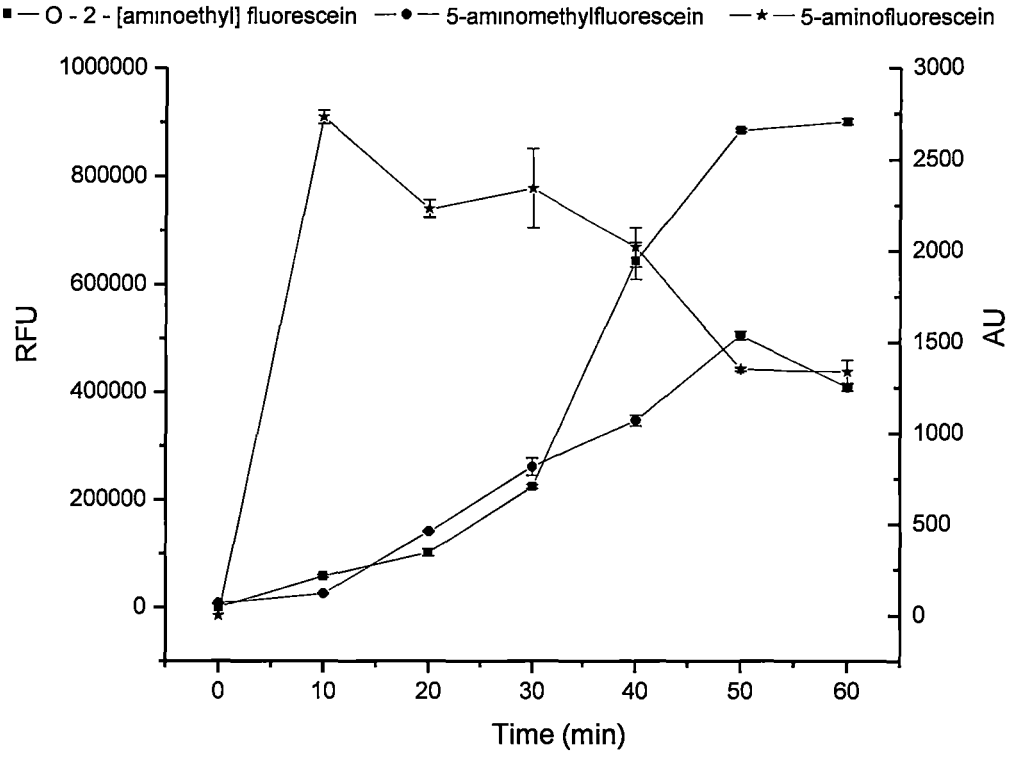

Figure 4.7. Kinetic studies expressed as labelling performance over time for the three tags: 5-aminofluorescein, 5-aminomethylfluorescein and O-2-[aminoethyl]fluorescein. The y axis on the left hand side represent relative fluorescence units recorded for the 5-aminomethylfluorescein and O-2-[aminoethyl]fluorescein. The y axis on the right hand side are expressed in absorbance units describing the UV/Vis tag 5-aminofluorescein.

From the data in Figure 4.7, 5-aminomethylfluorescein and O-2-[aminoethyl]fluorescein show very similar reaction kinetics from 0 to 30 min. Over the next 10 min significant changes are observed as the area of O-2-[aminoethyl]fluorescein G7 complex is increased by approximately 200% while 5-aminomethylfluorescein G7 complex shows moderate 50% enhancement in the peak area. This is followed by further substantial signal enhancement for both the reagents up until 50 min reaction time. Furthermore the time interval of 50-60 min demonstrates a rapid reduction in the reaction rate for the O-2-[aminoethyl]fluorescein G7 complex, while 5-aminomethylfluorescein tag shows a decrease in the peak area and possible decomposition of the tag-carbohydrate complex. Comparison of the two tag motifs shows that at the end of 60 min 5-aminomethylfluorescein yields an area which is approximately half of the area produced by O-2-[aminoethyl]fluorescein, making the newly synthesised label the fluorescent tag of choice as it obviously gives a better response to the maltoheptaose. Figure 4.7 also shows the kinetics of the UV/Vis tag 5-aminofluorescein where the signal is recorded in absorbance units. The tag is studied over the same time interval, however the derivatisation pattern obtained demonstrates very unexpected results. The collected data indicates that the highest area of 5-aminofluorescein G7 complex is recorded at the 10 min reaction time followed by gradual decrease and the lowest peak area recorded at the end of 60 min. The observed declining derivatisation trend highlights the exact opposite pattern to the one observed by the fluorescent tags discussed previously. One of the possible explanations for recording high intensity peaks at the start of the reaction could be attributed to the formation of an imine complex which does not form a permanent bond yet could still be detected in the imine form before reduction with sodium cyanoborohydride can occur [8]. In order

to test the hypothesis another set of kinetic studies was examined where sodium cyanoborohydride was excluded from the reaction mix to ensure only the imine complex can be formed and detected. The results showed no presence of the imine complex which negates the proposed hypothesis. This suggests that the 5-aminofluorescein tag is highly reactive showing the best labelling efficiency at the 10 min reaction time. Comparison of this visible tag to the newly synthesised fluorescein derivative indicates that the aromatic amine illustrates higher reactivity then the aliphatic amine. Although the outcomes are not as expected the newly synthesised tag has the advantage of being fluorescent and does show better labelling when compared to a commercial fluorescein motif such as 5-aminomethylfluorescein.

4.3.5 Application in oligosaccharide analysis

The next important step in evaluating the performance of the tag was to assess its ability to label typical commercially available oligosaccharides. A known standard of corn syrup was used containing a number of oligosaccharides with various dp starting from 4 and ending with 10, thus encompassing 7 analytes. It is important to note that it is not our intention in this work to describe an optimised method for this analysis but rather to demonstrate the potential of the newly synthesised tag to analyse carbohydrates. In order to assess the performance of the new tag, a comparison was made with the two related commercial fluorescein derivatives: 5-aminomethylfluorescein and 5-aminofluorescein (Figure 4.8).

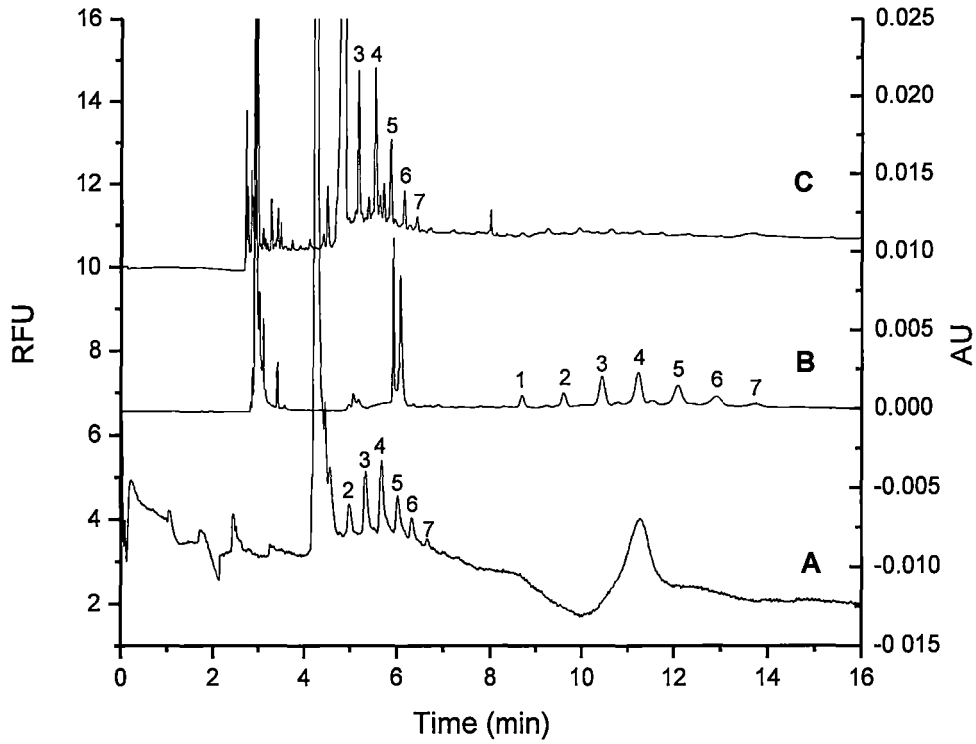

Figure 4.8. Three electropherograms identified as A, B, C showing labelling of G4-G10 corn syrup where peak 1: G4, 2: G5, 3: G6, 4: G7, 5: G8, 6: G9, 7: G10 (G meaning glucose, and number referring to degree of polymerisation). The separation conditions for electropherograms are A) 20 times dilution of 5-aminofluorescein ,10 s injection 50 mbar, 5×10^{-7} mol of 5-aminomethylfluorescein, 2.5×10^{-4} g of the G4-G10 corn syrup ; current -15 µA, detection, DAD, 214 nm; B) 100 times dilution of O-2-[aminoethyl]fluorescein, -15 µA, detection, LIF, 488 nm, other conditions as per A; C) 100 times dilution f 5-aminomethylfluorescein, -15 µA, detection, LIF, 488 nm, other conditions as per A. Conditions: capillary, fused silica (50 µm I.D.); 40 cm (30 cm effective length); electrolyte 100 mM boric acid, pH 8.65; voltage -30 kV; temperature, 30°C.

Calculation of the resolution parameters for electropherogram C indicates values of 1.92 between the G6 and the 5-aminomethylfluorescein, while the oligosaccharides ranging from G6 to G9 are better resolved with values recorded at 3.02 to 3.42. Further assessment indicates a slight drop down to 2.38 for the resolution of G9 and G10 oligosaccharides. Meanwhile electropherogram B, illustrates the well resolved separation of all seven analytes using the newly synthesised tag, with relatively broad peaks in under 14 min. Careful analysis of this electropherogram reveals an impressive resolution of 10.59 between the O-2-[aminoethyl]fluorescein and the G4 oligosaccharide, followed by a resolution of 2.79 between G4 and G5 and 2.33 for G5, G6 peaks. All the other oligosaccharides between G6 to G10 are still baseline resolved however their resolution is reduced to the range of 1.67-1.89. Electropherogram C also demonstrates a rapid separation in under 7 min with 6 analytes being detected with low resolution values recorded in the 1.28-1.86 range, where only the G10 oligosaccharide is completely baseline resolved from the G9. Further examination shows that electropherogram A describes similar migration times when compared with electropherogram C. Such observation was expected as both 5-aminomethyl and 5-aminofluorescein are very similar in structure both containing a phenolic and a carboxylic acid functions and hence their mobilities have similar magnitude. In contrast O-2-[aminoethyl]fluorescein contains only one ionisable functionality (carboxylic acid) which equates to less charge, as well as the additional bulk of the spacer group making the tag less mobile. Even though the peaks obtained in electropherogram B are broader and the sensitivity and in some cases the resolution is not as desirable as in C all the analytes are separated at approximately 1 min intervals and baseline resolved suggesting the tag could be well suited to the separations of simple sugars such as mono- and di-saccharides. To

ensure the results were reproducible intra-day RSD values were calculated for the fluorescent tags and their labelled oligosaccharides and the results were recorded where O-2-[aminoethyl]fluorescein showed 0.55-0.82 and 3.46-6.57 RSD value range for migration time and peak area respectively. 5-Aminomethylfluorescein separation highlighted slightly higher RSD values with 1.78-2.23 range for migration time and 2.88-10.56 spread for the peak area values. Finally 5-aminofluorescein labelled to a mixture of oligosaccharides showed some improvement compared to the other two tags where the migration time RSD range was 0.062-0.17 and the peak area was recorded at 2.21-5.62.

LODs for the system were also estimated using maltoheptaose, which has been utilised throughout the study to confirm the suitability of the novel O-2-[aminoethyl]fluorescein tag in carbohydrate analysis. Considering the parameters in the system such as the reaction temperature: 70°C, time: 1 h, excess of the tag: 100 times, reductive amination conditions described previously and a typical CE injection of 3%, the proposed system demonstrated low LOD of 1 nM. Further summary of the study is shown in Table 4.1 where a number of parameters such as spectral properties, QY, LOD and prices for the three tags are compared against each other. It is important to note that the prices for the tags vary considerably highlighting the significant cost benefit from using the novel tag.

Table 4.1. Comparison of maximum excitation (λ_{ex}) and emission (λ_{em}) wavelength, molar absorptivity (MA), quantum yield (QY), limit of detection (LOD) and price in Australian dollars for 5-aminomethylfluorescein, 5-aminofluorescein and O-2-[aminoethyl]fluorescein.

Fluorophore chromophore	λ_{ex}	λ_{em}	MA ($L\ mol^{-1}cm^{-1}$)	QY	LOD (nM)	Price (AUD per g)
5-Aminomethyl fluorescein	492[a]	516[a]	68,000[a]	-	0.29	$37,900
5-Aminofluorescein	492[b]	-	75,400[b]	0.003[c]	-	$75
O-2-[Aminoethyl]fluorescein	504[d]	526[d]	13,230[d]	0.24[d]	1	$1[e]

4.4 Conclusion

This chapter describes a successful synthesis of a novel fluorescent tag using three consecutive steps from fluorescein namely, esterification, alkylation and hydrolysis. The fluorescent properties of the tag are confirmed recording a QY of 0.24. Kinetic studies of various fluorescein motifs revealed that the aromatic fluorescein derivative has better reactivity than the newly synthesised aliphatic fluorescein complex. Application of the newly synthesised tag in carbohydrate analysis showed successful results with all 7 carbohydrates being detected and baseline separated. In contrast to both 5-aminofluorescein and 5-aminomethylfluorescein which showed inability to separate all of the carbohydrates. Overall the study showed that the new tag has been successfully synthesised, purified and applied to study a mixture of commercially available carbohydrates. The results also demonstrate a good potential of the novel tag to be used for the separation of simple mono- and di-saccharides. Intricate design of the tag and the flexibility of its synthesis demonstrates great capabilities to synthesise future fluorescein analogues which may display outstanding performance

[a] Reference [1]
[b] Reference [17]
[c] Reference [18]
[d] Obtained from experimental work in this chapter
[e] Price of starting reagent fluorescein

in terms of selectivity, resolution and efficiency. Careful modification of the alkylation step of the synthesis should allow an assortment of tags to be designed providing lower synthesis cost and potentially providing the desired spectral, kinetic and separation properties for further analysis of biomolecules. Future consideration of the charge bearing functions of the fluorescein derivatives can also assist in preconcentration mechanisms, such as dynamic pH junction which can ultimately improve the sensitivity of the method.

4.5 References

(1) Haugland, R. P. *Handbook of Fluorescent Probes and Research Products* 9th ed.; Molecular Probes: Eugene 2002.

(2) Du, X. L.; Wang, H.; Ma, M.; Deng, Y. H.; Zhang, H. S. *J. Sep. Sci.* **2008**, *31*, 999-1006.

(3) Deng, Y. H.; Zhang, H. S.; Du, X. L.; Wang, H. *J. Sep. Sci.* **2008**, *31*, 990-998.

(4) Urano, Y.; Kamiya, M.; Kanda, K.; Ueno, T.; Hirose, K.; Nagano, T. *J. Am. Chem. Soc.* **2005**, *127*, 4888-4894.

(5) Still, W. C.; Kahn, M.; Mitra, A. *J. Org. Chem.* **1978**, *43*, 2923-2925.

(6) Adamczyk, M.; Chen, Y. Y.; Johnson, D. D.; Reddy, R. E. *Tetrahedron* **1997**, *53*, 12855-12866.

(7) Stefansson, M.; Novotny, M. *Anal. Chem.* **1994**, *66*, 1134-1140.

(8) Sundberg, R. J.; Carey, F. A. *Advanced Organic Chemistry*; Plenum Press: Charlottesville, 1990.

(9) Rabjohn, N. *Organic Synthesis*; John Wiley & Sons: New York, 1963.

(10) Lohse, J.; Nielsen, P. E.; Harrit, N.; Dahl, O. *Bioconjugate Chem.* **1997**, *8*, 503-509.

(11) Shubert, F.; Cech, D.; Reinhardt, R.; Wiesner, P. *DNA Seq.* **1992**, *5*, 273-279.

(12) Brannon, J. H.; Magde, D. *J. Phys. Chem.* **1978**, *82*, 705-709.

(13) Du, X. L.; Zhang, H. S.; Guo, X. F.; Deng, Y. H.; Wang, H. *J. Chromatogr. A* **2007**, *1169*, 77-85.

(14) Jackson, P. *Biochem. J.* **1990**, *270*, 705-713.

(15) Klockow, A.; Widmer, H. M.; Amado, R.; Paulus, A. *Fresenius J. Anal. Chem.* **1994**, *350*, 415-425.

(16) Guttman, A.; Chen, F. T. A.; Evangelista, R. A.; Cooke, N. *Anal. Biochem.* **1996**, *233*, 234-242.

(17) Brando, T.; Pardin, C.; Prandi, J.; Puzo, G. *J. Chromatogr. A* **2002**, *973*, 203-210.

(18) Ballard, D. W.; Kranz, D. M.; Voss, E. W. *Proc. Natl. Acad. Sci. U.S.A.* **1983**, *80*, 5071-5074

Chapter 5

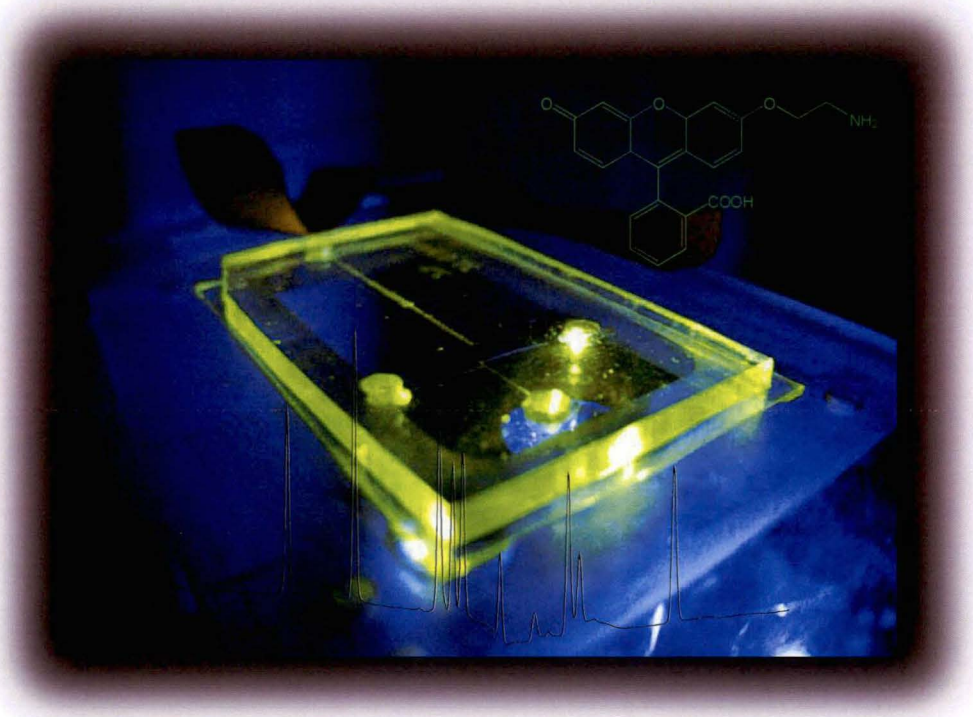

5 Capillary electrophoretic separation of mono- and di-saccharides with dynamic pH junction and implementation in microchips.

5.1 Introduction

Preconcentration is an essential step for many applications in CE, and with the growing trend towards miniaturisation and implementation on the microchip platform, preconcentration strategies that can be implemented on this platform need to be developed. According to the literature a wide diversity of biomolecules have been studied using the concept of microfluidic devices and preconcentration. Such biomolecules include carbohydrates, proteins, amino acids, DNA, fluorescent dyes, mono-chloro-phenols, and various other anionic, neutral and cationic small analytes have been concentrated in microchips. Analytes such as proteins and amino acids have gained a lot of interest and a number of approaches have been reported, including isoelectric focusing[1], solid phase extraction [2] and a number of other preconcentration approaches [3-6], but there is a clear appeal to employ ion selective [7], size exclusion [8] and nanopore membranes [9, 10] for preconcentration as these can produce remarkable enhancement factors of up to 10^6. An assortment of dyes have also been examined over the years primarily as a means to develop and examine the behaviour of on-line concentration methods in microchips, ranging from transient trapping [11] and sweeping [12] to field amplified sample stacking (FASS) [13] with temperature focusing [5] and electrokinetic double-focusing [14]. DNA has also been of interest with tr-ITP [15], tr-ITP/capillary gel electrophoresis [16], electrokinetic supercharging [17], solid-phase reversible immobilisation [18], as well as stacking using laminar or biased laminar loading [19]. Anionic compounds [20] have also

been analysed using a polyacrylamide preconcentrator allowing impressive 10^5 concentration factors while a group by Jacobson *et al.* implemented electrokinetic focusing to induce sample stacking of various cationic neutral and anionic analytes [21]. Ro *et al.* preconcentrated a neutral compound BODIPY, allowing 100 times enhancement in the signal using capillary electrochromatography [22]. Further research by Augustin and colleagues [23] employed the use of monoliths for preconcentration of mono-chloro-phenols demonstrating 3,500 enrichment factors while Wainright *et al.* [24] analysed ACLARA eTag molecules by ITP-zone electrophoresis resulting in 400-fold increase in sensitivity. Surprisingly the analysis of carbohydrates has been shown in very few studies especially related to preconcentration techniques. To my knowledge only one report using oligosaccharides and preconcentration on a microchip format has been published where the use of FASS was explored [25]. The outcomes revealed high resolution of oligosaccharide isomers performed on a poly(methyl methacrylate) microchip with a factor of preconcetration not stated in the study. Based on this, the summary of the literature reveals that up to this date very little research has been done involving carbohydrate preconcentration methods using microfluidic systems.

This current chapter aims to investigate separations of mono- and di-saccharides using both capillary and microchip electrophoresis while applying preconcentration using dynamic pH junction. If developed properly, dynamic pH junction can be used to concentrate analytes from a large volume of sample into a very narrow zone, as was first demonstrated by Britz-McKibbin in the late 90's [26, 27]. Since then a large number of systems have been developed, with a major contribution from the group of Cao, who use MCRB to describe the pH discontinuity around which analytes are concentrated [28-35]. The use of a pH discontinuity for concentration is an ideal

approach for derivatised carbohydrates as the derivatisation reaction is performed in acidic media. If sugars are derivatised with an ionisable reagent, then it is possible to directly inject large volumes of the derivatisation mixture into the capillary and achieve highly efficient sensitive separations, as we previously demonstrated in Chapter 3 using a highly absorbing fluorescein based chromophore. To improve the sensitivity further, fluorescence detection is more desirable than absorbance, however the requirement that the fluorophore contains an ionisable functional group means that the use of APTS is not feasible. This led us to synthesise a new ionisable fluorescent tag, O-2-[aminoethyl]fluorescein, as described in Chapter 4 which showed its suitability in electrophoretic separation of carbohydrates in corn syrup samples. This reagent has a high molar absorptivity, a moderate QY and was shown to be suitable for the separation of seven corn syrup oligosaccharides and a number of simple mono- and di-saccharides. The merits of this work are highlighted by the use of CE to design a microchip based dynamic pH junction method and we believe that this is the first report of the implementation of this preconcentration strategy on the microchip platform.

In this work, we demonstrate the suitability of the previously synthesised fluorescent reagent for on-line concentration of mono- and di-saccharides using a dynamic pH junction. The separation and dynamic pH junction conditions are optimised in capillaries, with this information used to design and implement the system in polydimethylsiloxane (PDMS)/glass microchips to demonstrate dynamic pH junction on a microchip for the first time.

5.2 Experimental

5.2.1 CE

A Beckman Coulter P/ACE MDQ, equipped with a LIF detector interfaced to the Karat software was utilised for fluorescence detection in CE experiments. LPA-coated fused silica capillary (Polymicro, Phoenix, AZ, USA) and bare fused silica capillary coated with poly(styrene sulfonate), PSS, or poly (diallyldimethylammonium chloride), PDADMAC, with a 50 μm I.D., 375 μm O.D, were used for all separations. Detection windows were created with hot sulfuric acid for acrylamide coated capillaries and using a butane torch for bare fused silica capillaries at 10 cm from the capillary end to fit the LIF detection system. Injection of the sample solutions was performed hydrostatically by applying a pressure of 50 mbar for 4 to 120 s. Electrophoretic separations were performed at -30 kV and +30 kV with the capillary thermostated at 25°C. LPA-coated capillaries were used to suppress the EOF and to improve the resolution of carbohydrates, while PSS and PDADMAC coatings were utilised to enable separation and detection in both CE and microchips.

5.2.2 Microchip electrophoresis

Microchip electrophoresis was carried out using an in-house built four channel power supply (CSL, University of Tasmania) which was connected to an interface containing four electrodes. Each electrode was placed into its designated reservoir assigned as 1-separation buffer, 2-sample waste, 3-separation waste, and 4-sample. A blue LED was used as a light source for confocal fluorescence detection. The LED was passed through a 470 nm exciter filter (ET470/40 ×,Chroma Technology, Rockingham, VT, USA) followed by a 10 × objective, through to a dichroic

(T495lpxr, Chroma Technology) and a 50 × objective (Mitutoyo, 0.55 NA, 13 mm working distance, Edmund Optics, Singapore) to focus the LED onto the microchannel. Fluorescence on the micro channel was passed back through the 50 × objective and dichroic, focused with a tube lens (Mitutoyo, 200 mm, Edund Optics) through two 525 nm long-pass filters (ET525/50 m, Chroma Technology) onto the photon counting unit (R4632-03, Hammamatsu, Japan). Data collection was accomplished using a USB photon counter (Hammamatsu) and files were saved using the NI LabVIEW program equipped with the photon counting unit where data acquisition was set to 50 Hz.

5.2.3 Microchip fabrication and PSS/PDDMAC coating of channels

An office laminator (Peach 3500, Laminator Systems, Australia) was used to create a template to make PDMS microchips with slight modification [36]. A piece of dry film photoresist (30 μm thick) (Ordyl 330, Elga Europe, Italy) was placed onto a ProSciTech microscope slide 75 mm × 50 mm × 1 mm after removing the back protective film layer. The dry film was then adhered to the slide by passing through the laminator set at 100°C at speed 2. The slide was then placed under a UV Shark series high-flux LED array as a light source (OTLH-0480-UV, Opio Technology, Wheeling, II, USA) and exposed at 0.8 mw/cm^2 for 2 min, followed by baking on a hotplate (ECHOtherm^{TM} MODEL HS40, Torrey Pines Scientific, CA, USA) set at 110°C. This was left to cool to room temperature, after which the top protective film layer was removed and a second layer of dry film was adhered to the first one using the previously described procedure. The second layer was exposed and processed as previously discussed, with the only exception being the use of a transparency mask during exposure. The addition of a layer of resist on the substrate was found to improve the quality of the templates. This was followed by baking for 2 min, cooling

to room temperature and removing the top protective film layer. The channels were developed by immersing for 90 s into BMR developer (Elga Europe), rinsing with BMR rinse (Elga Europe) for 60 s and leaving to hard bake on the hotplate for 30 min. PDMS was then prepared according to the standard method of Mcdonald *et al.* [37] and smeared on top of the previously described template. This was baked in an oven for 45-60 min at 80°C, after which the PDMS was left to cool and peeled off the template. Appropriate size wells were cut in the PDMS and this was placed on a new clean microscope slide. The channels of the PDMS microchip were coated under vacuum with PSS and PDADMAC coatings following the procedure of Graul and Schlenoff [38]. Firstly the PDMS chip was flushed with a 0.2 M NaOH solution for 60 s to deprotonate the surface of PDMS, followed by rinsing with water for 30 s. Next 0.5 M NaCl, 0.1% PDADMAC solution was flushed for 60 s followed by a rinsing step with water for 30 s. Following on 0.5 M NaCl, 0.1% PSS solution was flushed and the chip was rinsed again with water for 30 s. The procedure was repeated introducing another layer of PDADMAC and PSS in the previously described order. The coated microchip contained a network of two PSS and two PDADMAC layers where the outer most layer was PSS providing suitable surface for dynamic pH junction and separation of mono- and di-saccharides.

5.2.4 Labelling reaction

The choice of solvent used for the labelling of the carbohydrates in the current study was an important parameter. The solvent composition was carefully picked to ensure the appropriate solubility of O-2-[aminoethyl]fluorescein as well as good labelling performance. A bulk solution containing 120 µL methanol, 33.6 µL water and 6.4 µL glacial acetic acid was made up and stored in an eppendorf tube and refrigerated at 4°C. A 7 µL aliquot was taken and added to 2 µL sodium cyanoborohydride (1 M in

THF), 1 μL glacial acetic acid (99.7%) of 1×10^{-6} mol dry derivatisation reagent. The mixture was sonicated for 5 min to ensure dissolution of the tag. The mixture was then added to an eppendorf tube containing nine dry mono- and di-saccharides (5×10^{-8} mol each). Another eppendorf tube was used to prepare a control sample. The above steps were repeated excluding the addition of the dry mono- and di-saccharides. Both eppendorf tubes were placed on a dry bath incubator (Edwards Instrument Co, Model: MD-01N-220) and heated at 70°C for 1 hour. After completion of the reaction the solution was cooled and homogenised in a Griffin and George, UK (type: UJI 100) centrifuge. The reaction mixture was then injected into the CE with appropriate dilution as described in the text. All the reaction mixtures were kept at pH close to 4 after appropriate dilutions, while the BGE pH was kept at 8.60 after the system was optimised. The pH for the sample and the BGE was carefully matched to induce dynamic pH junction.

5.3 Results and discussion

The aim of the work was to implement on-line concentration and electrophoretic separation of mono- and di-saccharides in a microchip. As carbohydrates are most frequently derivatised prior to separation, we used a novel fluorophore that contained ionisable groups making it compatible with the use of a dynamic pH junction to exploit the acidic nature of the sample after derivatisation. Conditions for derivatisation, separation and dynamic pH junction are all optimised in capillaries prior to implementation in microchips.

5.3.1 Derivatisation considerations

One of the issues encountered in this study with the new reagent, O-2-[aminoethyl]fluorescein, was the incomplete solubility of the reaction mixture on

dilution with water prior to injection. As the water was being added, the reaction mixture precipitated out followed by further dissolution. Water was an ideal solvent for the dilution and further preconcentration and therefore was not substituted by any other solvents. Studies revealed that 5 hours after the dilution of the reaction mixture there was no increase in peak areas and peak heights of the mono- and di-saccharides, indicating that all of the precipitated sugars had resolubilised. Hence the labelling protocol was modified such that the reaction mixture was diluted on completion of the reaction, left at room temperature for 5 hours to dissolve completely, followed by the injection and analysis of the reaction mixture.

5.3.2 Optimisation of the separation selectivity

As O-2-[aminoethyl]fluorescein is a novel tag that has been used in Chapter 4, it was first necessary to optimise the separation selectivity of the mono- and di-saccharides in this work. An acrylamide coated capillary was selected for use as this substantially eliminated EOF allowing fast separations with high efficiencies. In Chapter 4, we described the synthesis of O-2-[aminoethyl]fluorescein and its suitability for the electrophoretic separation of simple sugars using a borate/tris buffer based on its frequent use to analyse oligosaccharides and simple sugars [39-42]. The use of this buffer to separate galactose, allose, arabinose, mannose, glucose, xylose, rhamnose, lactose and maltose proved unsuccessful due to poor resolution and selectivity. This was rationalised when considering the fact that borate can complex with tris which reduces the amount of free borate in the system available for complexation with vicinal diol groups on the mono-and di-saccharides.

Tris was replaced with ammonia and the system was optimised. Optimisation of the separation selectivity was undertaken by varying the pH and concentration of boric acid. Figure 5.1 demonstrates the separation of the saccharides at five different pH values ranging from 8.25 to 9.00 described by electropherograms A to E respectively. The trend shows that as pH increases the migration time becomes quicker which is consistent with the predictions since more borate is available to complex with vicinal diols on the sugars. It is also quite interesting to notice that the migration order for certain sugars such as glucose and xylose changes dramatically where the initial one has no vicinal diols while the latter one contains cis diols to allow complexation with borate allowing extra charge and additional selectivity.

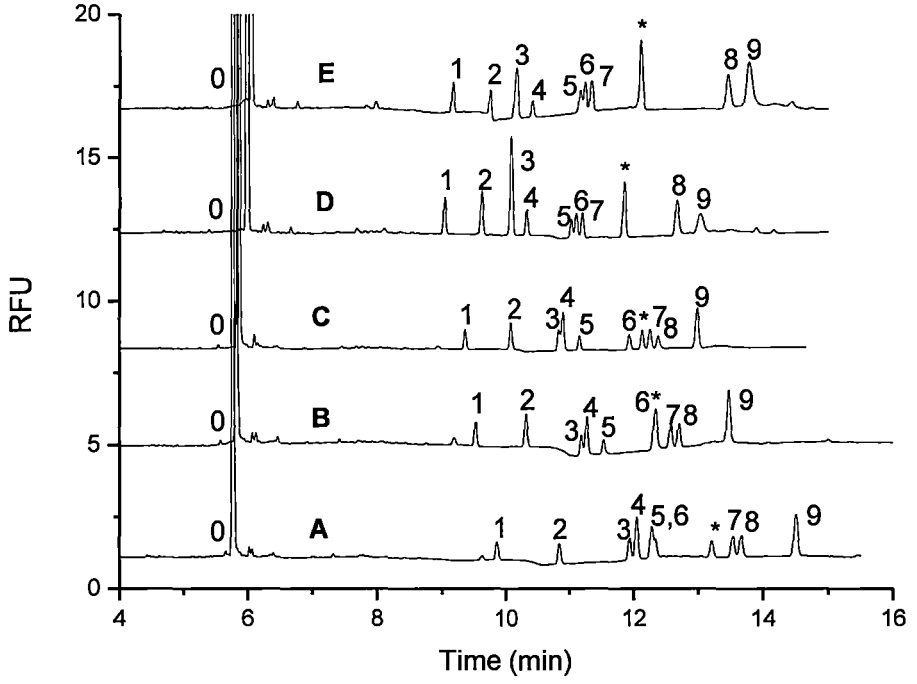

Figure 5.1. Optimisation of buffer pH ranging from pH 8.25-9.00 where A) pH 8.25; B) pH 8.40; C) pH 8.60; D) pH 8.85; E) pH 9.00; 0: O-2-[aminoethyl]fluorescein; 1: galactose; 2: allose; 3: arabinose; 4: mannose; 5: glucose; 6: xylose; 7: rhamnose, 8: lactose; 9: maltose; *: derivatisation peak. Conditions: sample diluted 10,000, acrylamide capillary (50 µm I.D.), 60 cm (50 cm effective length); electrolyte: boric acid 100 mM, pH 8.25-9.00; sample: pH 4.20; voltage -30 kV; injection at 50 mbar, 4 s; temperature: 30°C; detection: LIF 488 nm.

At the initial pH of 8.25 it was not possible to separate all of the analytes with only 6 peaks being well resolved. As the pH was increased to 8.60 only two peaks, arabinose and mannose co-migrated leaving the other analytes well resolved and separated. Further increase of the pH to 9.00 resulted in deterioration in resolution illustrated by the inability to resolve the three analytes (glucose, xylose and rhamnose) as shown in Figure 5.1 E. Thus pH 8.60 was chosen as the optimum in the separation of the nine mono- and di-saccharides.

To try and improve the resolution further, the borate concentration in the buffer was varied. Figure 5.2 highlights the changes in selectivity achieved at different borate concentration ranging from 100 mM to 200 mM.

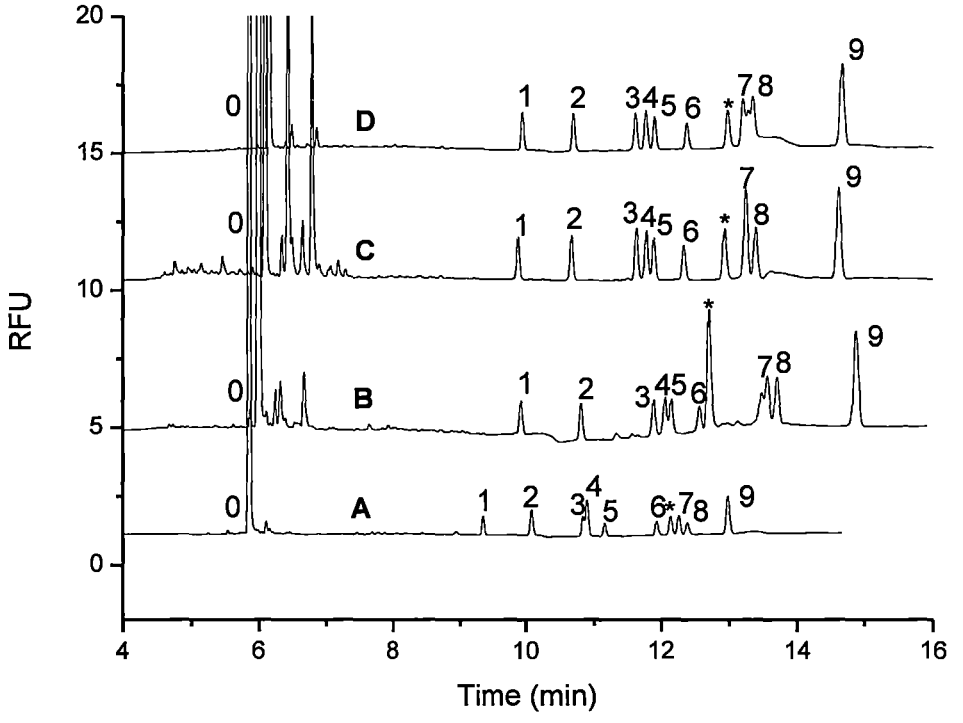

Figure 5.2. Optimisation of boric acid concentration ranging between 100-200 mM where A) 100 mM; B) 150 mM; C) 170 mM; D) 200 mM. Conditions: electrolyte: boric acid 100-200 mM, pH 8.60; other conditions as per Figure 5.1.

Increasing the amount of borate in the buffer from 100 mM to 170 mM clearly demonstrates a well resolved separation of all the nine saccharides showing an optimum borate concentration while further addition of borate to 200 mM compromises resolution resulting in co-migration of rhamnose and lactose peaks at around the 13.5 min mark. Identification of the peaks revealed that all the saccharides are well resolved except lactose which produced two peaks one of which co-migrated with rhamnose. A possible explanation for the presence of the two peaks derived from lactose is that these correspond to the α and β isomers which have hydroxyl groups in equatorial and axial positions accordingly. This would ultimately result in *cis* and *trans* conformation of the hydroxyl groups producing a charged borate complex for the initial conformation and no charge for the latter one.

The optimised separation for the nine mono- and di-saccharides obtained in acrylamide coated capillaries is shown in Figure 5.3.

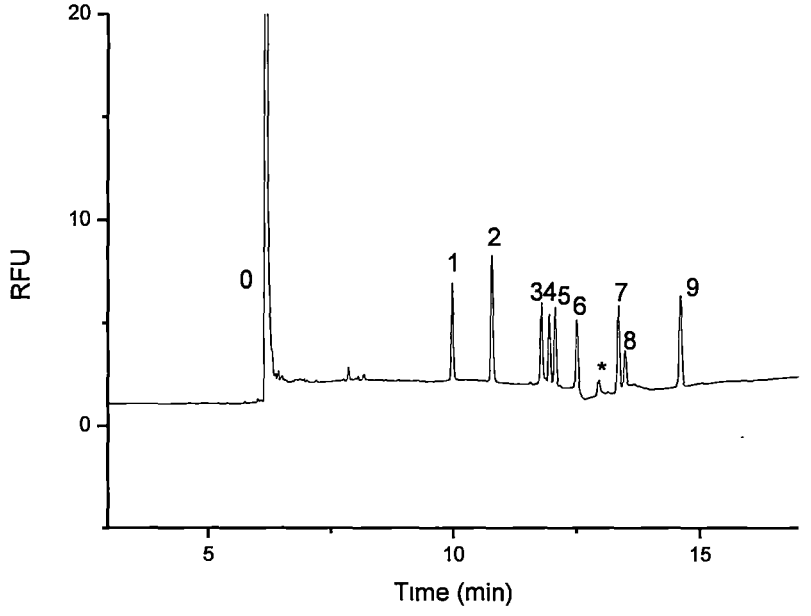

Figure 5.3. Optimised separation of the nine mono- and di-saccharides. Conditions: electrolyte: boric acid 170 mM, pH 8.60; other conditions as per Figure 5.1.

The conditions used in the system were as follows: Argon laser at 488 nm, acrylamide coated capillaries 60 cm × 50 μm I.D., BGE consisting of 170 mM boric acid and ammonia at pH 8.60. All the nine mono- and di-saccharides are clearly shown in the separation, although one of the lactose peaks co-migrates with the rhamnose peak as previously discussed. Using this method the RSD of the peak area and migration time were 0.42-6.05 and 0.12-0.21 respectively.

LODs calculated for the system were in the range of 0.74-2.6 nM which is approximately two orders of magnitude more sensitive compared with the work described in Chapter 3 using dynamic pH junction and LED absorbance detection of mono-, di- and tri- saccharides. These lower LODs are unsurprising given the superiority of fluorescence detection over absorbance detection, even though the later was used with significant on-line concentration. This clearly suggests that when combined LIF detection is introduced in conjunction with on-line concentration, even lower LODs will be obtained.

5.3.3 Stacking *via* dynamic pH junction

The next part of the study focused on preconcentration of the saccharides using dynamic pH junction to further improve the sensitivity. Such preconcentration strategy has been reported by numerous groups and has been used to analyse various compounds. This is the same buffer system used in Chapter 3 to stack mono-, di- and tri-saccharides namely glucose, lactose, maltotriose using a non-fluorescent reagent. Here, we use a novel fluorescent reagent and a BGE comprising borate/ammonia at pH 8.60, instead of borate/tris.

The stacking mechanism involved in this study is identical to the one described in Chapter 3 section 3.3.2 and is based on the fact that the sample has a distinctly different pH to that of the separation electrolyte. In order to demonstrate the potential of dynamic pH junction the sample was introduced at different injection times ranging from 4 to 120 s (from 0.7% to 20% of the capillary volume) shown in Figure 5.4.

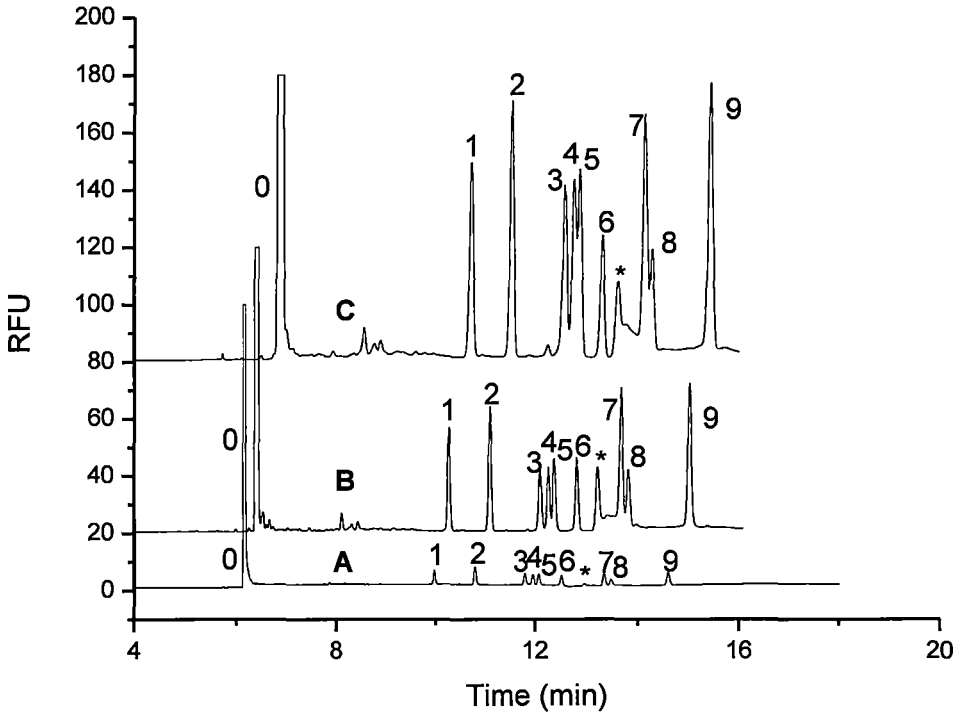

Figure 5.4. Electropherogram demonstrating dynamic pH junction where A) typical CE injection of 4 s at 50 mbar, B) dynamic pH junction at 40 s, 50 mbar, C) de-stacking effects at higher injection of 120 s at 50 mbar. Other conditions are as per Figure 5.3.

The electropherograms A to C show the results where electropherogram B is the optimum, with an injection time of 40 s equating to 7% of the capillary volume. Calculation of resolution values for electropherograms A and B shows very similar results where electropherogram B describes a very minor drop in resolution of up to 5% for all the saccharides. The only considerable change is observed between the fluorescent tag and the galactose peak where electropherogram A shows resolution of 26.98 while electropherogram B yields the resolution of 20.08, however the two sugars are clearly very well resolved under these conditions. Larger injections of up to 20% were studied although some peaks show poor resolution, a clear sign of de-stacking and no marginal improvements in the signal were observed as shown in electropherogram C. From this, the dynamic pH junction mechanism clearly works for moderate injection volumes of 7% showing close to ten times enhancement in the signal-to-noise ratio, and producing LODs as low as 0.13 nM for maltose, which is 650 times lower than our previous result.

5.3.4 Microchip compatible dynamic pH junction

The next goal and ultimately the most difficult aspect of the study was to transfer the dynamic pH junction method from the capillary system to a microchip. In order to do this, a number of parameters have to be modified. It is vital to understand that acrylamide based systems in microchips can not be made easily compatible with dynamic pH junction. The sample, which is at a low pH, must be introduced into an offset cross where it is sandwiched between the BGE. Pressure injections of the sample can not be performed easily and accurately and electrokinetic injections are the preferred strategy on chips. Nevertheless it is worth noticing that a report by Chen *et al.* conducted semihydrodynamic injections of a human estrogen receptor where sample loading was controlled by hydrodynamic forces and focused using

voltage application resulting in prevention of injection bias [43]. Thus while hydrodynamic injection is possible, it is not as simple as voltage-based injections. In the current study considering that the sample is at an acidic pH (a requirement for derivatisation), the analytes in the reaction mixture are neutral and therefore have no electrophoretic mobility (a requirement for dynamic pH junction) they must be introduced into the cross by EOF. However, this is complicated by the fact that EOF in glass/PDMS microchips is pH dependant and thus as the sample enters the microchip, the EOF will be reduced. Therefore the presence of the EOF flow needed to be kept constant in its magnitude throughout the separation medium regardless of the pH of the buffer or the sample zone. It was therefore essential to explore systems which will allow separation of mono- and di-saccharides in the presence of a pH independent EOF that could be easily implemented in a PDMS/glass microchip. Approaches for surface modification of PDMS have been recently discussed by Zhou *et al.* [44] and of the possible approaches, we selected the use of multiple layers of polyelectrolytes. These were originally developed in capillaries independently by Graul and Schelnoff [38] and Katayama *et al.* [45, 46] and have been shown to provide excellent stability and repeatability in capillaries and also when used in PDMS microchips [47, 48]. In the current study two different options were considered. The first utilised PDADMAC coating, producing a pH independent positive surface inside the capillary, while the second used as PSS coating to introduce a pH independent negative surface. Both coatings can be easily and quickly introduced inside fused silica capillaries making this a very attractive method for the analysis. The charge inside the capillary can be simply altered by either flushing PSS and PDADMAC one after the other, which explains why only one capillary is required to accommodate the two systems [38, 45, 46].

PDADMAC coated capillaries were initially evaluated as this would provide co-EOF separations leading to rapid and highly efficient separations. However, this system did not show any viable separation of the analytes, most likely due to the electrostatic interactions between the derivatised sugars and the cationic coating and therefore this option was abandoned. Counter-EOF separations with a PSS coated capillary were much more successful, as can be seen in Figure 5.5, although there was clearly a loss in resolution when compared to the acrylamide coated capillary with most of the analytes not being completely resolved and baseline separated.

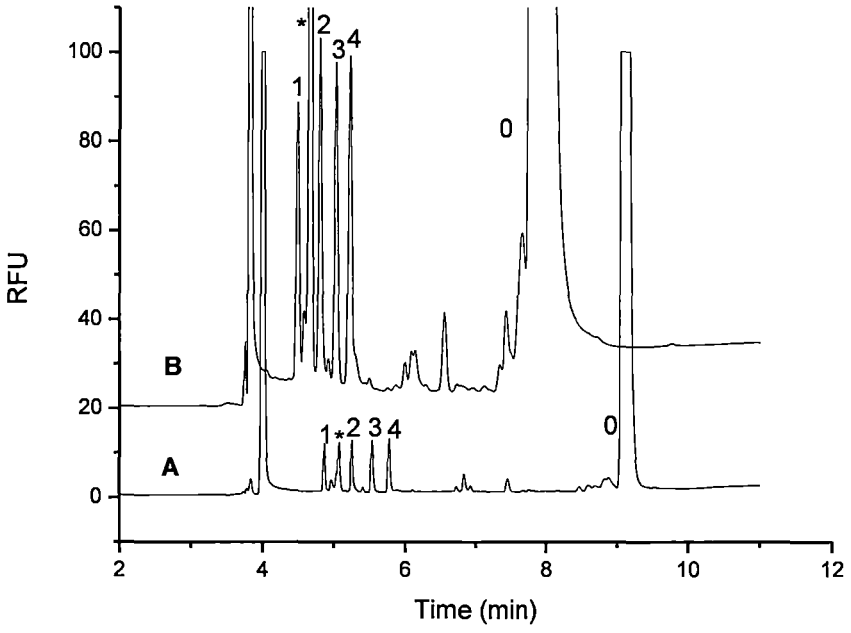

Figure 5.5. Electropherogram demonstrating preconcentration *via* dynamic pH junction in a fused silica capillary where A) typical CE injection of 4 s at 50 mbar, B) dynamic pH junction at 40 s, 50 mbar. The analyte peaks were assigned as follows: 0: O-2-[aminoethyl]fluorescein , 1: maltose, 2: glucose, 3: allose, 4: galactose, *: derivatisation peak. Conditions: sample diluted 1,000, fused silica capillary coated with PSS and PDADMAC where PSS is the outer most layer, voltage: +30 kV; injection at 50 mbar 4 and 40 s. Other conditions as per Figure 5.3.

The system was not further optimised to separate all the nine saccharides but rather four selected analytes were chosen from the set of the nine mono- and di-saccharides to obtain a baseline separation which could later be applied to microchip studies. Maltose, glucose, allose and galactose were labelled to O-2-[aminoethyl]fluorescein and analysed to yield a nice baseline separation as shown in Figure 5.5. The electropherogram in Figure 5.5 A, clearly demonstrates the presence of all four saccharides, as well as a derivatisation peak and O-2-[aminoethyl]fluorescein as the last peak at 10 min. Subsequently preconcentration *via* dynamic pH junction was applied to the system where the results are shown in Figure 5.5 B. The mechanism of dynamic pH junction appears to be clearly working at the 40 s injection time which corresponds to a 7% injection followed by de-stacking at higher injection volumes. Interestingly this is the same optimal volume as obtained in the acrylamide coated capillary suggesting that there is no impact on stacking performance by the EOF. The stacking capability of the system is once again confirmed by assessing the resolution parameters of the analytes. Electropherogram A demonstrates a baseline resolution between all the analytes ranging from 3.84 to 1.94 except for the glucose and the derivatisation peak pair where the resolution is practically baseline, recorded at 1.46. Similarly electropherogram B also demonstrates a baseline resolution between all the analytes recording resolution values of 2.83-1.50 except for the previously mentioned glucose/derivatisation peak pair showing a value of 1.15 which equates to a minor decline in resolution. Overall the observed decline in resolving power for electropherogram B is relatively low when compared to the increase in injection volume suggesting that dynamic pH junction is working. RSD values obtained for this method showed peak areas and migration times in the range of 0.61-2.53 and

0.17-0.26 respectively. Utilisation of dynamic pH junction enabled approximately 6 times enhancement in the sensitivity resulting in LODs of 0.62 nM for maltose. The mechanism of dynamic pH junction for the PSS system was identical to the acrylamide system except the direction of the movement of the ions was switched due to the change in polarity, where the initial system utilised normal while the latter one applied reversed polarity. It is worth discussing the mechanism to understand the fundamental reasons behind the stacking accomplished using the PSS coating. In this case the preconcentration is carried out in the presence of EOF which takes the analytes to the detection site as shown in Figure 5.6. This figure considers a chip based approach where the sample is injected electrokinetically.

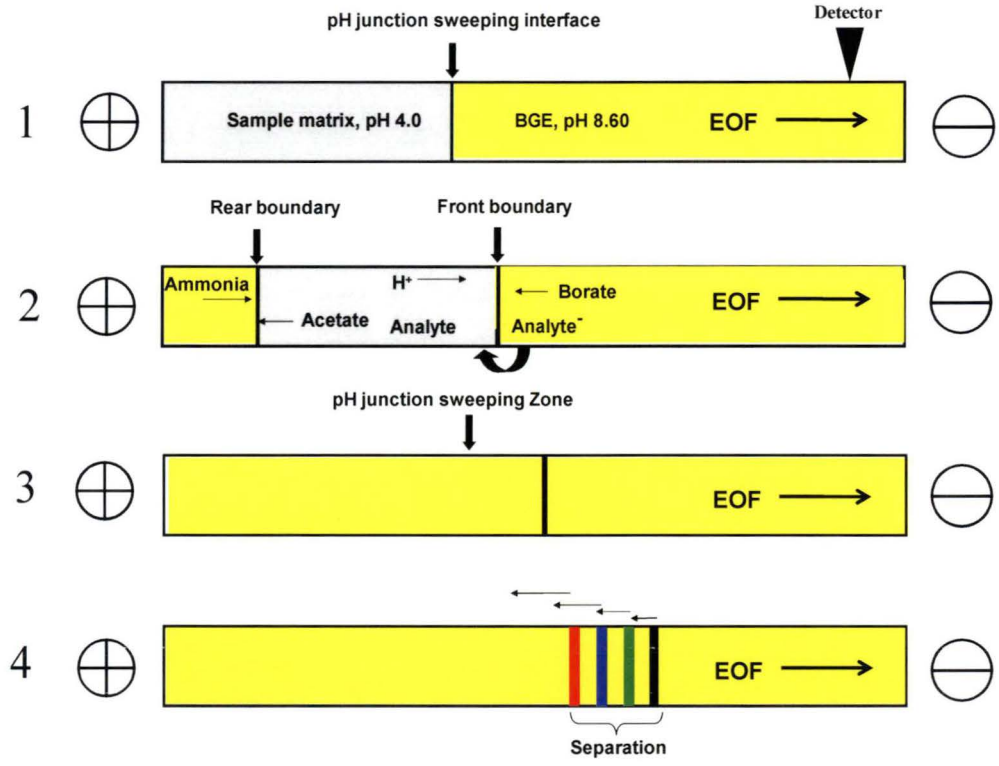

Figure 5.6. Mechanism of stacking *via* dynamic pH junction mode where 1: sample is injected electrokinetically, 2: formation of rear and front boundary resulting in stacking of the analytes, 3: formation of pH junction sweeping zone after the sample has stacked, 4: separation and detection of the analyte.

As the sample is introduced into the capillary between the borate/ammonia electrolyte, application of electric field causes borate and acetate ions to move to the anode while ammonia and hydrogen travel to the cathode, creating a pH junction interface (1). Such arrangement and mobility of ions results in formation of the rear and the front boundaries which are responsible for the pH stacking mechanism. The rear boundary located closer to the inlet (anode) is a product of the neutralisation reaction between ammonia and acetate, while the front boundary is established due to reaction between borate and hydrogen ions (2). In order for the sample to stack, the front boundary must move quicker than the rear boundary towards the anode to consume the sample matrix and concentrate the sample analytes around the moving pH boundary (3). While the front boundary is moving through the sample plug the analytes originally in the low pH zone become exposed to the high pH electrolyte. The derivatised analytes bear a negative charge, as well as additional effect of borate complexation, allowing significant electrophoretic mobility which enables the analytes to move back into the low pH zone. As this boundary moves through the low pH sample zone, analytes concentrate around this moving pH boundary. Once the entire sample has been stacked, the boundary must be allowed to dissipate so that the analytes can separate on the basis of their electrophoretic mobilities (4). Meanwhile the separation is performed in the counter-EOF mode where the EOF carries the separated analytes to the detection site.

The crucial role of this CE based PDADMAC/PSS system is realised by the direct translation of the CE method to a microchip based format as well as applying cathodic pH independent EOF to allow introduction of the low pH sample *via* EOF in chip electrophoresis which will become evident in the next section of the study.

5.3.5 Dynamic pH junction on a chip

While the use of a PSS coating ensures that the dynamic pH junction system should be readily transferred to the microchip platform, several process modifications were made during fabrication of the microchip without which there was inadequate coating of the PDMS. First the PDMS was baked in the oven for strictly 45-60 min at 80°C. Time longer than 60 min led to extensive oxidation of the PDMS surface and limited the amount of PDADMAC that was adsorbed onto the surface. Second, the microchip required thorough conditioning with NaOH to hydrolyse as much of the PDMS as possible to provide a suitable surface for interaction with PDADMAC. After initial adsorption of the prime PDADMAC layer, it was possible to coat with PSS and to build up multiple layers easily. To ensure the PDADMAC/PSS coating provided reproducible EOF inside PDMS microchips RSD values for migration times and peak areas of O-2-[aminoethyl]fluorescein were calculated. At n=3 the results were very impressive reporting RSD values of 4.72 for the peak area and 1.30 for the migration time which suggests the credibility of the coating and ultimately of the EOF. Separation of the mixture of sugars shown in Figure 5.5 A is shown in Figure 5.7 C which shows the previously discussed four saccharides namely maltose, glucose, allose and galactose followed by a broad peak identified as the novel tag O-2-[aminoethyl]fluorescein at the 100 s mark. It is very impressive to notice that this separation closely matches that shown in Figure 5.5 A undoubtedly showing the applicability of the method and its utility for the microchip based separations. However, while this separation is impressive because of its speed, the resolution is inferior and the peak capacity has been reduced when compared to the capillary separation which would ultimately complicate separations of complex mixtures of sugars and their stereoisomers.

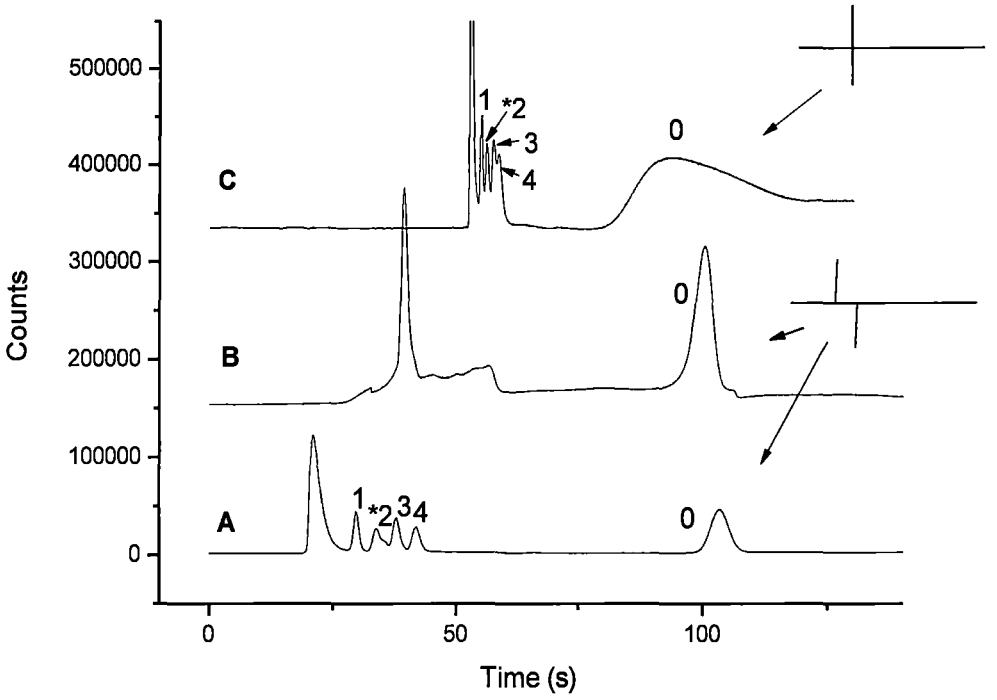

Figure 5.7. Electropherogram demonstrating preconcentration *via* dynamic pH junction on a microchip format where A) dynamic pH junction with sample at pH 4.10, B) reference injection under non-stacking conditions with sample at pH 8.40, C) normal injection using cross microchip configuration with sample at pH 4.00. Conditions: PDMS microchip coated with PSS and PDADMAC where PSS is the outer most layer, (channel: 50 μm wide 30 μm deep), electrolyte: boric acid 170 mM, pH 8.60 using channel architecture described in the experimental section. The following voltages were applied to the reservoirs of the microchip: load: (1) +420 V, (2) -400 V, (3) +800 V, (4) +880 V; separation: (1) +220 V, (2) -380 V, (3) -1100 V, (4) -520 V, all samples diluted 20 times. Other conditions as per Figure 5.1.

Optimisation of the microchannel geometry and voltages would improve this separation, however, as this was not the main emphasis of this work, we did not pursue this further.

Having established the compatibility of microchip coating procedure, the final step was to perform dynamic pH junction on a chip which was one of the main goals of the study. These experiments were performed using an offset cross, with an offset of 7% of the separation length to the detection point, which was the optimum injection length determined from capillary studies using both the acrylamide and PSS coatings. Figure 5.7 A presents the dynamic pH junction injection with sample prepared at pH 4.10 while Figure 5.7 B shows a control separation performed under non-stacking conditions where the sample is at pH 8.40 closely matching that of the BGE. The outcomes clearly illustrate the presence of preconcentration in Figure 5.7 A where sharp peaks are obtained and are nearly baseline separated. In contrast the control sample injection demonstrated no separation of the analytes but rather a continuous broad peak with no resolved saccharides. LODs for the microchip system using dynamic pH junction were calculated to be between 790-1,420 nM. This translates to a three orders of magnitude decrease in sensitivity when compared with the CE based acrylamide and PSS coated capillaries, which is unsurprising given the significant difference between the LED used in the microchip work and the 488 argon ion laser used in the capillary experiments. Comparison of the current study with the literature values indicates similar outcomes where Maeda and colleagues [49] managed to achieve 0.86 μM while Lee et al. [50] obtained 2.3 μM detection limits for glucose. The current system has a great a potential for further improvement by considering other ionisable fluorescent tags suitable for dynamic for pH junction,

as well as applications of other excitation sources to allow better signal-to-noise output resulting in better sensitivity.

5.4 Conclusion

This chapter unequivocally demonstrated the applicability of the novel tag O-2-[aminoethyl]fluorescein for the analysis of a set of the nine mono- and di-saccharides. The designed method was optimised and enabled dynamic pH junction using acrylamide coated capillaries with maximum injections of up to 7% sample plug volume to the detection window. Application of fused silica capillaries and incorporation of pH independent EOF flow *via* the use of PSS coating assisted the separation of the four mono- and di-saccharides. Alteration of the CE method to suit the chip format *via* the use of fused silica capillaries and incorporation of pH independent EOF flow through the use of PSS coating assisted the stacking and the separation of the four mono- and di-saccharides. Finally the method was successfully transferred to the chip format allowing preconcentration *via* dynamic pH junction and a quick, near baseline separation of the four analytes. Microchip based instrumentation offer great advantages in regards to rapid analysis time, small sample volumes as well as the ability to observe separations real time potentially giving further future insights into preconcentration and separation mechanisms in microfluidic devices. Consequently this should enable further enhancement in sensitivity for analysis of various biomolecules using micro chip format.

5.5 References

(1) Cong, Y. Z.; Zhang, L. H.; Tao, D. Y.; Liang, Y.; Zhang, W. B.; Zhang, Y. K. *J. Sep. Sci.* **2008**, *31*, 588-594.

(2) Yu, C.; Davey, M. H.; Svec, F.; Frechet, J. M. J. *Anal. Chem.* **2001**, *73*, 5088-5096.

(3) Lichtenberg, J.; Verpoorte, E.; de Rooij, N. F. *Electrophoresis* **2001**, *22*, 258-271.

(4) Kim, S. M.; Burns, M. A.; Hasselbrink, E. F. *Anal. Chem.* **2006**, *78*, 4779-4785.

(5) Munson, M. S.; Danger, G.; Shackman, J. G.; Ross, D. *Anal. Chem.* **2007**, *79*, 6201-6207.

(6) Mohamadi, M. R.; Kaji, N.; Tokeshi, M.; Baba, Y. *Anal. Chem.* **2007**, *79*, 3667-3672.

(7) Lee, J. H.; Song, Y. A.; Han, J. Y. *Lab Chip* **2008**, *8*, 596-601.

(8) Hatch, A. V.; Herr, A. E.; Throckmorton, D. J.; Brennan, J. S.; Singh, A. K. *Anal. Chem.* **2006**, *78*, 4976-4984.

(9) Song, S.; Singh, A. K.; Kirby, B. J. *Anal. Chem.* **2004**, *76*, 4589-4592.

(10) Wu, D. P.; Steckl, A. J. *Lab Chip* **2009**, *9*, 1890-1896.

(11) Sueyoshi, K.; Kitagawa, F.; Otsuka, K. *Anal. Chem.* **2008**, *80*, 1255-1262.

(12) Liu, Y. J.; Foote, R. S.; Jacobson, S. C.; Ramsey, J. M. *Lab Chip* **2005**, *5*, 457-465.

(13) Gong, M. J.; Wehmeyer, K. R.; Limbach, P. A.; Arias, F.; Heineman, W. R. *Anal. Chem.* **2006**, *78*, 3730-3737.

(14) Zhuang, G. S.; Li, G.; Jin, Q. H.; Zhao, J. L.; Yang, M. S. *Electrophoresis* **2006**, *27*, 5009-5019.

(15) Nagata, H.; Ishikawa, M.; Yoshida, Y.; Tanaka, Y.; Hirano, K. *Electrophoresis* **2008**, *29*, 3744-3751.

(16) Liu, D. Y.; Ou, Z. Y.; Xu, M. F.; Wang, L. H. *J. Chromatogr. A* **2008**, *1214*, 165-170.

(17) Xu, Z. Q.; Hirokawa, A. *Electrophoresis* **2004**, *25*, 2357-2362.

(18) Witek, M. A.; Llopis, S. D.; Wheatley, A.; McCarley, R. L.; Soper, S. A. *Nucl. Acids Res.* **2006**, *34*.

(19) Easley, C. J.; Karlinsey, J. M.; Landers, J. P. *Lab Chip* **2006**, *6*, 601-610.

(20) Yamamoto, S.; Hirakawa, S.; Suzuki, S. *Anal. Chem.* **2008**, *80*, 8224-8230.

(21) Jacobson, S. C.; Ramsey, J. M. *Anal. Chem.* **1997**, *69*, 3212-3217.

(22) Ro, K. W.; Chan, W. J.; Kim, H.; Koo, Y. M.; Hahn, J. H. *Electrophoresis* **2003**, *24*, 3253-3259.

(23) Augustin, V.; Proczek, G.; Dugay, J.; Descroix, S.; Hennion, M. C. *J. Sep. Sci.* **2007**, *30*, 2858-2865.

(24) Wainright, A.; Williams, S. J.; Ciambrone, G.; Xue, Q. F.; Wei, J.; Harris, D. *J. Chromatogr. A* **2002**, *979*, 69-80.

(25) Dang, F. Q.; Zhang, L. H.; Jabasini, M.; Kaji, N.; Baba, Y. *Anal. Chem.* **2003**, *75*, 2433-2439.

(26) Britz-Mckibbin, P.; Kranack, A. R.; Paprica, A.; Chen, D. D. Y. *Analyst* **1998**, *123*, 1461-1463.

(27) Britz-Mckibbin, P.; Wong, J.; Chen, D. D. Y. *J. Chromatogr. A* **1999**, *853*, 535-540.

(28) Cao, C. X.; He, Y. Z.; Li, M.; Qian, Y. T.; Gao, M. F.; Ge, L. H.; Zhou, S. L.; Yang, L.; Qu, Q. S. *Anal. Chem.* **2002**, *74*, 4167-4174.

(29) Cao, C. X.; He, Y. Z.; Li, M.; Qian, Y. T.; Yang, L.; Qu, Q. S.; Zhou, S. L.; Chen, W. K. *J. Chromatogr. A* **2002**, *952*, 39-46.

(30) Oin, W. H.; Cao, C. X.; Li, S.; Zhang, W.; Liu, W. *Electrophoresis* **2005**, *26*, 3113-3124.

(31) Wang, Q. L.; Fan, L. Y.; Zhang, W.; Cao, C. X. *Anal. Chim. Acta* **2006**, *580*, 200-205.

(32) Li, M.; Fan, L. Y.; Zhang, W.; Cao, C. X. *Anal. Bioanal. Chem.* **2007**, *387*, 2719-2725.

(33) Wang, X.; Zhang, W.; Fan, L. Y.; Hao, B.; Ma, A. N.; Cao, C. X.; Wang, Y. X. *Anal. Chim. Acta* **2007**, *594*, 290-296.

(34) Cao, C. X.; Fan, L. Y.; Zhang, W. *Analyst* **2008**, *133*, 1139-1157.

(35) Zhu, W.; Zhang, W.; Fan, L. Y.; Shao, J.; Li, S.; Chen, J. L.; Cao, C. X. *Talanta* **2009**, *78*, 1194-1200.

(36) Vulto, P.; Glade, N.; Altomare, L.; Bablet, J.; Del Tin, L.; Medoro, G.; Chartier, I.; Manaresi, N.; Tartagni, M.; Guerrieri, R. *Lab Chip* **2005**, *5*, 158-162.

(37) McDonald, J. C.; Whitesides, G. M. *Accounts Chem. Res.* **2002**, *35*, 491-499.

(38) Graul, T. W.; Schlenoff, J. B. *Anal. Chem.* **1999**, *71*, 4007-4013.

(39) Stefansson, M.; Novotny, M. *Anal. Chem.* **1994**, *66*, 1134-1140.

(40) Kamoda, S.; Nomura, C.; Kinoshita, M.; Nishiura, S.; Ishikawa, R.; Kakehi, K.; Kawasaki, N.; Hayakawa, T. *J. Chromatogr. A* **2004**, *1050*, 211-216.

(41) Kakehi, K.; Funakubo, T.; Suzuki, S.; Oda, Y.; Kitada, Y. *J. Chromatogr. A* **1999**, *863*, 205-218.

(42) Liu, J. P.; Shirota, O.; Novotny, M. V. *Anal. Chem.* **1992**, *64*, 973-975.

(43) Chen, C. C.; Yen, S. F.; Makamba, H.; Li, C. W.; Tsai, M. L.; Chen, S. H. *Anal. Chem.* **2007**, *79*, 195-201.

(44) Zhou, J. W.; Ellis, A. V.; Voelcker, N. H. *Electrophoresis*, *31*, 2-16.

(45) Katayama, H.; Ishihama, Y.; Asakawa, N. *Anal. Chem.* **1998**, *70*, 2254-2260.

(46) Katayama, H.; Ishihama, Y.; Asakawa, N. *Anal. Chem.* **1998**, *70*, 5272-5277.

(47) Boonsong, K.; Caulum, M. M.; Dressen, B. M.; Chailapakul, O.; Cropek, D. M.; Henry, C. S. *Electrophoresis* **2008**, *29*, 3128-3134.

(48) Liu, B. F.; Ozaki, M.; Hisamoto, H.; Luo, Q. M.; Utsumi, Y.; Hattori, T.; Terabe, S. *Anal. Chem.* **2005**, *77*, 573-578.

(49) Maeda, E.; Hirano, K.; Baba, Y.; Nagata, H.; Tabuchi, M. *Electrophoresis* **2006**, *27*, 2002-2010.

(50) Lee, H. L.; Chen, S. C. *Talanta* **2004**, *64*, 210-216.

Chapter 6

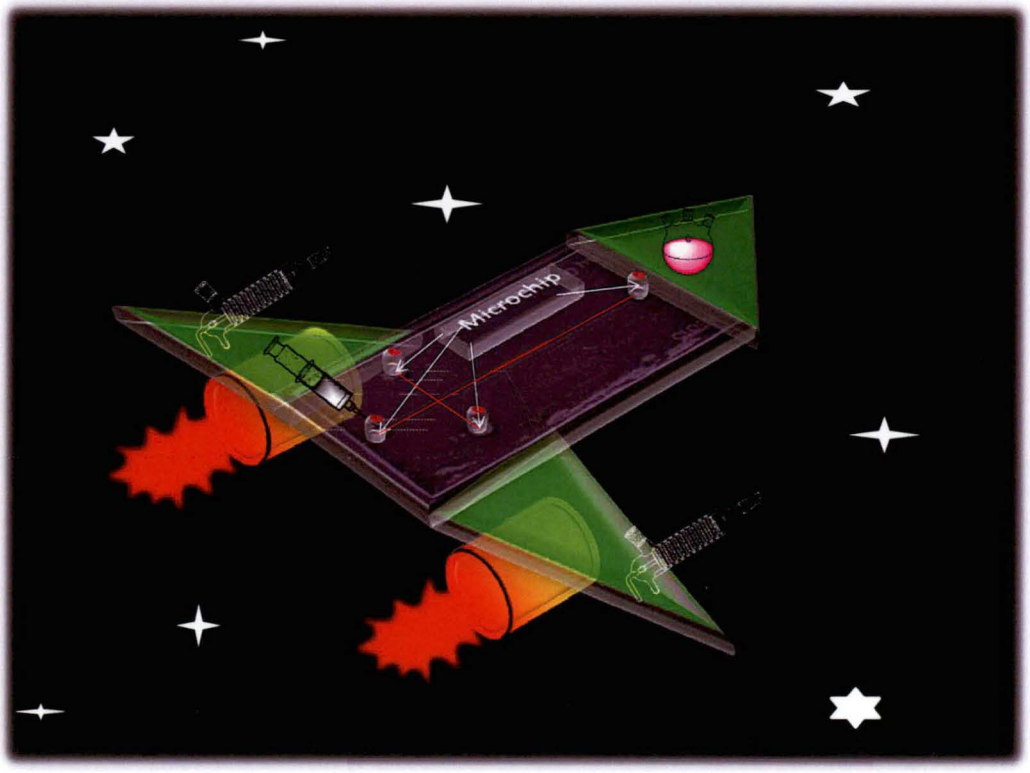

6 Conclusions and future directions

A number of conclusions can be drawn from the current study relating to development of novel strategies in CE to improve the sensitivity of carbohydrates. Utilisation of commercially available chromophore such as 5-aminofluorescein enables successful application of preconcentration *via* dynamic pH junction as a result of a close match between pK_a values of the chromophore, and pHs of the sample and the BGE allowing stacking for mono, di and tri saccharides. The present work involving 5-aminofluorescein enabled injection of large volumes of undiluted samples as a consequence of cleverly tailored sample and buffer composition allowing further enhancement in the sensitivity of the system. The amount of acid in the sample governs the movement of the boundary, affecting the distance travelled by the boundary and the degree of stacking of the analytes in the capillary. Careful consideration of these parameters presents a clever system which produces an optimum capillary length for stacking of the analytes to allow better sensitivity, and an ideal separation length to achieve outstanding efficiency and baseline resolution.

Incorporation of an in-house built cheap alternative such as an LED detector facilitated improved signal-to-noise ratio when compared to the commercially available DAD which once again translated to better sensitivity for absorbance detection. It is unsurprising that the LEDs offered better sensitivity than DAD and hopefully future methods can establish further enhancements by offering better focusing of this cheap light source.

The use of the 5-aminofluorescein chromophore is a substitute for fluorophores based on the fluorescein backbone which strongly implies the ability to directly transform this system to LIF detection.

Development of the new fluorescein based analogue O-2-[aminoethyl]fluorescein was accomplished using a straightforward, three step synthesis composed of esterification, alkylation and hydrolysis. The intricate design of the tag and the flexibility of the synthesis offered a way in which to construct a variety of fluorophores starting from an inexpensive, readily available fluorescein reagent. This current study demonstrated the utility of this tag for the analysis of simple oligosaccharides such as those found in corn syrup with the hope that other research groups may replicate the relatively simple synthesis and that it could be eventually commercialised. Future fluorescent tags need to be designed to ensure the reactive group-spacer combination allows the best labelling of carbohydrates and provides optimum electron transfer mechanism for maximum fluorescence which in turn can be used to achieve the best sensitivity. Tailored functionalities have to be also designed to allow the best resolution and selectivity of carbohydrates for future studies.

Application of O-2-[aminoethyl]fluorescein in the analysis of simple mono and di-saccharides demonstrated great separation outcomes for nine analytes in terms of efficiency, selectivity and resolution when using borate/ammonium buffers and acrylamide coated capillaries. Modification of the method to fused silica capillaries with capillary coatings such as PSS and PDADMAC decreased the resolution and the stacking ability of the saccharides due to the presence of substantial EOF, nevertheless it enabled direct translation from CE to a microchip format. The use of PDADMAC as the outer positive layer showed no viable separation most probably due to the electrostatic interaction between the derivatised sugars and the cationic surface of PDADMAC. In contrast the PSS coating with its anionic surface enabled a separation of four analytes.

The CE method was successfully designed and transferred to a microchip format allowing a separation of four mono- and di-saccharides in under 2 minutes. From this it was established that CE as a more reliable platform to microchips can be used to design and test methods which can eventually be converted without any modification to microchip scale separations. More importantly the biggest merit of the study is the first account of dynamic pH junction on a chip which with no doubt would be of great interest to the scientific community. Such results could be applied towars developing portable instruments for detection of simple sugars or other analytes for routine analyses in hospitals where analysis time is of great importance and sensitivity is required to allow detection of minute quantities of analytes.

However it is important to realise that chapter 5 of the study does bear some limitations in regards to sample dilution and implementation of dynamic pH junction. Eventhough this preconcentration method was achieved in this work, future studies should consider methods where sample is preconcentrated without any prior dilution.

The overview of the thesis suggests that preconcentration *via* dynamic pH junction was one of the main strategies to improve the sensitivity in carbohydrate analysis. The current study does have some limitations in regards to sample dilution which was necessary to carry out dynamic pH junction as . This ultimately constraints the preconcentration technique due to inability to inject samples straight as shown in chapter 4 and 5. Nevertheless chapter 3 demonstrated a clear ability to inject undiluted samples which gives the study a clear merit. More work is required to improve the current method however a firm foundation was established for future research using dynamic pH junction. This work has also been able to provide a cheap alternative to sensitive detection as described by chapter 3 and 5 where homebuilt detectors and power supplies were utilised.

There are other stacking strategies that could be considered in the scope of the study where very little method modification is required. One of such preconcentration methods is known as electrokinetic supercharging. This preconcentration method is very appealing and could potentially offer improvement factors in the order of 1,000. Something that must be considered is the choice of the fluorophore where the fluorescein based analogues are not compatible for this particular stacking strategy. Consideration of other commercially available fluorophores on the market unveils APTS as an attractive preference which is currently recognised as an excellent and one of the best tags for the analysis of oligosaccharides. APTS still is the golden standard offering impressive LODs in the order of 10^{-12}M for complex carbohydrates, nevertheless this thesis successfully covered mostly simple carbohydrates and enabled LODs at 10^{-10} M which is still quite significant. Preliminary assessment of rice starch samples using the APTS in conjunction with electrkinetic supercharging suggested sensitivity enhancements close to 1,000 times. Future directions of the current study will focus on detailed research aiming to understan the potential of this technique towards achieving superior sensitivity. Other future goals strive to reduce analysis times by manipulating the hardware through implementation of micro fluidic formats and decrease preparation times using on-line derivatisation methodology using zone passing and sandwich derivatisation configuratons. To supplement this, novel tags will also be designed with the aim of simple reaction protocols using minimal reagents and offering highly sensitive detection with tailored properties to enable a variety of stacking techniques. To conclude, this work is heading towards faster, smaller and more sensitive formats for the analysis of biomolecules with a primary focus on carbohydrates. Some of the

major challenges in carbohydrate research are related to the ability to detect and resolve numerous isomeric structures of these biocomposites with the utlimate aim of conducting rapid analyses. The workdescribed in the current thesis addressed issues of sensitivity and with the ultimate goal of rapid detection using microchip platforms. This thesis mainly deals with sensitive detection, resolution and separation of more simple carbohydrates nevertheless it describes a promising foundation towards the field of glycobiology.